MULTI-MODEL BASED FORMATION CONTROL OF A FLEET OF UAVS

BY

Mohammed Ataur Rahman

A Thesis Presented to the
DEANSHIP OF GRADUATE STUDIES

KING FAHD UNIVERSITY OF PETROLEUM & MINERALS

DHAHRAN, SAUDI ARABIA

In Partial Fulfillment of the
Requirements for the Degree of

MASTER OF SCIENCE

In

SYSTEMS AND CONTROL ENGINEERING

December 2017

KING FAHD UNIVERSITY OF PETROLEUM & MINERALS

DHAHRAN- 31261, SAUDI ARABIA

DEANSHIP OF GRADUATE STUDIES

This thesis, written by **Mohammed Ataur Rahman** under the direction of his thesis advisor and approved by his thesis committee, has been presented and accepted by the Dean of Graduate Studies, in partial fulfillment of the requirements for the degree of **MASTER OF SCIENCE IN SYSTEMS & CONTROL ENGINEERING.**

15/5/2018

Dr. Abdul Wahid A. Al-Saif
(Advisor)

15/05/2018

Dr. Sami El Ferik
(Member)

Dr. Hesham K. Al-Fares
Department Chairman

16/05/2018

Dr. Muhammad Faizan Mysorewala
(Member)

Dr. Salam A. Zummo
Dean of Graduate Studies

عمادة الدراسات العليا
DEANSHIP OF GRADUATE STUDIES

21/5/18

Date

Dedicated to my beloved parents, who are the biggest support and inspiration of my life

ACKNOWLEDGMENTS

All praises and thankfulness be to Allah (S.W.T.), the Most Gracious and the Most Merciful. I have been blessed by Him with countless privileges and bounties and without Him, this would not have been possible. May His peace be upon the Prophet Muhammed and His family.

I would like to thank King Fahad University of Petroleum and Minerals and The Systems Engineering department for accepting my admission and giving me the opportunity to pursue my Masters here.

And then, I am quite privileged to have Dr. Abdul Wahid A. Al-Saif as my thesis advisor. I thank him very much for his continuous support and guidance throughout this thesis especially during times when I got stuck.

I am also thankful to my committee members Dr. Sami El Ferik and Dr. Muhammed Faizan Mysorewala for their support and helpful inputs.

I would also like to thank my parents and my family members for their love and constant support. I am particularly indebted to my parents for raising me well and providing all the benefits and luxuries possible for my better future.

Finally, I would like to thank all my colleagues and friends from KFUPM and elsewhere for their support and advises. Special thank goes to Safi Khaja, Abdul Majeed Kabir, Raghib, Amer, Faisal, Basheer, Allah Bakash and Inayat Basha without whose company this journey would not have been this pleasant.

TABLE OF CONTENTS

LIST OF TABLES

LIST OF FIGURES

ABSTRACT

Full Name : [Mohammed Ataur Rahman]

Thesis Title : Multi-Model Based Formation Control of a Fleet of UAVs

Major Field : [Systems and Control Engineering]

Date of Degree : [December 2017]

In this thesis, the formation control of a set of quadrotors is achieved using the Takagi-Sugeno Multi-Model approach to linearize the UAVs. First the nonlinear model of the quadrotor is linearized using the Taylor series about a set of operating points and local models are obtained. These local models are then interpolated using the Fuzzy Takagi-Sugeno approach to obtain the approximation of the entire nonlinear model. Comparison of the nonlinear and the T-S model shows a good approximation of the system. Then a nonlinear state-feedback controller is synthesized using the Parallel Distributed Compensation (PDC). The gains of the controller are obtained by Linear Quadratic Regulator (LQR) optimization to stabilize the system and obtain desired response. This is followed by the formation control of a set of quadrotors using the leader-follower method. In this method, the potential field technique is used to obtain the desired shape formations. An attractive potential is generated that attracts the followers towards the leader and a repulsive potential is generated that repels adjacent quadrotors to avoid collisions. Simulations are performed to obtain the desired shape formation for different cases. It is observed that the formation control proposed gives a good tracking response.

ملخص الرسالة

الاسم الكامل: محمد عطا الرحمن

عنوان الرسالة: السيطرة على تشكيل أسطول من الطائرات بدون طيار استنادا إلى نماذج متعددة

التخصص: هندسة النظم والتحكم

تاريخ الدرجة العلمية: ديسمبر 2017 م

في هذه الأطروحة، تم التحكم في تشكل/تكوين مجموعة من المركبات رباعية الدوار باستخدام طريقة تاكاجي-سوغينو متعددة النماذج لتحويل المركبات بدون طيار لنظيرها الخطي .في البداية يتم الحصول على نموذج غير خطي لمركبة رباعية الدوار وتم إستخدام متسلسلة تايلور حول مجموعة من نقاط التشغيل لتقريب النموذج الي نموذج خطي بالكامل وتم التحصل علي نماذج محلية .تم إستيفاء النماذج المحلية بنهج تاكاجي-سوغينو الضبابي للتحصل علي تقريب للنموذج الغير خطي الكامل .تُظهر المقارنة بين النموذج غير الخطي ونموذج تاكاجي-سوغينو تقريبًا جيدًا للنظام .ثم تم بعد ذلك تأليف وحدة تحكم غير خطية بطريقة التغذية العكسية لمتغيرات الحالة باستخدام تعويض التوزيع الموازي .(PDC) يتم الحصول على كسوب وحدة التحكم عن طريق منظم التربيع الخطي (LQR)لتحسين وتحقيق إستقرار للنظام والحصول على الاستجابة المطلوبة .ويتبع ذلك تدريب مجموعة من المركبات رباعية الدوار باستخدام طريقة القائد والتابع .في هذه الطريقة ، يتم استخدام تقنية المجالات المحتملة للحصول على تكوينات الشكل المطلوب .يتم إنشاء مجال جاذب لجذب الأتباع نحو زعيم/قائد ومجالات منفرة لصد المركبات المجاورة لتجنب الإصطدامات .تم تنفيذ عمليات المحاكاة للحصول على الشكل/التكوين المطلوب للحالات المختلفة .يلاحظ أن متحكم التشكيل المقترح يعطي إستجابة تتبع جيدة.

CHAPTER 1

INTRODUCTION

1.1 Motivation

Unmanned air vehicles, simply known as the UAVs, have seen a significant attention and progress in the past decade due to their innumerous advantages and applications. UAV as the name stands for is an air borne robot that can fly autonomously or semi autonomously without a pilot on board. The tasks that are needed to be performed by the UAVs are given through a control system which may be mounted on the vehicle or somewhere else. UAVs consists of multivariable nonlinear dynamics whose complexity depends on the required operation and objectives. There are different types of UAVs such as the fixed wing, the helicopter, the quadrotor etc. The quadrotor is one of the most popular and researched on UAV these days because of its advantages over the others that includes more reliability, less size and low maintenance. Quadrotor is a multirotor which is lifted and propelled by 4 rotors. Each rotor is attached to a dc motor that governs the motion of the vehicle. The front and back rotor rotate in anticlockwise direction and the left and right rotor rotates in clockwise direction. Thus, the gyroscopic effects and the torques are cancelled out in the stationary trimmed state. Figure (1.1) shows a quadrotor which is the Parrot AR. Drone 2.0 built in Nevada in 2012.

Figure 1.1 Parrot AR. Drone 2.0 takeoff

UAVs are reliable to replace manned aerial vehicles in many areas such as military, civilian communities, and agriculture. In military tasks, UAVs are used to carry different loads, such as radars, sensors, cameras, or weapons too. In addition, UAVs can be used for observation and exploring unfriendly environments [1]. In civilian environments, UAVs are useful for several applications such as watching natural resources, home security, scientific research, and search and rescue operations.

The concept of 'Divide and Conquer' is generally used to solve any complex problem in day to day life. The problem can be divided into several easier parts, which when solved individually and combined can give the solution to the entire problem. Similar concept can even be used in controlling nonlinear systems, in which the complex nonlinear model can be divided into set of locally linearized models and then interpolated together to obtain the overall system. This method is called the Multi-Model Approach (MMA) also known as the Takagi-Sugeno (T-S) modelling [6]. The interpolation of all the individual models is done using Fuzzy logic.

Recently, the use and control of groups of UAVs to achieve tasks cooperatively together has been attracted much interest of researchers in the related fields. This is because of the advantages that are obtained from using multiple vehicles instead of using a more elaborated single vehicle. If a task outcome of a team of multiple unmanned vehicles is compared with that of an individual vehicle, one can realize that the multiple vehicles overall performance can develop mission allocation, performance, the required time, and the system efficiency and safety.

Multi-UAV formation flight is a combination of the study of both Quadrotors and synchronization, so it has received substantial interest from both autonomous systems and control groups. Cooperative coordination can be described as set of UAVs those are assigned to track a predefined path of flight while obtaining useful information through their sensors and maintaining a prescribed formation structure. The flight trajectory could be a set of coordinates that the UAVs must follow or a prescribed region of fly within certain boundaries.

In this thesis, first the nonlinear model of a Quadrotor is taken and linearized using the Taylor series linearization around a set of operating points to obtain the individual local T-S models. These models are combined using the Fuzzy logic to obtain the overall T-S model. Then, a nonlinear state-feedback controller is implemented using the parallel distributed compensation technique. The gains of the controller are obtained using the linear quadratic regulator (LQR) optimization to stabilize the system and achieve desired response. This is now implemented in the formation control of the UAVs in which we use the leader-follower method. The leader is set to track a desired reference trajectory and the followers track the position of the leader with predefined offsets. These offsets are

calculated using the potential fields technique to obtain a desired shape formation. An attractive potential is generated that attracts the followers towards the leader and a repulsive potential is generated that repels adjacent quadrotors to avoid collisions and a desired shape formation is obtained.

1.2 Thesis Objectives

- Study of a Quadrotor UAV with Multiple Model Approach technique and T-S Fuzzy Logic.
- Developing the State Feedback controller using Linear Quadratic Regulator on a single quadrotor.
- Implementing the control technique for the Formation of a set of Quadrotors using leader-follower potential fields technique.
- Simulation of all the results to test stability and performances.

CHAPTER 2

LITERATURE REVIEW

There have been a lot of research and contribution going on for the quadrotor UAVs. The literature mainly focuses on the modelling and the control for the nonlinear dynamics of the system. One of the earliest work done is by Samir Bouabdallah in [1,2] where he formulated the dynamics of the quadrotor model and presented briefly different control techniques applied to it. The dynamics modelling, simulation and system identification has also been addressed in other papers like [3,4]. The application of a simple PID controller for the quadrotor is given in [7]. Attitude control techniques using observers are given in [10].

The applications of fuzzy theory in control systems is widely seen in the literature. The Takagi-Sugeno (TS) model which uses the multiple model approach (MMA) for the quadrotor is shown in [6]. The concept of approximation based on multiple models is not new. Since the work and publications of Johansen and Foss in this topic, the multiple-models approach obtained a significant attention [2], at the beginning certain authors have tried to represent nonlinear systems by the piece-wise linear approximations [5], which use the set of local models and switching, A few years afterwards, Jacob and al [6] have presents the multi-experts approach which is the combination of different experts via activation functions such as an expert is a model describing the local behaviour of a system. Due to the structure of the local model networks and the similarity to the neural networks,

it is hard to decide whether local model networks belong to the category of fuzzy systems or neural networks.

Many non-linear techniques have been employed on the quadrotors to stabilize the system. In [11], feedback linearization method was developed to control the quadrotor and track a predefined trajectory. Voos [12] developed a control structure based on feedback linearization and its decomposition into a nested structure. Backstepping method was proposed by Altug et al [13] in which the positions and the yaw angle were kept constant while the pitch and the roll angle regulate to zero to stabilize the quadrotor. Zuo [14] employed the backstepping technique with command-filtered compensation. Sliding mode techniques was developed in [15], and a combination of sliding mode control and backstepping technique has been considered in [16]. Stabilization of the attitude of the UAV based on compensation of the Coriolis and gyroscopic torques has been studied in [17]. In [18], Merabti employed the Nonlinear Model Predictive control technique for the trajectory tracking of a quadrotor in the presence of an external perturbation. Bialy in [19] presents a robust adaptive controller for a UAV in the existence of linear uncertainties in the parameters and exogenous disturbances.

In [20] Guerrero and Rogelio investigated a leader/follower type approach based on the combination of nested saturations and a multi-agent consensus control to design a nonlinear controller to achieve flight formation for a multiple mini rotorcraft system. Young-Cheol and Hyo-Sung [21] used a three-dimensional formation controller based on inter-agent distances. The controller is constructed from the time derivative of the Euclidean distance matrix related to the team realization. Turpin et al. [22] studied formation control for a team of quadrotors where the vehicles track a specified group

trajectory with ability to change the shape of the formation safely according to specifications. Shape vectors prescribe the formation and command the relative separations and bearings between the quadrotors. In [23], a Multimodel Predictive Control technique is used on the leader-follower formation of the quadrotor by using Fuzzy logic.

There are many techniques of formation control in Quadrotors: leader-follower, behavioural, and virtual structure approaches, However, in [24], the authors added the artificial potential field techniques as a fourth approach while Chen et al. [25] combined the behavioural approach and the artificial potential field techniques in one approach.

In leader-follower technique, one of the members is selected to be the leader and the others are nominated as followers [26], however sometimes multiple agents are considered as leaders [27]. The followers must locate themselves with respect to their leader and to keep a desired position relative to the leader [28]. Control systems with the leader-following strategy exhibit satisfactorily well performance for flight vehicle formations. Simplicity and reliability are characters of this method. However, disadvantage in this scheme is that the leader doesn't receive an explicit feedback from the followers.

The leader-follower formation control methods have been studied widely including various methodologies like PID control approach [29], decentralized control based on Linear Quadratic Regulator (LQR) [30], nonlinear techniques, and adaptive methods. In [31] simulation comparison studies have been done between baseline constant gain control algorithms and adaptive control laws which adapt to the uncertainties caused by the aerodynamic interactions.

In Behavioral approach is always combined with potential field approach in the applications of formation control. In behavioral approach, each member is assigned with several desired behaviors and the control action is described by a weighted average of the control that corresponds to each desired behavior for the member. These desired behaviors may include formation maintaining, collision avoidance, and obstacle avoidance [32] Mathematical analyses are difficult for behavioral approaches and formation characteristics, such as stability, cannot generally be guaranteed.

In virtual structure approach, the whole formation of members is considered as a single unit. Using the desired motion for the virtual structure, which is given, the desired motions for the members are found. In virtual structure method, three steps are needed to design the controller. The first step is to define the desired virtual structure dynamics. The second step is to convert the desired virtual structure motion to desired motions for each member in the group. The Last step is to design separate tracking controllers for each member.

This structure is mainly used to implement sensor and manipulator systems. The advantage of this method is that formation control is uncomplicated. The centralization, however, is a disadvantage in the Virtual structure implementation and this leads to the whole system failure in the case of an agent failure [33].

CHAPTER 3

Preliminary: Quadrotor Dynamics and Mathematical Modelling

3.1 Introduction

In this chapter, the mathematical non-linear model of a quadrotor is first obtained by using theoretical approach. This model is then linearized using the Taylor series linearization and Takagi-Sugeno Multiple-Model Approach and a network of linearized models are obtained. The overall network of models is then compared with the original model to validate our system.

3.2 Quadrotor Dynamics Modelling

The quadrotor consists of four rotating propellers which are driven by four dc motors that governs the motion of the vehicle. The orientation of the quadrotor is determined by the Euler angles which are the Roll angle (φ), Pitch angle (θ) and Yaw angle (ψ). The dynamics of the quadrotor can be explained in Figure (3.1). The system consists of the inertial frame R^b and the body frame R^m as shown. The forces appearing on the quadrotor are the Roll, Pitch and Yaw torques and the total thrust force.

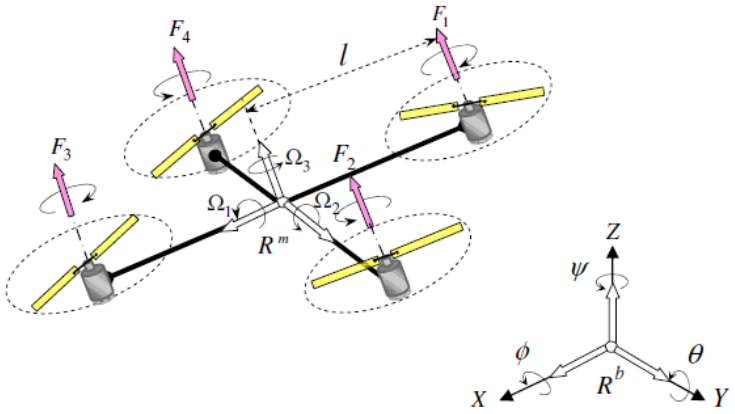

Figure 3.1 Quadrotor Dynamics

As stated previously, rotors (1, 3) and rotors (2, 4), rotate in different directions to negate the moments generated by each other. By increasing the angular velocity of the 2nd rotor and decreasing the angular velocity of the 4th rotor while keeping the whole thrust constant, we can get the roll movement in the x-axis direction of the vehicle. Similarly, by increasing the angular velocity of the 3rd rotor and decreasing the angular velocity of the 1st rotor produces the pitch movement along the y-axis. And for the yaw motion along the z-axis, the speed of rotors (1, 3) can be increased and the speed of rotors (2, 4) can be decreased. This mechanism is explained in Figure (3.2).

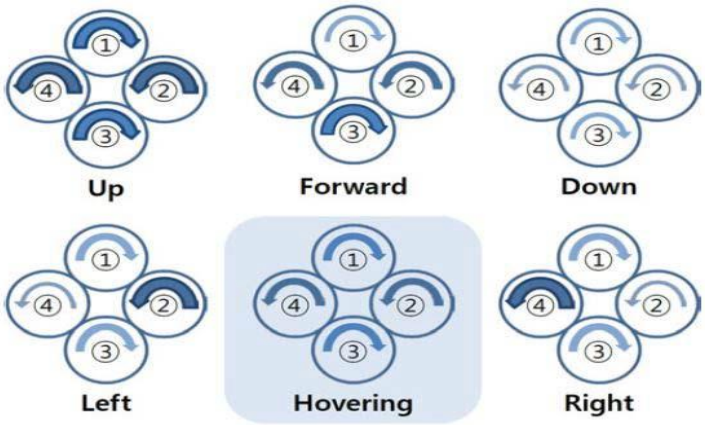

Figure 3.2 Movement mechanism of the quadrotor

The transformation matrix used for the transformation of the system from the inertial or ground frame to the body frame in terms of the Euler angles is,

$$R = \begin{pmatrix} c\psi c\theta & s\varphi s\theta c\psi - s\psi c\varphi & c\varphi s\theta c\psi + s\psi s\varphi \\ s\psi c\theta & s\varphi s\theta s\psi + c\psi c\theta & c\varphi s\theta s\psi - s\varphi c\psi \\ -s\theta & s\varphi c\theta & c\varphi c\theta \end{pmatrix} \tag{3.1}$$

where *s(x)* and *c(x)* represents *sin(x)* and *cos(x)* respectively.

Now, by considering the Euler angles of rotation and Newton-Euler or Lagrange method of developing models, the equations of motion are derived in terms of the translational and rotational parameters which are [$\varphi, \Theta, \psi, x, y, z$]. Thus, the set of nonlinear equations obtained are:

$$\begin{aligned}
\ddot{\varphi} &= \frac{\dot{\theta}\dot{\psi}\left(I_y - I_z\right)}{I_x} - \frac{J_r}{I_x}\Omega_r\dot{\theta} - \frac{K_{fax}}{I_x}\dot{\varphi}^2 + \frac{l}{I_x}u_2 \\
\ddot{\theta} &= \dot{\varphi}\dot{\psi}\frac{(I_z - I_x)}{I_y} + \frac{J_r}{I_y}\Omega_r\dot{\varphi} - \frac{K_{fay}}{I_y}\dot{\theta}^2 + \frac{l}{I_y}u_3 \\
\ddot{\psi} &= \dot{\theta}\dot{\varphi}\frac{\left(I_x - I_y\right)}{I_z} - \frac{K_{faz}}{I_z}\dot{\psi}^2 + \frac{l}{I_x}u_4 \\
\ddot{x} &= -\frac{K_{ftx}}{m}\dot{x} + \frac{l}{m}(c\varphi s\theta c\psi + s\varphi s\psi)u_1 \\
\ddot{y} &= -\frac{K_{fty}}{m}\dot{y} + \frac{l}{m}(c\varphi s\theta s\psi - s\varphi c\psi)u_1 \\
\ddot{z} &= -\frac{K_{ftz}}{m}\dot{z} - g + \frac{l}{m}(c\varphi c\theta)u_1
\end{aligned} \tag{3.2}$$

where *l* is the length of each arm and *m* is the mass of the quadrotor. I_x, I_y and I_z are the moments of inertia around *x*,*y* and *z* axes respectively. u_1, u_2, u_3 and u_4 are the control inputs.

The control inputs are related to the angular velocities of the rotors by the following relation,

$$\begin{pmatrix} u_1 \\ u_2 \\ u_3 \\ u_4 \end{pmatrix} = \begin{pmatrix} b & b & b & b \\ 0 & -b & 0 & b \\ -b & 0 & b & 0 \\ d & -d & d & -d \end{pmatrix} \begin{pmatrix} {\omega_1}^2 \\ {\omega_2}^2 \\ {\omega_3}^2 \\ {\omega_4}^2 \end{pmatrix} \tag{3.3}$$

$$\Omega_r = \omega_1 - \omega_2 + \omega_3 - \omega_4$$

where b is the thrust and d is the drag parameter. ω_i is the angular velocity of the i^{th} rotor.

The detailed derivation of the above equations can be seen in [4].

3.3 Linearization of the Quadrotor Model

The linearized model is obtained using Takagi-Sugeno representation which involves the Multiple Model Approach (MMA). It is based on the rule 'Divide and conquer'. According to MMA, the complete nonlinear complex system is divided into several simpler linear sub-systems. The solutions of these sub-systems when combined should give the solution of the complete system. Generally, the complex system is divided into linear models which describe the dynamics of the system in different regions of the operating space. The entire system can be achieved by interpolation. This can be shown in Figure (3.3) as follows.

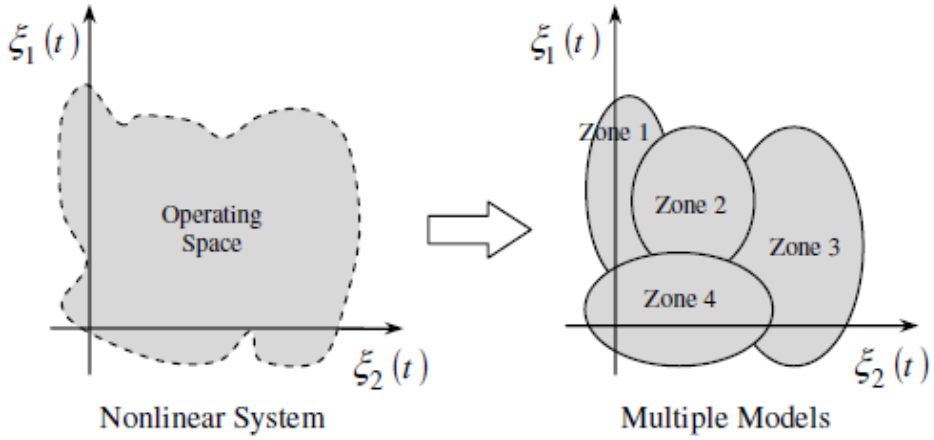

Figure 3.3 Multiple model Approach (MMA)

For convenience, the nonlinear model of the quadrotor is represented in state space form as follows,

$$\dot{x}(t) = A(x)x(t) + B(x)u(t)$$
$$\dot{y}(t) = C(x)x(t) + D(x)u(t) \tag{3.4}$$

The state, input and output vectors are,

$$x(t) = (\varphi \quad \dot{\varphi} \quad \theta \quad \dot{\theta} \quad \psi \quad \dot{\psi} \quad x \quad \dot{x} \quad y \quad \dot{y} \quad z \quad \dot{z})^T$$
$$u(t) = (u_1 \quad u_2 \quad u_3 \quad u_4)^T \tag{3.5}$$
$$y(t) = (\varphi \quad \dot{\varphi} \quad \theta \quad \dot{\theta} \quad \psi \quad \dot{\psi} \quad x \quad \dot{x} \quad y \quad \dot{y} \quad z \quad \dot{z})^T$$

To obtain the state matrices *A*, *B*, *C* and *D*, Taylor series linearization process is used. For this purpose, the state function *f* is defined as,

$$f\big(x(t),u(t)\big)=\dot{x}(t)=\begin{pmatrix}\dot{\varphi}\\ \frac{\dot{\theta}\dot{\psi}(I_y-I_z)}{I_x}-\frac{J_r}{I_x}\Omega_r\dot{\theta}-\frac{K_{fax}}{I_x}\dot{\varphi}^2+\frac{l}{I_x}u_2\\ \dot{\theta}\\ \dot{\varphi}\dot{\psi}\frac{(I_z-I_x)}{I_y}+\frac{J_r}{I_y}\Omega_r\dot{\varphi}-\frac{K_{fay}}{I_y}\dot{\theta}^2+\frac{l}{I_y}u_3\\ \dot{\psi}\\ \dot{\theta}\dot{\varphi}\frac{(I_x-I_y)}{I_z}-\frac{K_{faz}}{I_z}\dot{\psi}^2+\frac{l}{I_z}u_4\\ \dot{x}\\ -\frac{K_{ftx}}{m}\dot{x}+\frac{l}{m}(c\varphi s\theta c\psi+s\varphi s\psi)u_1\\ \dot{y}\\ -\frac{K_{fty}}{m}\dot{y}+\frac{l}{m}(c\varphi s\theta s\psi-s\varphi c\psi)u_1\\ \dot{z}\\ -\frac{K_{ftz}}{m}\dot{z}-g+\frac{l}{m}(c\varphi c\theta)u_1\end{pmatrix} \tag{3.6}$$

The behavior of the nonlinear system about an operating point (x_i,u_i) can be approximated by a linear time-invariant system (LTI). We use the Taylor series of the first order to obtain:

$$\dot{x}(t)=A_i(x(t)-x_i)+B_i(u(t)-u_i)+f(x_i,u_i) \tag{3.7}$$

Which can be written as,

$$\dot{x}(t)=A_ix(t)+B_iu(t)+d_i \tag{3.8}$$

where:

$$A_i=\left.\frac{\partial f(x,u)}{\partial x}\right|_{\substack{x=x_i\\u=u_i}};\ B_i=\left.\frac{\partial f(x,u)}{\partial u}\right|_{\substack{x=x_i\\u=u_i}};\ d_i=f(x_i,u_i)-A_ix_i-B_iu_i \tag{3.9}$$

Therefore, by performing the above derivation, the matrices A_i and B_i are obtained as,

$$A_i = \begin{pmatrix} 0 & 1 & 0 & 0 & 0 & 0 & 0 & 0 & 0 & 0 & 0 & 0 \\ 0 & a_1 & 0 & a_2\dot{\psi} + a_3 & 0 & a_2\dot{\theta} & 0 & 0 & 0 & 0 & 0 & 0 \\ 0 & 0 & 0 & 1 & 0 & 0 & 0 & 0 & 0 & 0 & 0 & 0 \\ 0 & a_5 + a_4\dot{\psi} & 0 & a_6 & 0 & a_4\dot{\varphi} & 0 & 0 & 0 & 0 & 0 & 0 \\ 0 & 0 & 0 & 0 & 0 & 1 & 0 & 0 & 0 & 0 & 0 & 0 \\ 0 & a_7\dot{\theta} & 0 & a_7\dot{\varphi} & 0 & a_8 & 0 & 0 & 0 & 0 & 0 & 0 \\ 0 & 0 & 0 & 0 & 0 & 0 & 0 & 1 & 0 & 0 & 0 & 0 \\ a_9 & 0 & a_{10} & 0 & a_{11} & 0 & 0 & a_{12} & 0 & 0 & 0 & 0 \\ 0 & 0 & 0 & 0 & 0 & 0 & 0 & 0 & 0 & 1 & 0 & 0 \\ a_{13} & 0 & a_{14} & 0 & a_{15} & 0 & 0 & 0 & 0 & a_{16} & 0 & 0 \\ 0 & 0 & 0 & 0 & 0 & 0 & 0 & 0 & 0 & 0 & 0 & 1 \\ a_{17} & 0 & a_{18} & 0 & 0 & 0 & 0 & 0 & 0 & 0 & 0 & a_{19} \end{pmatrix} \quad (3.10)$$

where,

$$a_1 = -\frac{K_{fax}}{I_x}\ ;\ a_2 = \frac{\left(I_y - I_z\right)}{I_x}\ ;\ \ a_3 = -\frac{J_r}{I_x}\Omega_r\ ;\ \ a_4 = \frac{(I_z - I_x)}{I_y}\ ;\ a_5 = \frac{J_r}{I_y}\Omega_r\ ;$$

$$a_6 = -\frac{K_{fay}}{I_y};\ a_7 = \frac{\left(I_x - I_y\right)}{I_z};\ a_8 = -\frac{K_{faz}}{I_z};\ a_9 = \frac{l}{m}(-s\varphi s\theta c\psi + c\varphi s\psi)u_{1i}\ ;$$

$$a_{10} = \frac{l}{m}(c\varphi c\theta c\psi)u_{1i};\ a_{11} = \frac{l}{m}(-c\varphi s\theta s\psi + s\varphi c\psi)u_{1i};\ a_{12} = -\frac{K_{ftx}}{m};$$

$$a_{13} = \frac{l}{m}(-s\varphi s\theta s\psi - c\varphi c\psi)u_{1i}\ ;\ a_{14} = \frac{l}{m}(c\varphi c\theta s\psi)u_{1i}$$

$$a_{15}\ = \frac{l}{m}(c\varphi s\theta c\psi + s\varphi s\psi)u_{1i}\ ;\ a_{16} = -\frac{K_{fty}}{m};\ a_{17} = \frac{l}{m}(-s\varphi c\theta)u_{1i}\ ;$$

$$a_{18} = \frac{l}{m}(-c\varphi s\theta)u_{1i}\ ;\ a_{19} = -\frac{K_{ftz}}{m}$$

$$B(x) = \begin{pmatrix} 0 & 0 & 0 & 0 \\ 0 & b_1 & 0 & 0 \\ 0 & 0 & 0 & 0 \\ 0 & 0 & b_2 & 0 \\ 0 & 0 & 0 & 0 \\ 0 & 0 & 0 & b_3 \\ 0 & 0 & 0 & 0 \\ b_4 & 0 & 0 & 0 \\ 0 & 0 & 0 & 0 \\ b_5 & 0 & 0 & 0 \\ 0 & 0 & 0 & 0 \\ b_6 & 0 & 0 & 0 \end{pmatrix} \tag{3.11}$$

where,

$$b_1 = \frac{l}{I_x} \; ; \; b_2 = \frac{l}{I_y} \; ; \; b_3 = \frac{l}{I_z} \; ; \; b_4 = \frac{l}{m}(c\varphi s\theta c\psi + s\varphi s\psi) \; ;$$

$$b_5 = \frac{l}{m}(c\varphi s\theta s\psi - s\varphi c\psi) \; ; \; b_6 = \frac{l}{m}(c\varphi c\theta)$$

The matrix *C(x)* is taken as an identity matrix and *D* is taken as zero.

$$C(x) = \begin{pmatrix} 1 & 0 & 0 & 0 & 0 & 0 & 0 & 0 & 0 & 0 & 0 & 0 \\ 0 & 1 & 0 & 0 & 0 & 0 & 0 & 0 & 0 & 0 & 0 & 0 \\ 0 & 0 & 1 & 0 & 0 & 0 & 0 & 0 & 0 & 0 & 0 & 0 \\ 0 & 0 & 0 & 1 & 0 & 0 & 0 & 0 & 0 & 0 & 0 & 0 \\ 0 & 0 & 0 & 0 & 1 & 0 & 0 & 0 & 0 & 0 & 0 & 0 \\ 0 & 0 & 0 & 0 & 0 & 1 & 0 & 0 & 0 & 0 & 0 & 0 \\ 0 & 0 & 0 & 0 & 0 & 0 & 1 & 0 & 0 & 0 & 0 & 0 \\ 0 & 0 & 0 & 0 & 0 & 0 & 0 & 1 & 0 & 0 & 0 & 0 \\ 0 & 0 & 0 & 0 & 0 & 0 & 0 & 0 & 1 & 0 & 0 & 0 \\ 0 & 0 & 0 & 0 & 0 & 0 & 0 & 0 & 0 & 1 & 0 & 0 \\ 0 & 0 & 0 & 0 & 0 & 0 & 0 & 0 & 0 & 0 & 1 & 0 \\ 0 & 0 & 0 & 0 & 0 & 0 & 0 & 0 & 0 & 0 & 0 & 1 \end{pmatrix} \tag{3.12}$$

3.4 Construction of the Takagi-Sugeno Model

3.4.1 Model Architecture

To build the T-S model, we use $r=9$ locally linearized models and these models are interpolated using the T-S Fuzzy logic. The architecture and the formulation of the model is described in Figure (3.4) below.

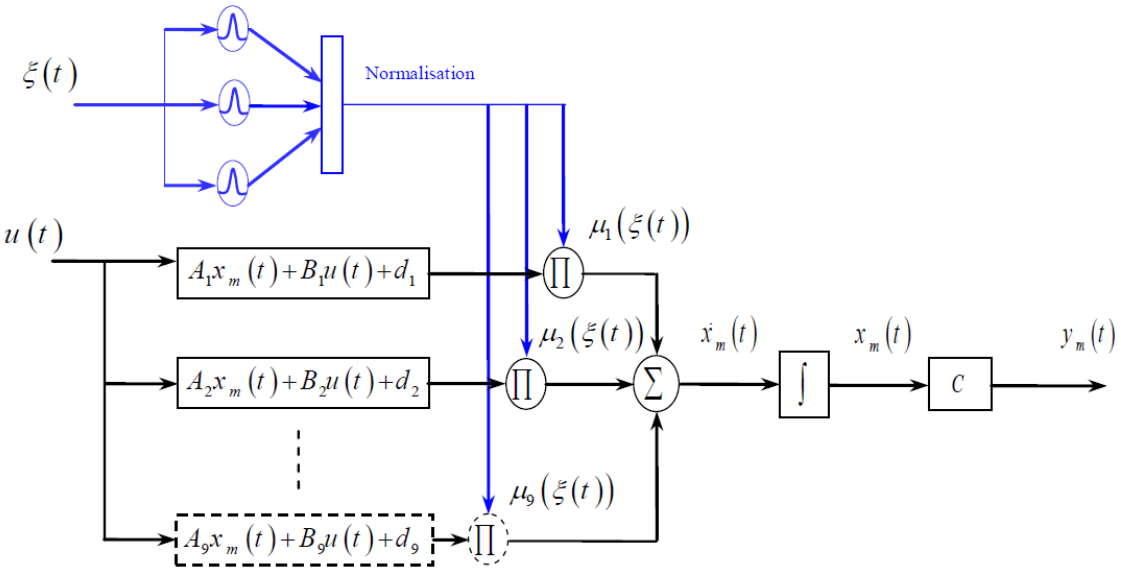

Figure 3.4 Takagi-Sugeno architecture

$$\dot{x}_m(t) = \sum_{i=1}^{r} \mu_i\big(\xi(t)\big)\big(A_i x_m(t) + B_i u(t)\big)$$
$$\dot{y}_m(t) = C x_m(t) \tag{3.13}$$

where r is the number of local linear models, x, y and u are the state, output and input vectors respectively. A and B are the state and input matrices, $\xi(t)$ is the Fuzzy decision variable. $\mu_i\big(\xi(t)\big)$ is the normalized activation function.

The activation function determines the degree of activation of the individual local model. It shows the amount of contribution of each local model to the entire system. The properties of the activation function are as follows,

$$\begin{cases} \sum_{i=1}^{r} \mu_i\big(\xi(t)\big) = 1 \\ 0 \le \mu_i\big(\xi(t)\big) \le 1 \end{cases} \tag{3.14}$$

There are different types of activation functions that can be used in Fuzzy theory like Triangular, Sigmoidal, Gaussian etc. In this work, we use the gaussian activation function which is defined as follows,

$$\mu_i\big(\xi(t)\big) = \frac{\omega_i\big(\xi(t)\big)}{\sum_{i=1}^{m} \omega_i\big(\xi(t)\big)} \quad ; \quad \omega_i\big(\xi(t)\big) = \prod_{j=1}^{m} M_{ij}\left(\xi_j(t)\right) \tag{3.15}$$

where *m* is the dimension of the decision variables vector *ξ(t)*.

M_{ij} are the membership functions defined based on the Gaussian Fuzzy rules as follows,

$$M_{ij}\left(\xi_j(t)\right) = \exp\left(-\frac{\left(\xi_j(t) - c_{i,j}\right)^2}{2\sigma_{i,j}^2}\right) \tag{3.16}$$

Now, to define the individual models, the operating points are first taken from [5] and the system is studied. As mention in [5],

- Three models are defined around the roll angle, ϕ=-30^0, 0^0, 30^0
- Three models are defined around the pitch angle, θ=-30^0, 0^0, 30^0
- Three models are defined around the yaw angle, ψ=-60^0, 0^0, 60^0

The decision variable vector is taken as,

$$\xi(t) = (\varphi \quad \theta \quad \psi)^T \tag{3.17}$$

The selected operating points are converted into radians and are summarized in Table 3.1 as follows,

Table 3.1 Operating Points

Operating Points	1	2	3	4	5	6	7	8	9
φ_i	-0.523	0	0.523	0	0	0	0	0	0
$\dot{\varphi}_i$	0.562	0	0.583	0	0	0	0	0	0
θ_i	0	0	0	-0.523	0	0.523	0	0	0
$\dot{\theta}_i$	0	0	0	0.527	0	0.585	0	0	0
ψ_i	0	0	0	0	0	0	-1.047	0	1.047
$\dot{\psi}_i$	0	0	0	0	0	0	0.942	0	0.856

3.4.2 Parameter Selection of Membership functions

The parameters of the membership function as seen in (3.15) are the centers, $c_{i,j}$ and dispersions, $\sigma_{i,j}$. They are defined as follows,

-The centres: The centers of membership functions, $c_{i,j}$, are defined from the operating points. They are given in Table (3.2).

Table 3.2 Centers $c_{i,j}$ of the membership function

j \ *i*	*1*	*2*	*3*	*4*	*5*	*6*	*7*	*8*	*9*
1	-0.523	0	0.523	0	0	0	0	0	0
2	0	0	0	-0.523	0	0.523	0	0	0
3	0	0	0	0	0	0	-1.047	0	1.407

-The Dispersions: The dispersions, $\sigma_{i,j}$, are obtained by using an optimization technique to minimize the error between the non-linear model and the linearized T-S model. This is explained in [5]. Thus, we obtain the dispersion parameters as shown in Table (3.3).

Table 3.3 Dispersions $\sigma_{i,j}$ of the membership function

i \ j	1	2	3	4	5	6	7	8	9
1	0.2424	0.5236	0.2769	0.3534	0.4597	0.1745	0.3563	0.1745	0.2638
2	0.3260	0.5231	0.5236	0.5236	0.1745	0.5236	0.4031	0.5236	0.1745
3	0.1745	0.1745	0.2462	0.2643	0.5236	0.1745	0.1855	0.5236	0.1814

3.4.3 Plots of the Membership Functions

Using the parameter values from Table 3.2 for centers $c_{i,j}$ and Table 3.3 for dispersions $\sigma_{i,j}$, and applying them in the equation (3.16), we can obtain the plots of the membership functions and observe their behavior. Therefore, the membership function plots for each decision variable (φ, θ, ψ) can be obtained as shown in Figure 3.5.

It can be observed from Figure 3.5 that based on the selection of centers, $c_{i,j}$ and dispersions, $\sigma_{i,j}$, the behavior of the membership function changes. Since the centers are taken around the operating points, the peak of each membership function occurs at their respective operating points. Also, we can see that the dispersions determine the width of each membership function.

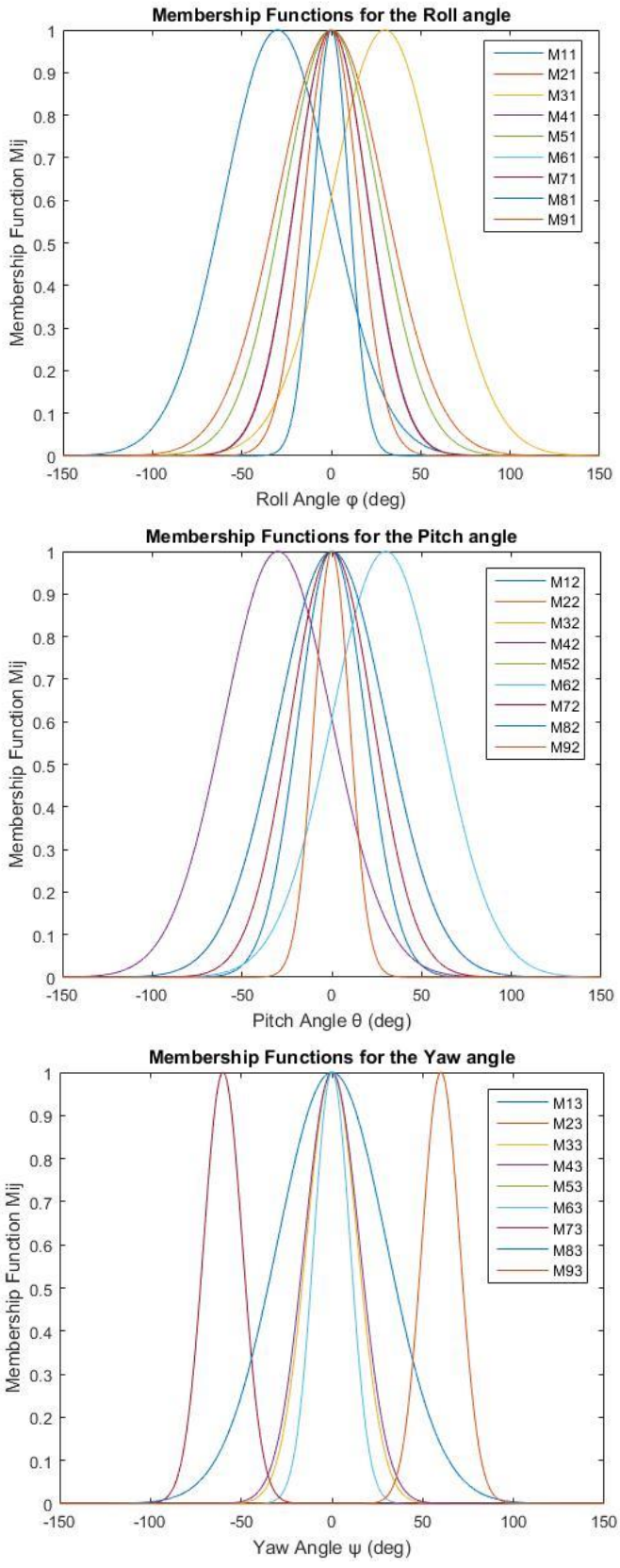

Figure 3.5 Membership Function Plots for *(φ, θ, ψ)*

3.5 Validation of the Takagi-Sugeno Model

To validate the T-S model, we use a Pseudo Random Binary Signal (PRBS) and apply as input to both the non-linear model and the T-S model. Then we simulate the two systems in parallel and the results are compared.

3.5.1 Pseudo Random Binary Signal (PRBS)

The PRBS is a signal obtained by using a pulse rectangular modulated signal whose length is defined randomly. This signal can be approximated to a discrete white noise and it has zero mean and variance close to one. Also, PRBS is rich in frequency and does not move the system away from the operating point. It is commonly used in the identification and validation tasks.

The PRBS is a pseudorandom signal, as it is characterized by a "length sequence in which the variations in the width of the pulses vary randomly, but on a large time space, they are periodic. The period is defined by the length of the sequence.

The amplitude of the PRBS can be very low, but it must be above the residual noise. If the signal to noise ratio is too low, it is necessary to increase the duration of the simulation to get a good estimate of the parameters. A typical value of the amplitude of the PRBS is 0.5% to 5% of the value of the operating point on which it is applied.

$$A_{PRBS} = w_{eq} \pm 0.005 * w_{eq} \; ; \text{ where } w_{eq} = \sqrt{\frac{mg}{4b}} \tag{3.18}$$

The PRBS can be generated in MATLAB Simulink using the predefined function block called Band Limited White Noise. The signals are generated as show in Figure (3.6).

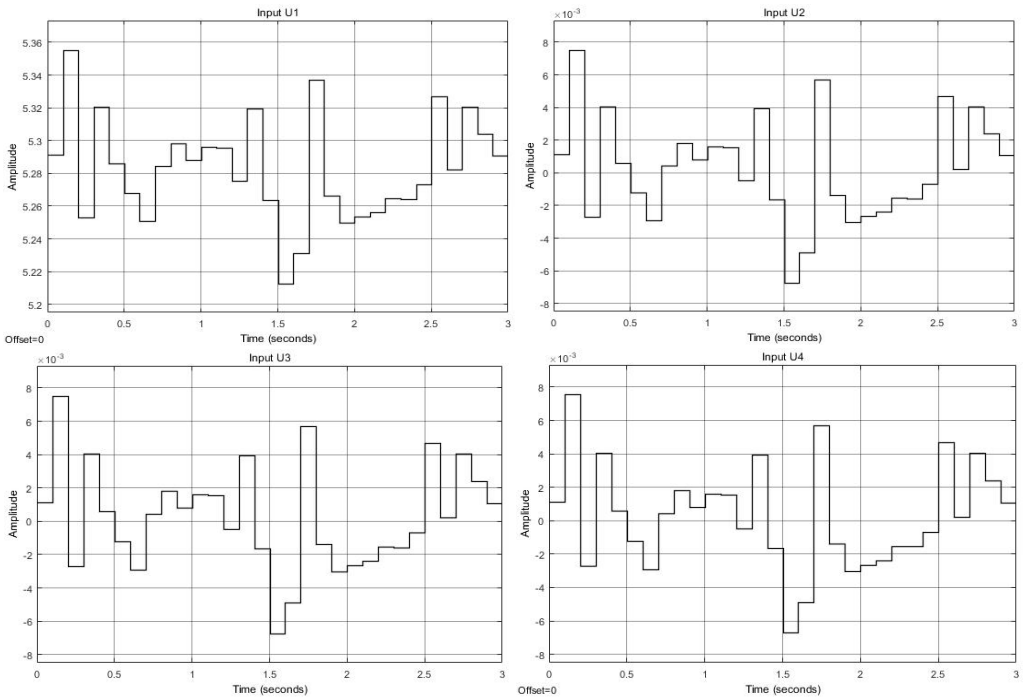

Figure 3.6 PRBS Input Signals

3.5.2 Simulation Results

The parameters of the quadrotor used in the simulations are taken from [6] and given in Table 3.4 as follows:

Table 3.4 Quadrotor Parameters

Parameter	Description	Value	Units
m	Mass of the Quadrotor	0.486	Kg
l	Length of the arm	0.225	m
I_x	Moment of inertia along x-axis	4.856 E-3	Kg.m^2
I_y	Moment of inertia along y-axis	4.856 E-3	Kg.m^2
I_z	Moment of inertia along z-axis	8.801 E-3	Kg.m^2
b	Lift coefficient	2.923 E-5	N/rad/s
d	Drag coefficient	1.12 E-6	N/rad/s

The simulation of the non-linear and the T-S models with PRBS inputs are carried out in MATLAB using all the parameters described. The behavior of all the states with the given inputs are obtained as shown in Figure (3.7).

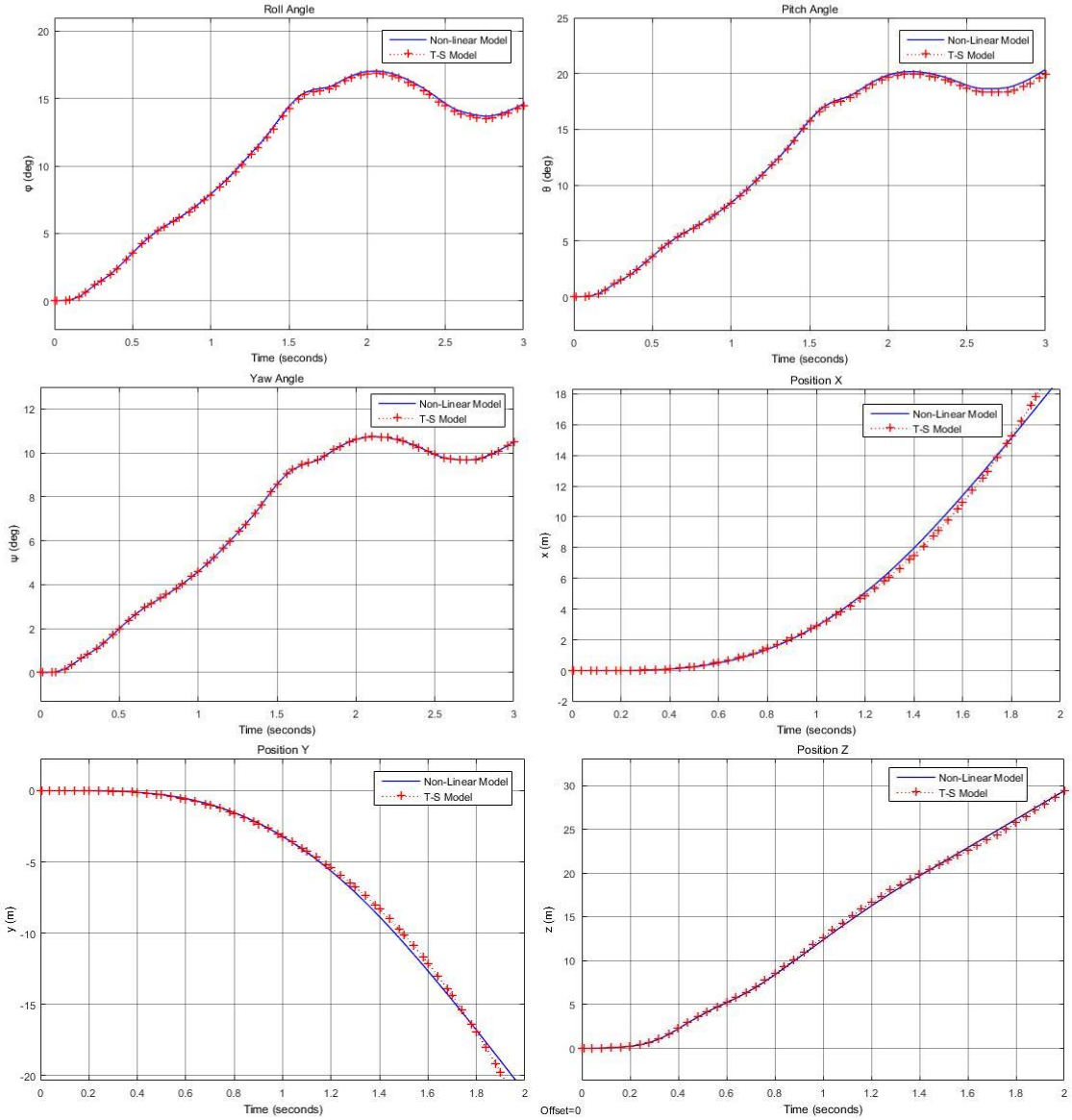

Figure 3.7 States of the Quadrotor Non-linear model vs T-S model

Therefore, it can be observed that the T-S model gives a good approximation of the dynamics of the non-linear quadrotor model within a range of operating points.

3.6 T-S Model of the Quadrotor using Different Operating Points

Now, we define our own operating points to obtain a different T-S model of the quadrotor and similar procedure is applied as shown in the previous section. We define the operating points such that they are uniformly distributed and cover more points in the operating space. They are selected as follows,

- Three models are defined around the roll angle, ϕ=*-30^0, -15, 0^0, 15, 30^0*
- Three models are defined around the pitch angle, θ=*-30^0, -15, 0^0, 15, 30^0*
- Three models are defined around the yaw angle, ψ=*-60^0, -30, 0^0, 30, 60^0*

The selected operating points are converted into radians and are summarized in Table 3.5 as follows,

Table 3.5 New Operating Points

Operating Points	1	2	3	4	5
φ_i	-0.523	-0.261	0	0.261	0.523
$\dot{\varphi}_i$	0.562	0.263	0	0.292	0.585
θ_i	-0.523	-0.261	0	0.261	0.523
$\dot{\theta}_i$	0.527	0.263	0	0.292	0.585
ψ_i	-1.047	-0.523	0	0.523	1.047
$\dot{\psi}_i$	0.942	0.471	0	0.428	0.856

Using these operating points, the parameters of the membership functions are obtained. The centers of the membership functions are defined in Table 3.6 as follows,

Table 3.6 Centers $c_{i,j}$ of the new membership functions

j \ *i*	*1*	*2*	*3*	*4*	*5*
1	-0.523	-0.261	0	0.261	0.523
2	-0.523	-0.261	0	0.261	0.523
3	-1.047	-0.523	0	0.523	1.047

Now, after doing some trial and error with various values of dispersions, the most optimal value of dispersion is taken as $\sigma_{i,j}=0.2$ for all membership functions. Using these centers and dispersions the membership functions are plotted for the Roll, Pitch and Yaw angles as shown in Figure 3.8.

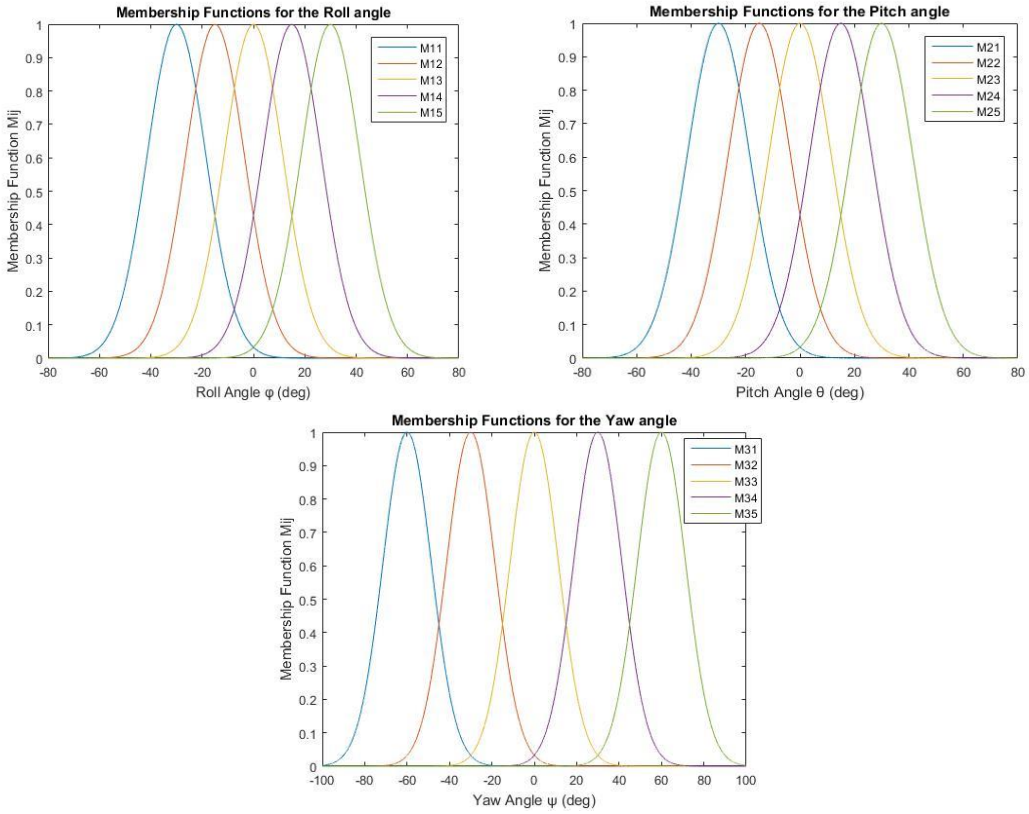

Figure 3.8 New Membership Function Plots for (φ, θ, ψ)

3.6.1 Validation of the new T-S model of the Quadrotor

The simulation of the nonlinear model and the new T-S model of the quadrotor is carried out by using the same PRBS inputs from Figure 3.6.The simulation results of the states are shown in Figure 3.9 as follows,

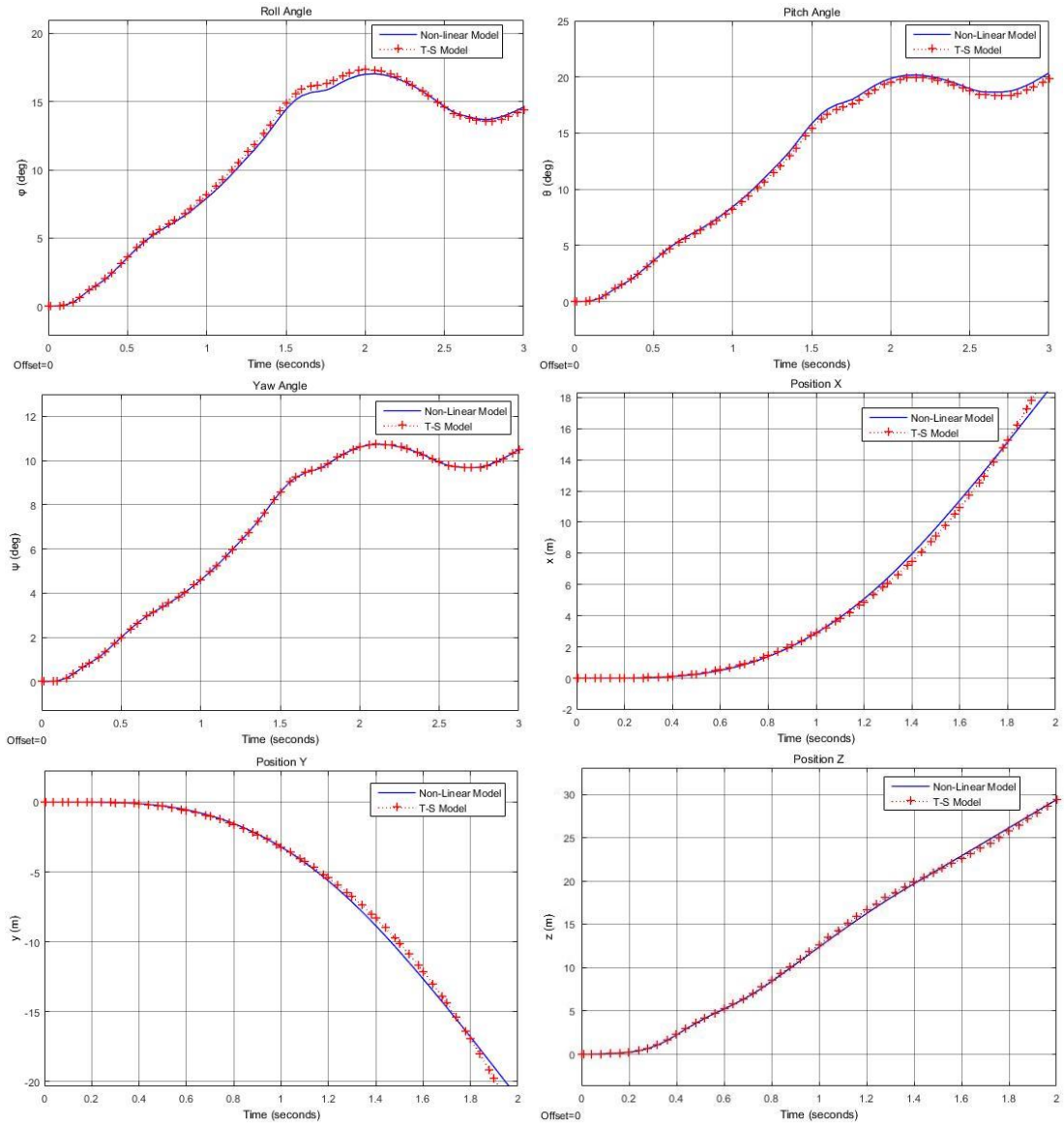

Figure 3.9 States of the Quadrotor Non-linear model vs new T-S model

Therefore, it can be observed that the new T-S model also gives a very good approximation of the dynamics of the non-linear quadrotor model within the range of operating points.

3.6 Conclusion

In this chapter, the dynamics and the operation of the quadrotor was explained. Then the non-linear mathematical model was formulated and the state equations were obtained. This model showed the non-linear, multivariable and under actuated behavior of the quadrotor which makes it relatively difficult to control.

Then the linearization of the model was done using Taylor series linearization method and nine linearized models were generated over a set of operating points that were taken from [5]. These individual models were interpolated using Gaussian membership functions and a Takagi-Sugeno model was obtained. Then simulations were carried out to compare the non-linear and the T-S models by giving PRBS input. The results confirmed the similarity of the T-S model with the non-linear system.

Then, we defined our own operating points and a new set of local models were obtained. The same strategy was applied to the local models as before and the new T-S model of the quadrotor was obtained. The validation of this new model was carried out and the results were compared with the nonlinear model of the quadrotor. The new T-S model also provides a good approximation of the system.

CHAPTER 4

STATE-FEEDBACK LQR CONTROL OF THE QUADROTOR

4.1 Introduction

The quadrotor is a rotary wing air vehicle. The difficulty of control of the quadrotor is mainly due to its complex dynamics, non-linearity, multi-variable nature and most of all the underactuated states. Thus, the problem of controlling a quadrotor has received a lot of attention in research in the last decade. Many techniques have been applied to successfully control the quadrotor and can be found in the literature which have been discussed earlier in chapter 2. In our work, we aim to use the state-feedback controller and optimize it using the Linear Quadratic Regulator (LQR) technique because of its reliability and efficiency.

In this chapter, we first study about the theory State-Feedback control systems. Then, the state-feedback controller for our system is defined and the control law is developed. This is followed by LQR optimization to obtain the state-feedback gains. Then, simulations are performed to control the T-S and the Nonlinear models of the quadrotor using the developed controller for both the operating points discussed in chapter 3 and the tracking of a desired trajectory is done.

4.2 State-Feedback Control Design

4.2.1 Definition

State-feedback is a control technique in which the closed-loop poles of a system are placed in pre-defined desired locations. The control law is defined based on an error function which is a function of the desired states and the actual states. This method is widely used in MIMO systems because of its simplicity. Consider a plant with state-space representation as follows,

$$\begin{aligned} \dot{x}(t) &= Ax(t) + Bu(t) \\ \dot{y}(t) &= Cx(t) + Du(t) \end{aligned} \tag{4.1}$$

We define the control law *u(t)* as follows,

$$u(t) = r(t) - Kx(t) \tag{4.2}$$

where *r(t)* is a function of the desired states and *K* is the feedback gain which is a real constant. Substituting (4.2) in (4.1), we get the closed loop system as follows,

$$\begin{aligned} \dot{x}(t) &= (A - BK)x(t) + Br(t) \\ \dot{y}(t) &= Cx(t) + Du(t) \end{aligned} \tag{4.3}$$

The structure of the state feedback control system is shown in Figure 4.1 as follows,

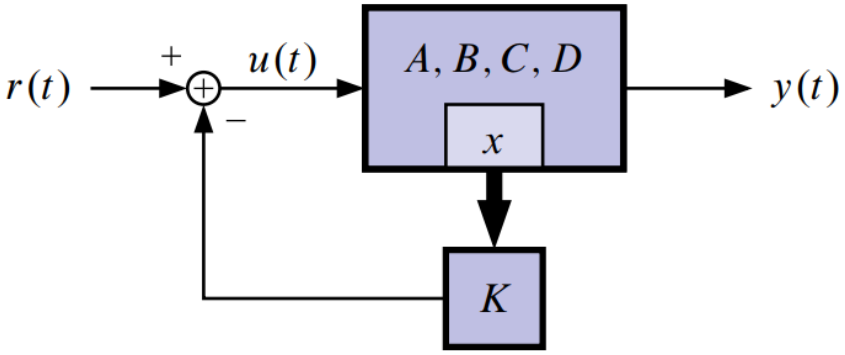

Figure 4.1 State-Feedback System

4.2.2 Parallel Distributed Compensation (PDC)

In this work, since we use the Takagi-Sugeno system, the Parallel Distributed Compensation (PDC) technique is used to develop the control law for multi-models. In PDC, the control design utilizes the multiple-model approach to mirror the structure of the T-S model. Consider the T-S model that has been discussed earlier,

$$\dot{x}_m(t) = \sum_{i=1}^{r} \mu_i\big(\xi(t)\big)\big(A_i x_m(t) + B_i u(t)\big)$$
$$\dot{y}_m(t) = C x_m(t) \tag{4.4}$$

Now, we define the control law *u(t)* as follows,

$$u(t) = r(t) - \sum_{i=1}^{r} \mu_i\big(\xi(t)\big)\big(K_i x_m(t)\big) \tag{4.5}$$

where *r(t)* is the desired states function and K_i is the state-feedback gain of the i^{th} model. Thus, the closed loop system becomes,

$$\dot{x}_m(t) = \sum_{i=1}^{r}\sum_{j=1}^{r} \mu_i\big(\xi(t)\big)\,\mu_j\big(\xi(t)\big)\big((A_i - B_iK_i)x_m(t) + B_ir(t)\big) \tag{4.6}$$

It should be noted that the parameters of the controller such as A_i, B_i and activation functions are respectively same as the parameters of T-S models.

4.3 LQR Optimization

Quadrotor is a MIMO system which cannot be controlled easily by simple pole placement techniques. Therefore, optimization techniques are essential to stabilize the system reach the desired states. The solutions of optimal control provide an automated design technique in which only the figure of merit is required [10]. The most widely used method is the Linear Quadratic Regulator (LQR) optimization because of its simplicity and efficiency. In this work, we use the LQR technique to obtain the state feedback gains of the controller described in the last section.

Consider a general plant with the state-space equations and control law as follows,

$$\dot{x}(t) = Ax(t) + Bu(t)$$

$$\dot{y}(t) = Cx(t) + Du(t) \tag{4.7}$$

$$u(t) = r(t) - Kx(t)$$

Now, to obtain the gain *K*, we define a cost function such that it is the sum of the penalties of the states and the input. These penalties represent how far the system is from the desired response. This can be represented as,

$$J = \int_0^\infty \left(x^T(t)Qx(t) + u^T(t)Ru(t)\right)dt \tag{4.8}$$

This cost function *J* is now minimized to reduce the penalties of the controller. This implies *Q* and *R*, are both selected as positive definite matrices. The gain *K* is calculated as,

$$K = R^{-1}B^T P \tag{4.9}$$

where *P* is obtained by solving the Algebraic Riccati Equation (A.R.E),

$$A^T P + PA - PBR^{-1}B^T P + Q = 0 \tag{4.10}$$

Now, the same procedure can be applied to our T-S state feedback controller and all the gains can be calculated as,

$$K_i = R^{-1}B_i^T P$$
$$A_i^T P + PA_i - PB_i R^{-1}B_i^T P + Q = 0 \tag{4.11}$$

where $i = 1,2,\dots,r$. r being the number of T-S models.

4.4 Simulation Results

The controller designed above is applied on both the T-S model and the nonlinear model of the Quadrotor and simulations are performed in MATLAB. The values of the parameters of the quadrotor are taken the same as mention in Table (3.4). The state-feedback gains are generated using the inbuilt MATLAB tool for LQR which has a syntax of the form,

$$K_i = lqr(A_i, B_i, Q, R) \tag{4.12}$$

4.4.1 Simulation of the T-S Model of the Quadrotor

The general control schematic applied on the T-S model of the quadrotor system can be represented in Figure (4.2) as follows,

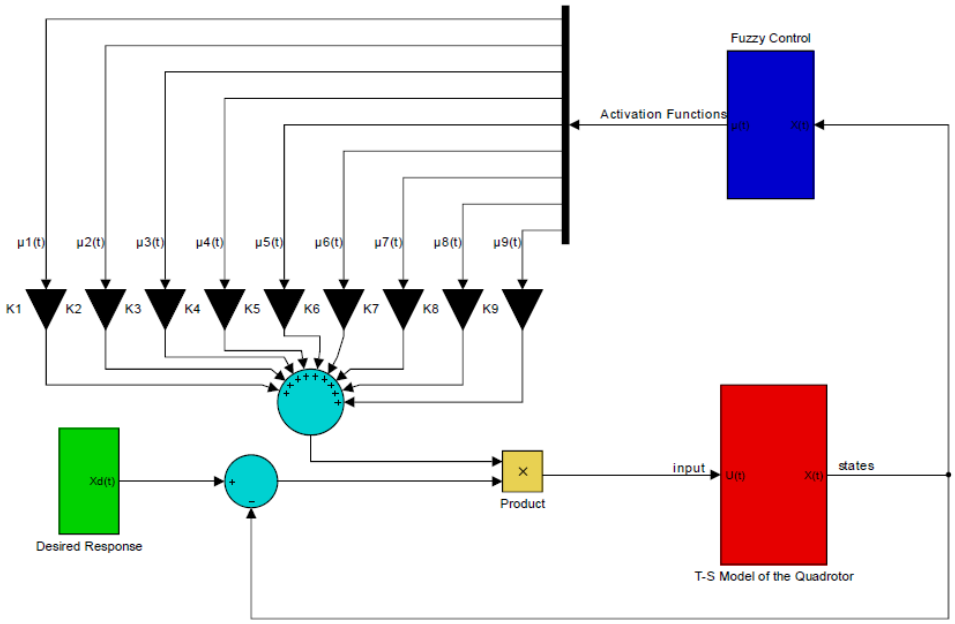

Figure 4.2 Block Diagram of the Control System for the T-S model of the Quadrotor

a) Step Response

The desired states are selected such that the positions are $x_d = 3\ m, y_d = 4\ m, z_d = 5\ m$ and the attitude corresponds to $\varphi_d = 0^0,\ \theta_d = 0^0,\ \psi_d = 60^0$. The initial conditions of the states are set to zero. The responses are obtained as shown in Figure (4.3).

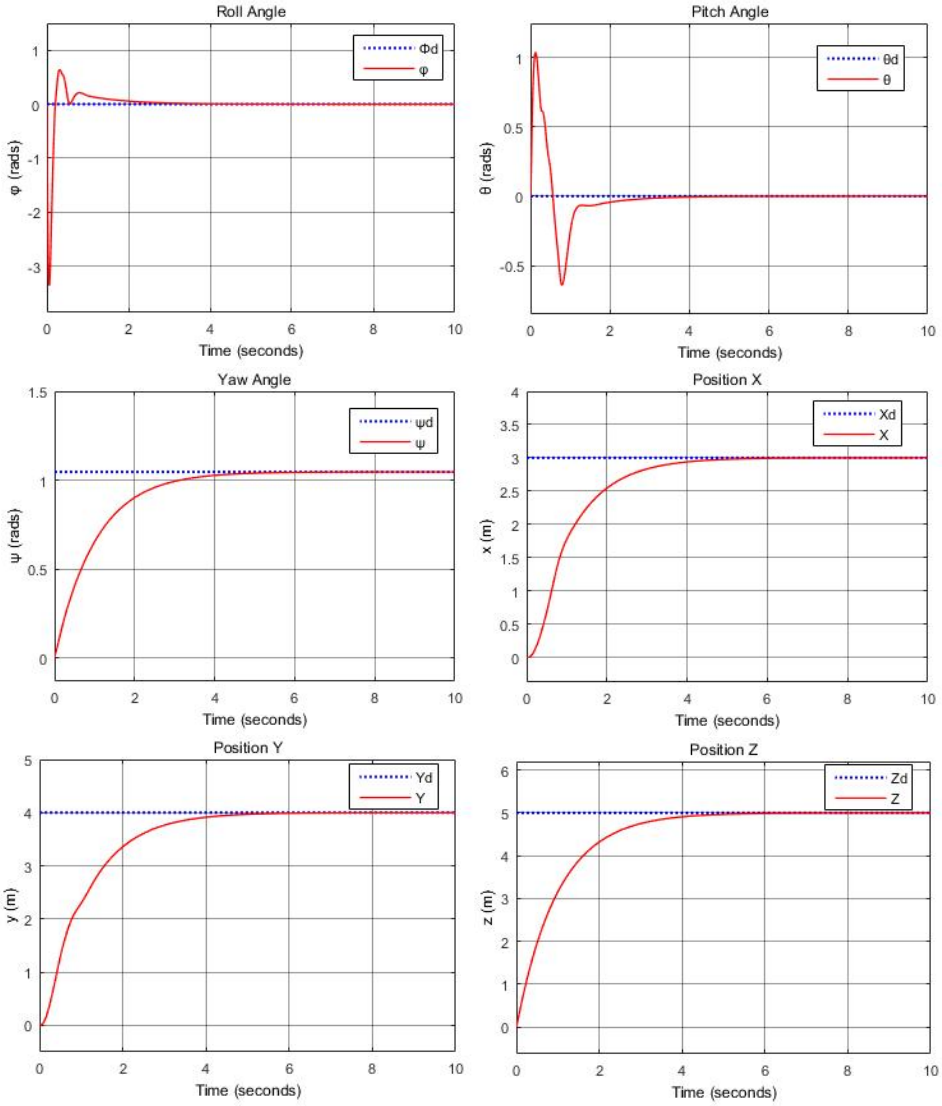

Figure 4.3 Step Response of the states of the T-S model of the Quadrotor

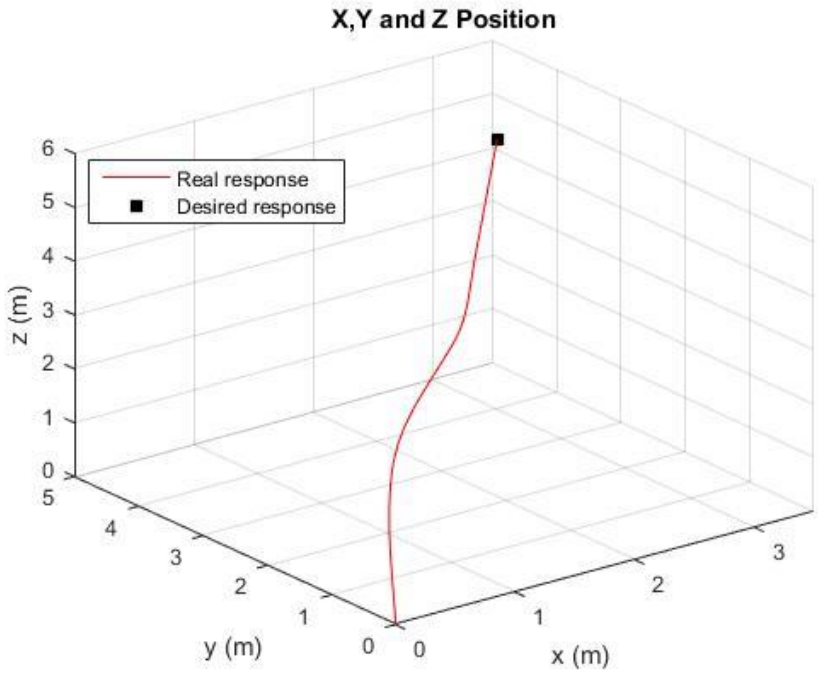

Figure 4.4 Step Response of the position of the T-S model of the Quadrotor in 3D view

Figure (4.4) shows the step response of the position trajectory of the quadrotor in 3D view. Therefore, it can be observed that the controller provides smooth performance of the system and all the states reach the desired step in less than 5 secs.

b) Sinusoidal Response

Now to further validate the controller, the desired states are taken in the form of sinusoidal signals. The signals are of the form $r(t) = Asin(wt + \phi)$. The sine response of the states can be seen in Figure (4.5) as follows,

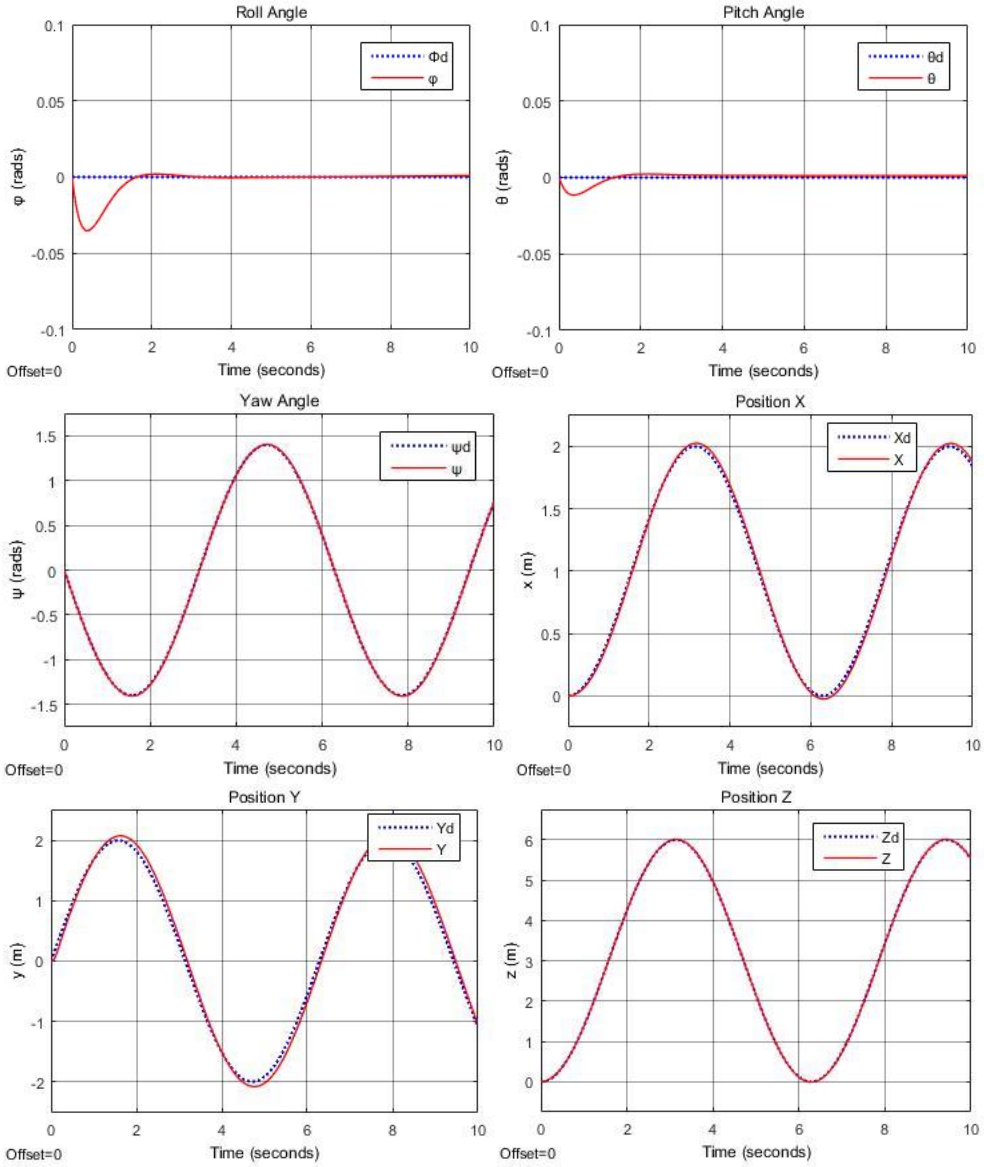

Figure 4.5 Sine Response of the states of the T-S model of the Quadrotor

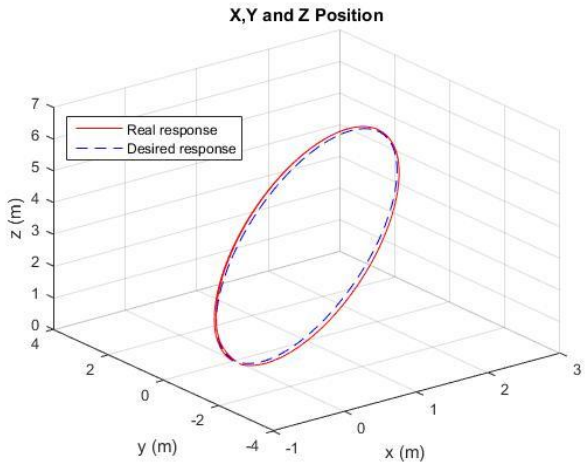

Figure 4.6 Sine response of the position of the T-S model of the Quadrotor in 3D view

Figure (4.6) shows the sine response of the position trajectory of the quadrotor in 3D view. Therefore, it can be observed that the controller provides smooth tracking for the sinusoidal reference signal.

4.4.2 Simulation of the Nonlinear Model of the Quadrotor

Now, to validate our T-S model, same controller is applied on the nonlinear model of the Quadrotor. Both step and sinusoidal reference signals described previously are taken to test the performance. The general control schematic can be seen in Figure (4.7)

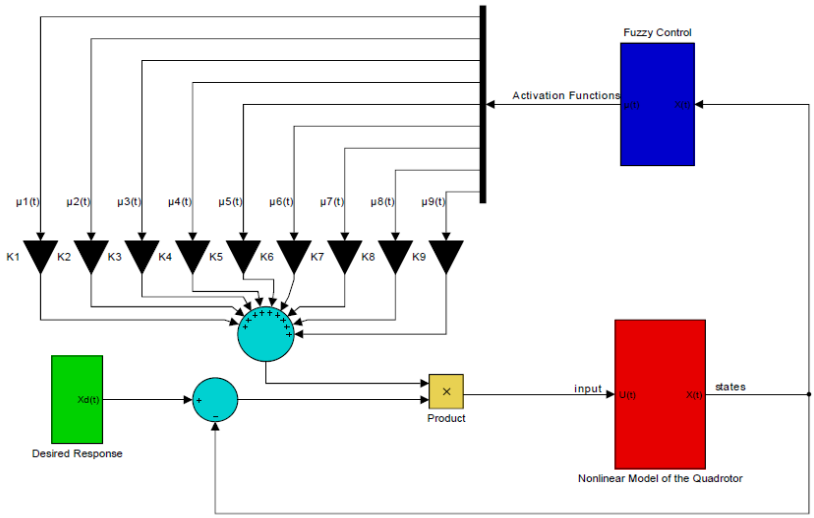

Figure 4.7 Block Diagram of the Control System for the nonlinear model of the Quadrotor

a) Step Response

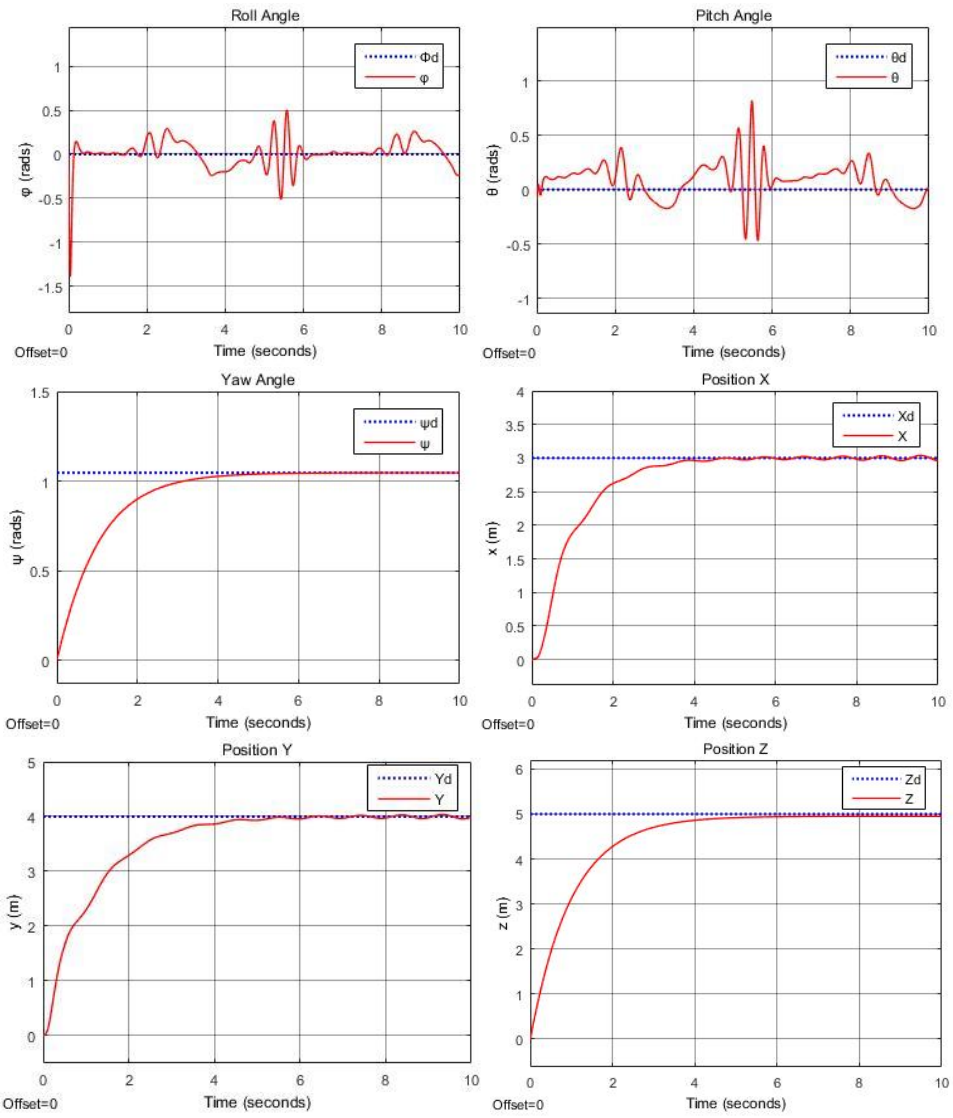

Figure 4.8 Step Response of the states of the Nonlinear model of the Quadrotor

From Figure (4.8), it can be observed that there are few ripples in the responses because of the nonlinearity and approximation but the overall tracking is smooth.

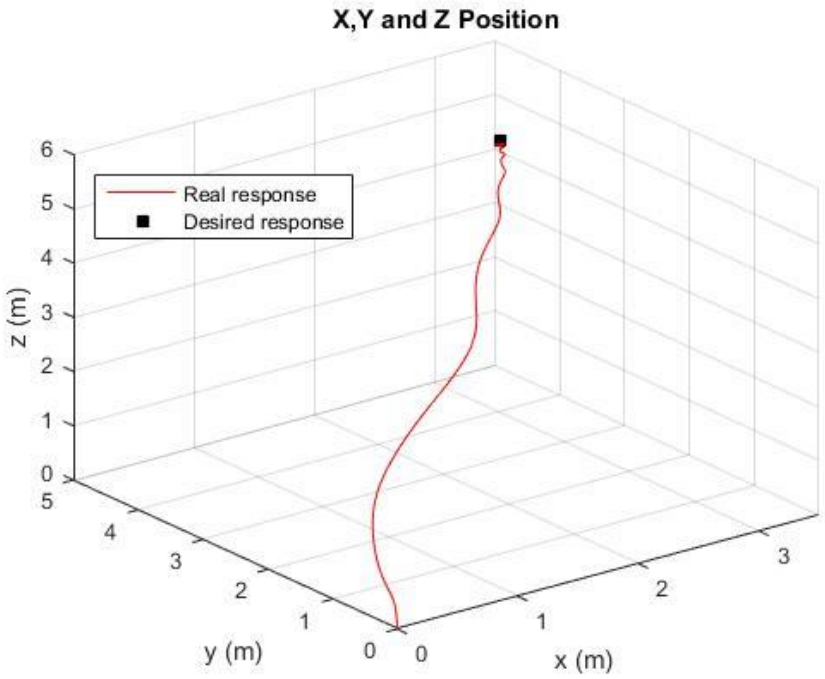

Figure 4.9 Step response of the position of the Nonlinear model of the Quadrotor in 3D view

Figure (4.9) shows the step response of the position trajectory of the nonlinear model of the quadrotor in 3D view. Therefore, it can be observed that the controller provides smooth performance of the system and all the states reach the desired step in less than 5 secs.

b) Sinusoidal Response

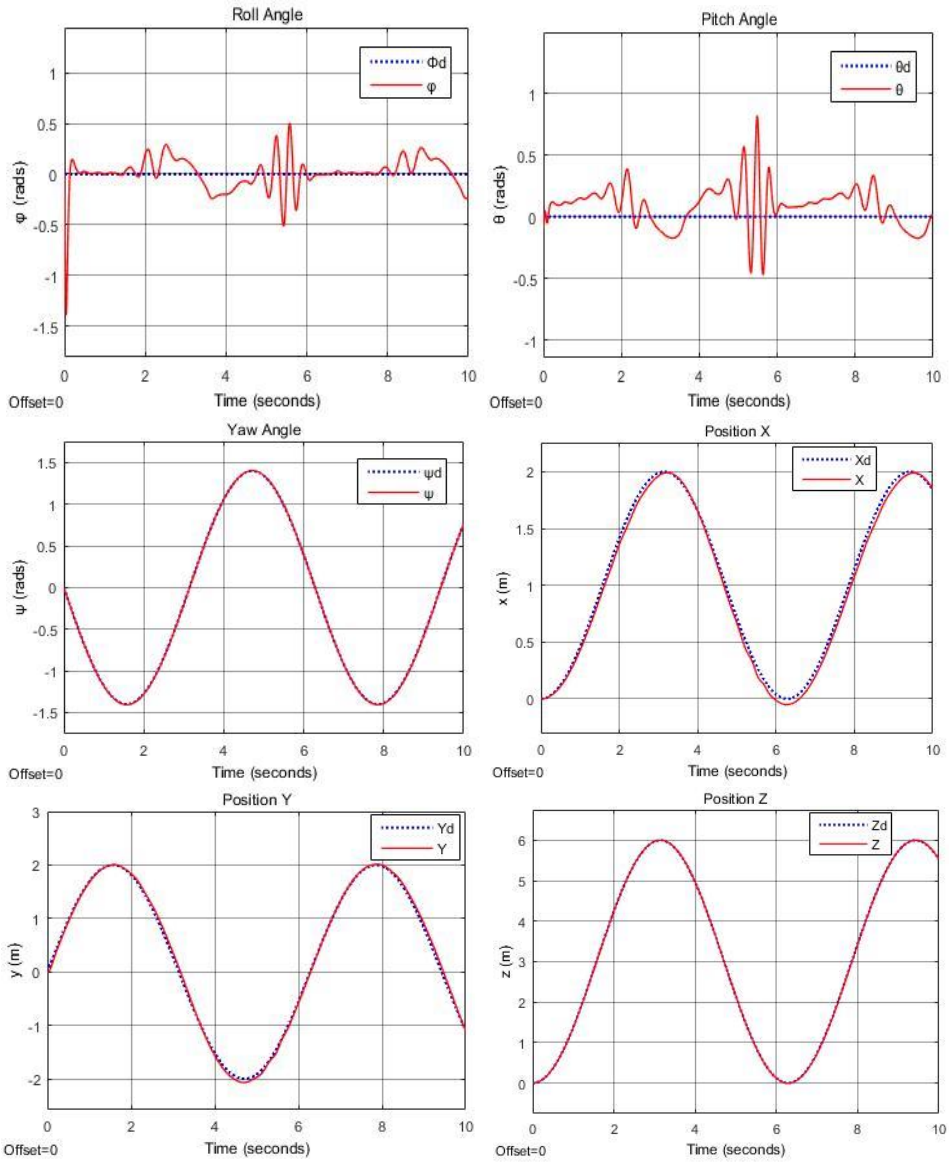

Figure 4.10 Sine Response of the states of the Nonlinear model of the Quadrotor

From Figure (4.10), it can be observed that there are few ripples in the responses because of the nonlinearity and approximation but the overall tracking is smooth.

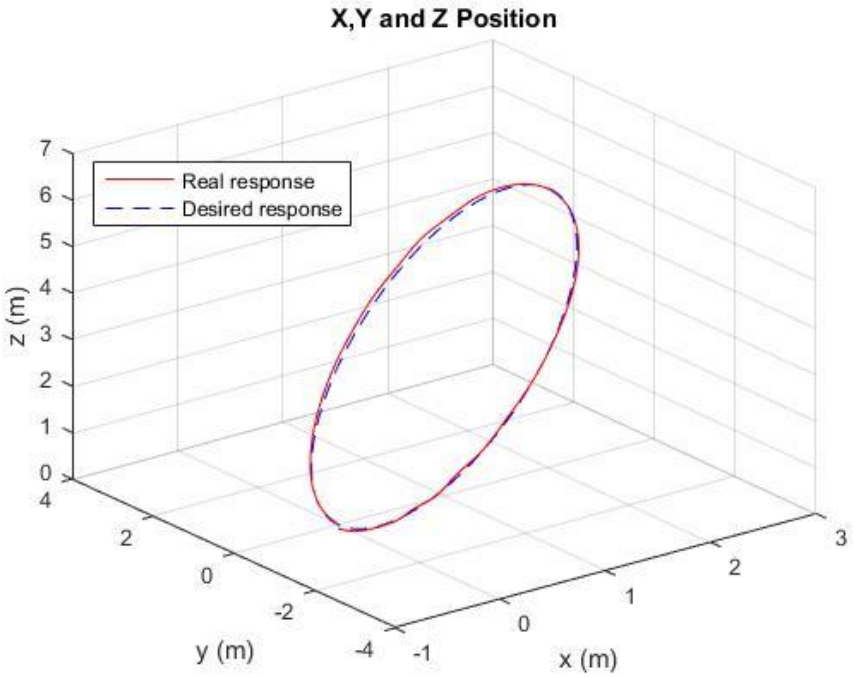

Figure 4.11 Sine response of the position of the Nonlinear model of the quadrotor in 3D view

Figure (4.11) shows the sine response of the position trajectory of the nonlinear model of the quadrotor in 3D view. Therefore, it can be observed that the controller provides smooth tracking of the sinusoidal reference signal for the nonlinear model of the quadrotor too.

4.4.3 Comparison of the T-S and Nonlinear Models

Now, Both the T-S and the nonlinear models are simulated parallelly at the same time and the responses are obtained together.

a) Step Response

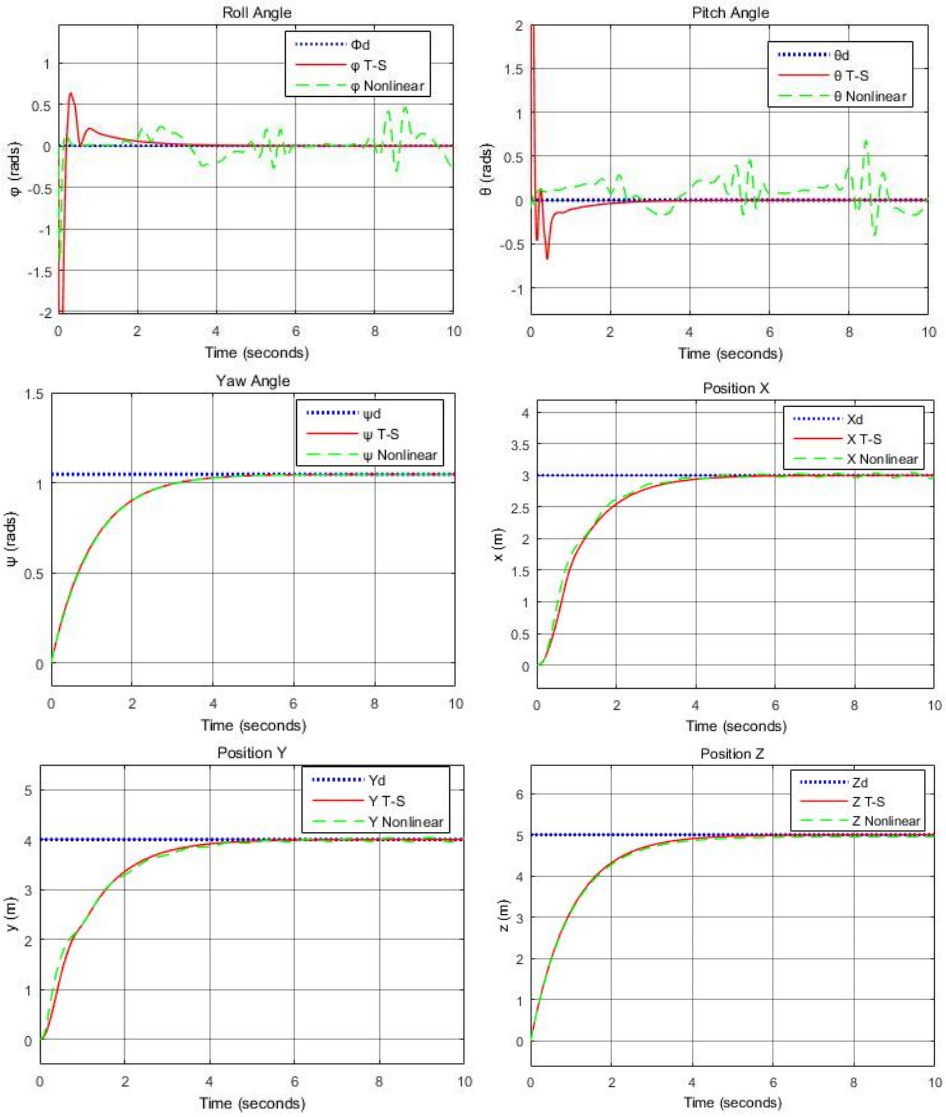

Figure 4.12 Step Response of the states of both the T-S and the Nonlinear models of the Quadrotor

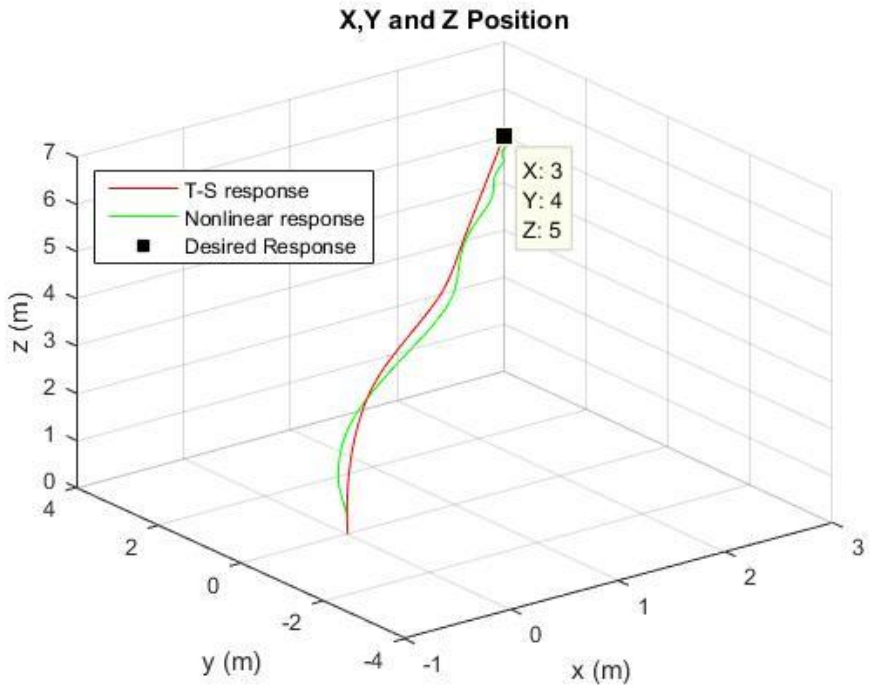

Figure 4.13 Step Response of the position of both the T-S and the Nonlinear models of the Quadrotor in 3D view

c) Sine Response

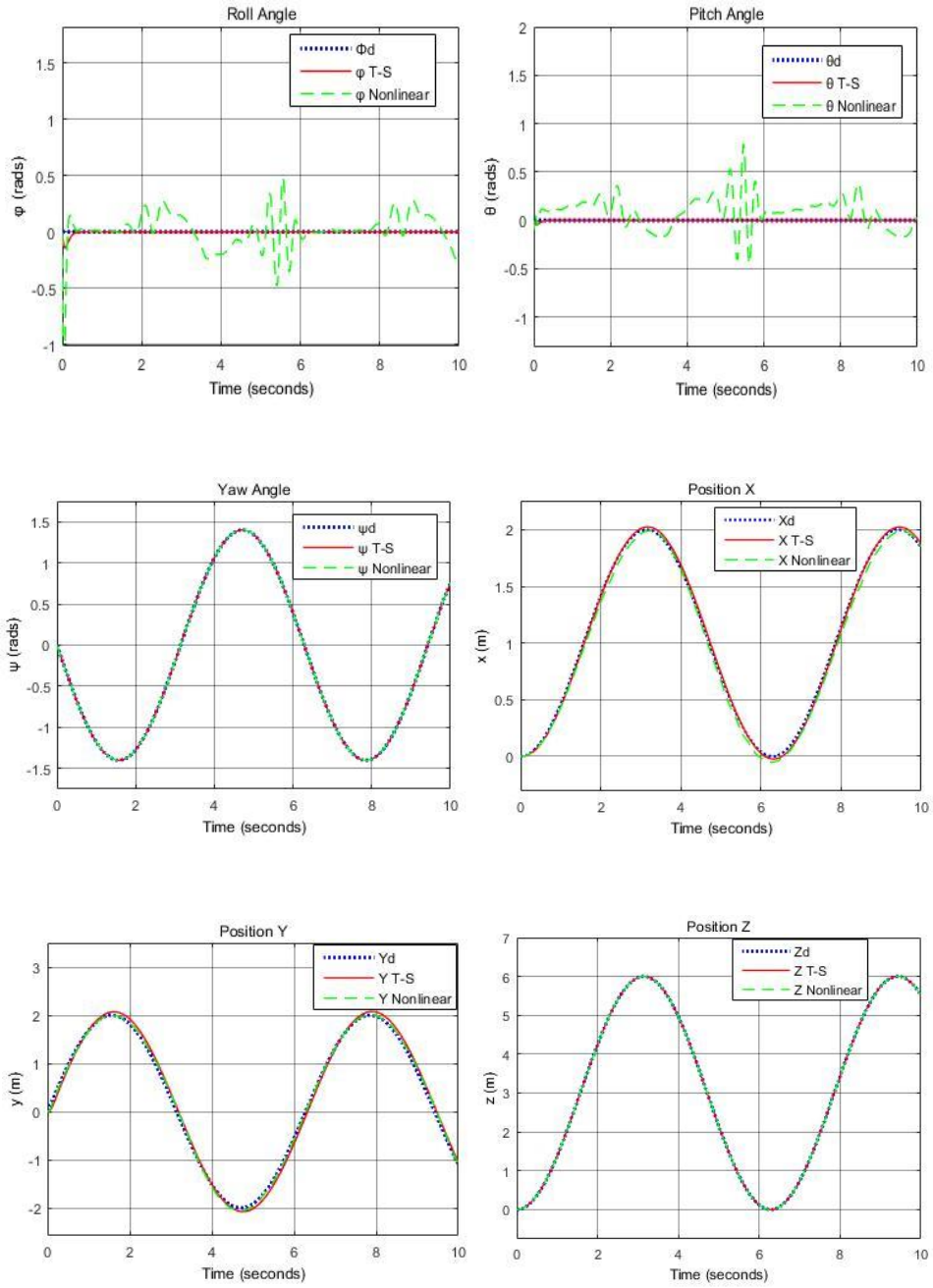

Figure 4.14 Sine Response of the states of both the T-S and the Nonlinear models of the Quadrotor

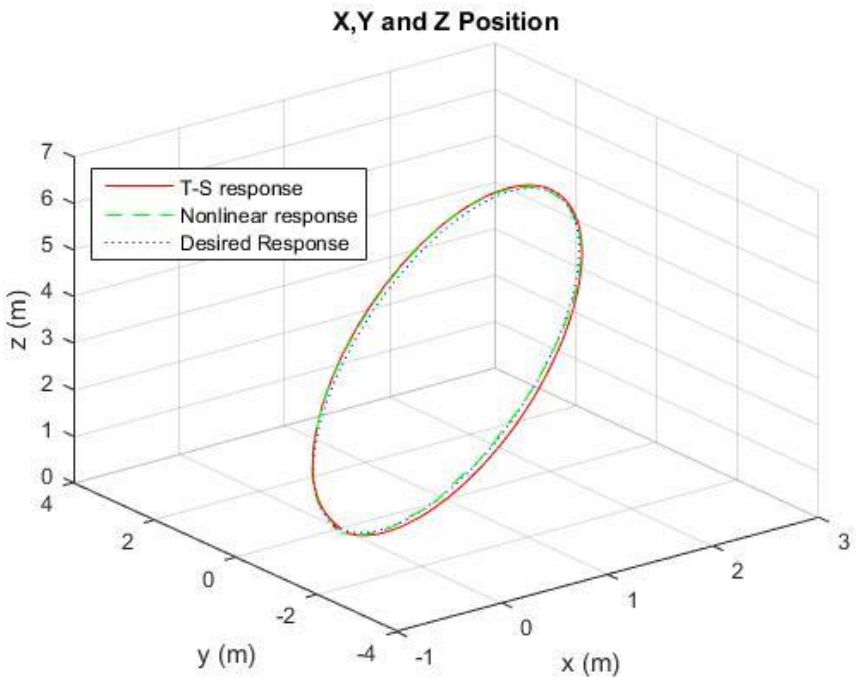

Figure 4.15 Sine Response of the position of both the T-S and the Nonlinear models in 3D view

Therefore, it can be concluded that the LQR controller designed gives good performance of the reference signals on both the T-S model and the Nonlinear model of the Quadrotor. Although there are small ripples in the nonlinear system, the overall tracking is smooth.

4.4.4 Simulation of the Nonlinear Model of the Quadrotor with New Operating points

Now, we consider the case when the T-S model of the quadrotor is taken with the new operating points as discussed in chapter 3. Because of the change in the operating points, the A_i and B_i matrices are different which results in different LQR gains, K_i. Therefore, using these gains, the controller is implemented to the nonlinear model of the quadrotor and simulation is done for both the step and sine responses. The results obtained are shown as follows.

a) Step Response

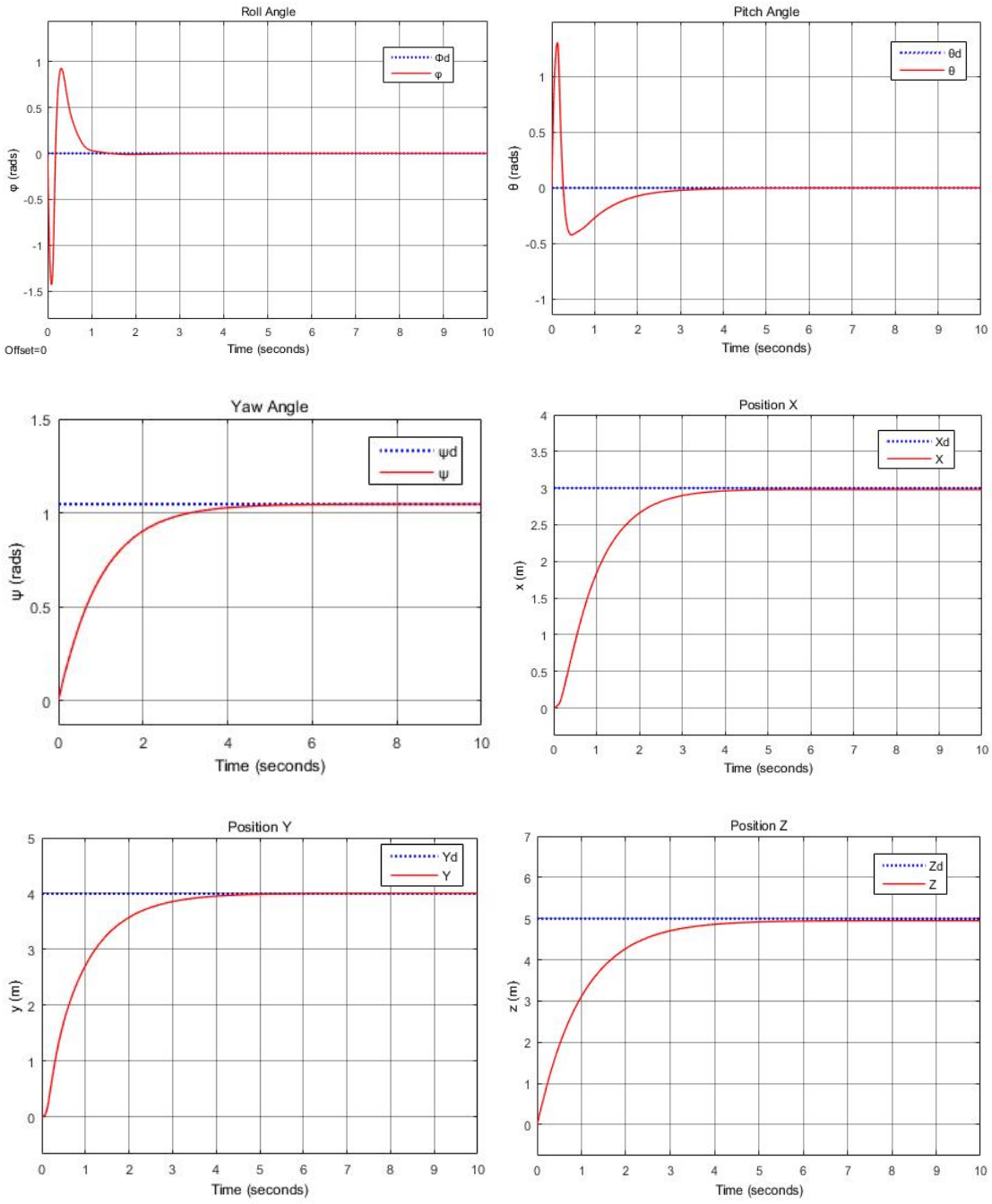

Figure 4.16 Step Response of the states of the Nonlinear model of the Quadrotor with new Operating Points

From Figure (4.16), it can be observed that the ripples have been reduced a lot when compared to the original operating points. Therefore, it provides a smoother response.

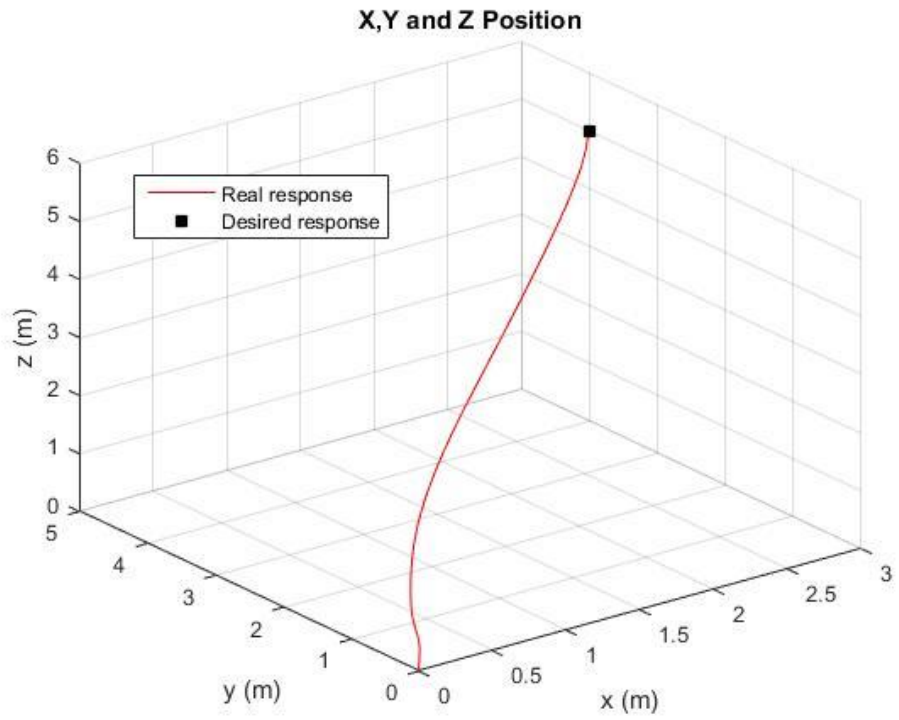

Figure 4.17 Step Response of the position of the Nonlinear model of the Quadrotor with new Operating Points in 3D view

Figure (4.17) shows the step response of the position trajectory of the nonlinear model of the quadrotor with new operating points in 3D view. Therefore, it can be observed that the controller with the new operating points provides a smoother tracking of the step reference signal for the nonlinear model of the quadrotor.

d) Sine Response

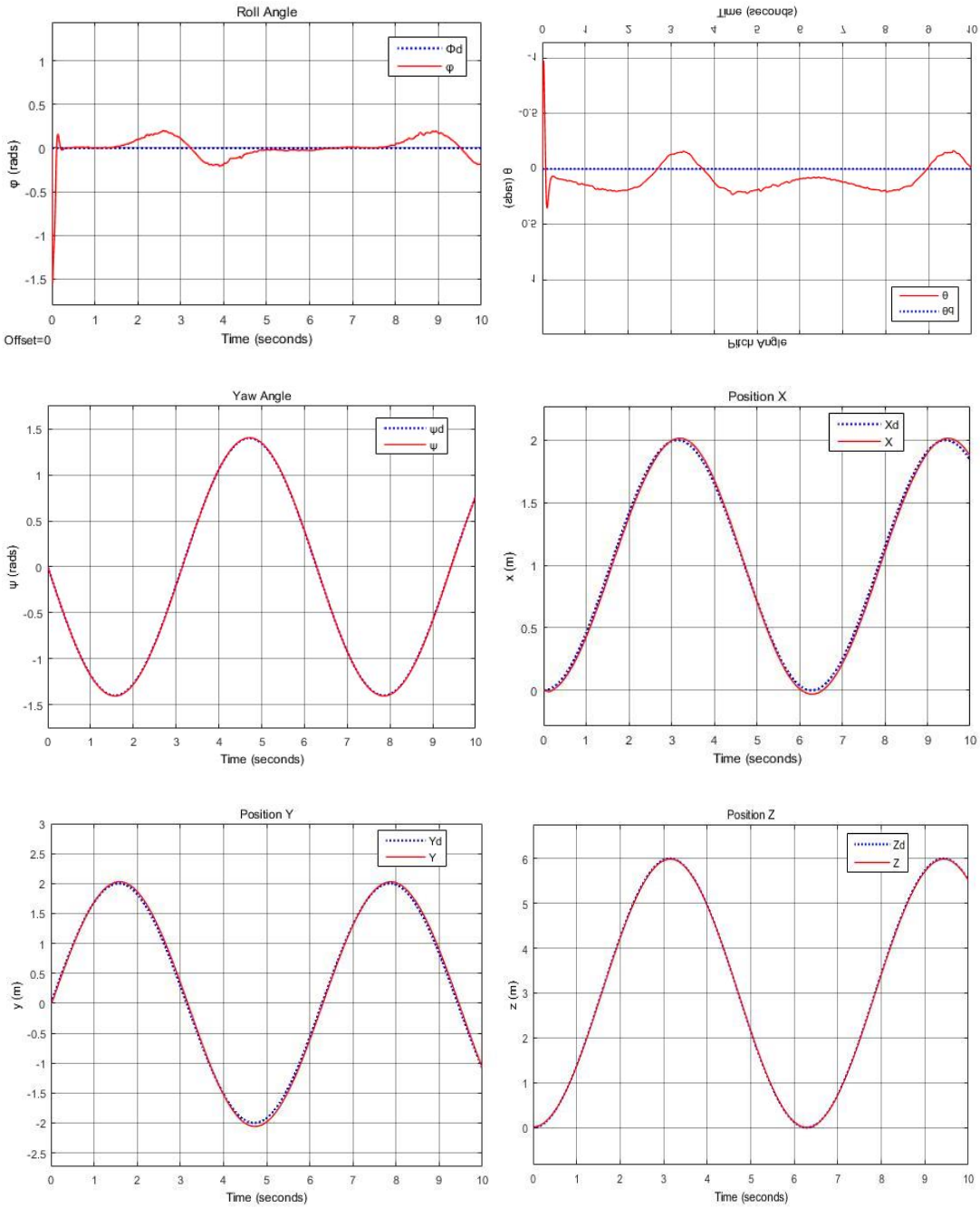

Figure 4.18 Sine Response of the states of the Nonlinear model of the Quadrotor with new Operating Points

From Figure (4.18), it can be observed that the ripples have been reduced a lot when compared to the original operating points. Therefore, it provides a smoother sine response.

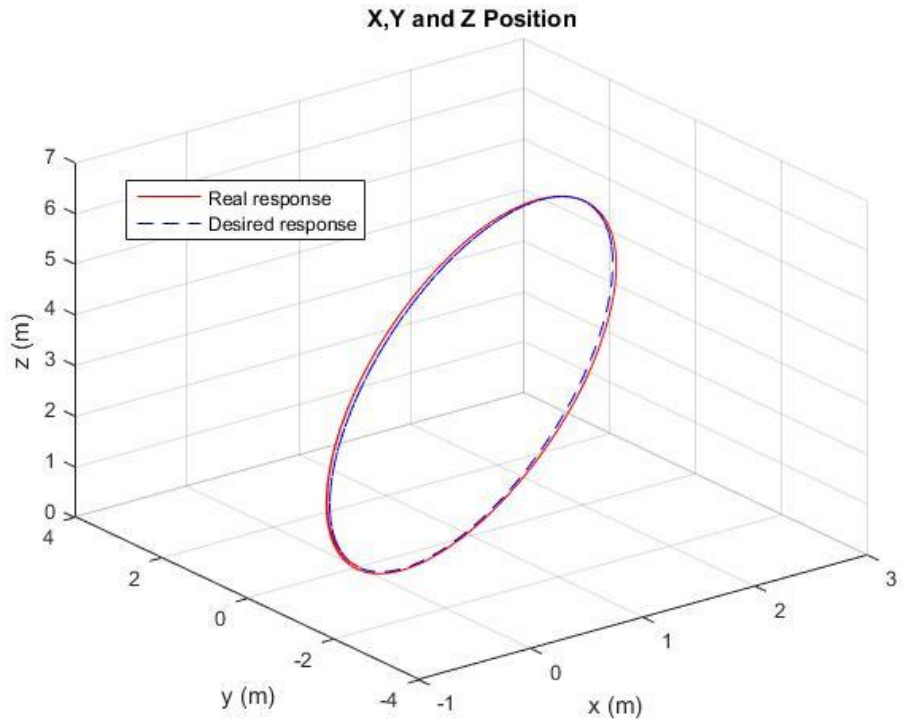

Figure 4.19 Sine Response of the position of the Nonlinear model of the Quadrotor with new Operating Points in 3D view

Figure (4.19) shows the sine response of the position trajectory of the nonlinear model of the quadrotor with new operating points in 3D view. Therefore, it can be observed that the controller with the new operating points provides a smoother tracking of the sine reference signal too for the nonlinear model of the quadrotor.

CHAPTER 5

FORMATION CONTROL OF A FLEET OF UAVs

5.1 Introduction

In recent years, the application of groups of UAVs to achieve tasks cooperatively together has been widely used. This is because of the advantages that are obtained from using multiple vehicles instead of using a more complex single vehicle. If a task outcome of a team of multiple unmanned vehicles is compared with that of an individual vehicle, one can realize that the multiple vehicles overall performance can develop mission allocation, performance, the required time, and the system efficiency and safety.

In this chapter, we first study about the theory of formation control, in particular about the leader-follower based approach. The leader is set to track a desired reference trajectory and the followers track the trajectory of the leader with some offsets. Then to calculate these offsets, potential fields technique is implemented and the overall architecture of the formation is obtained. This is followed by the simulation results in which we observe the behavior of the system for various cases.

5.2 Leader-Follower Formation Scheme

As the name suggests, this strategy consists of a leader quadrotor and several follower quadrotors. The leader is given a desired reference path which it tracks using the nonlinear controller. Simultaneously, the followers are set to track the path of the leader but with some offsets [33]. These offsets determine the shape of the formation control of the quadrotors.

Consider a system consisting of one leader quadrotor and *N* follower quadrotors. It is assumed that all these quadrotors have identical models and controllers as discussed in chapter 4. The T-S model for each quadrotor can be represented as,

$$\dot{x}_j(t) = \sum_{i=1}^{r} \mu_i\big(\xi(t)\big)\Big(A_i x_j(t) + B_i u_j(t)\Big)$$
$$\dot{y}_j(t) = C x_j(t) \tag{5.1}$$

where *x*, *y* and *u* are the state, output and input vectors respectively for each quadrotor. *A* and *B* are the state and input matrices, *ξ(t)* is the Fuzzy decision variable. $\mu_i\big(\xi(t)\big)$ is the normalized activation function and *r* being the number of local linear models which are same for all quadrotors. *j=0,1, 2,…,N* are the number of quadrotors.

Now, the state feedback LQR controllers for the quadrotors are given as,

$$u_j(t) = r_j(t) - \sum_{i=1}^{r} \mu_i\big(\xi(t)\big)\Big(K_i x_j(t)\Big) \qquad j = 0,1,2,\dots,N \tag{5.2}$$

Where *r* is the reference trajectory for each quadrotor and *K* are the state feedback gains that are calculated using LQR.

Now, to obtain the leader-follower formation, the reference signal for the leader $r_0(t)$ is selected as per our desired required response. But the reference signals for the followers, $r_j(t)$, $j=1,2,\ldots,N$ are defined as the trajectory of the leader with some offsets. This can be represented as,

$$r_j(t) = x_0(t) + x_{j_{OFF}} \tag{5.3}$$

where $x_0(t)$ is the current state vector of the leader and $x_{j_{OFF}}$ is the offset for all the states of the j^{th} follower with respect to the leader. Therefore, the control law for each follower becomes,

$$u_j(t) = x_0(t) + x_{j_{OFF}} - \sum_{i=1}^{r} \mu_i\big(\xi(t)\big)\Big(K_i x_j(t)\Big) \qquad j = 1,2,\ldots,N \tag{5.4}$$

Therefore, the closed loop system for each follower becomes,

$$\dot{x}_j(t) = \sum_{i=1}^{r}\sum_{k=1}^{r} \mu_i\big(\xi(t)\big)\,\mu_k\big(\xi(t)\big)\big((A_i - B_i K_i)x_j(t) + B_i(x_0(t) + x_{j_{OFF}})\big) \tag{5.5}$$

It should be noted that all the parameters of the Fuzzy functions and the states are identical for all the quadrotors. Also, in practice, the control of only the positions *(x, y, z)* is performed and the rest of the states of the quadrotors are set to track the leader. This means that the offsets are present only for the position states of the reference signals.

5.3 Potential Fields Technique for Shape Formation

5.3.1 Definition

To obtain desired shape formations, the offsets described above are calculated using a method called potential fields technique. Consider a set of quadrotors as shown in figure 5.1.

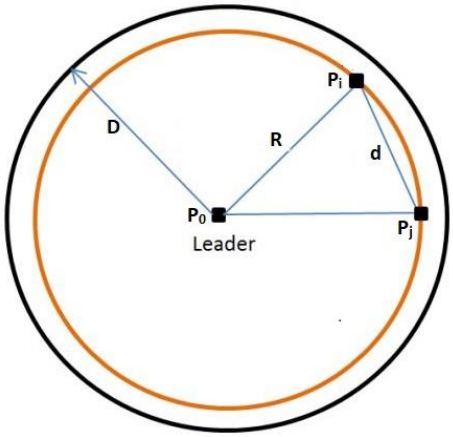

Figure 5.1 General Formation Structure

As shown in the figure, the position the leader is represented by P_0 and that of the followers by P_i and P_j. D is the sensing range of each quadrotor and is represented as a circle. The followers are set to form a shape of a polygon on a circle with radius R with leader located at the center of the circle. Also, to avoid collision, each adjacent follower must be a distance of $d \leq D$ apart from each other. Using geometry, the relation between R and d can be obtained as,

$$d = 2Rsin\left(\frac{\pi}{n}\right) \tag{5.6}$$

where *n* is the number followers.

5.3.2 Control Design

Potential fields technique is used to obtain cooperative control of the quadrotors. Each follower has the information of the positions of the leader and adjacent followers. Using this information, an attractive and a repulsive potential force is applied on each follower to obtain the desired shape formation. The attractive potential attracts the follower towards the leader whereas the repulsive potential repels adjacent followers and keep them at a distance *d*. Therefore, two potential field functions are defined based on this concept, one of them is U_{att}, the attractive potential and the other is U_{rep}, the repulsive potential. These functions are defined as follows,

$$U_{att} = \frac{1}{2} k_{att} (r_{oi} - R)^2 \tag{5.7}$$

$$U_{rep} = \begin{cases} \frac{1}{2} k_{rep} \left(r_{ij} - d\right)^2 & r_{ij} < d \\ 0 & otherwise \end{cases} \tag{5.8}$$

where r_{oi} is the current distance between the leader and the i^{th} follower, r_{ij} is the current distance between the i^{th} and the j^{th} followers, *R* is the desired distance between the leader and the followers, *d* is the desired distance between each adjacent follower and k_{att}, k_{rep} are positive tuning constants.

Now, the forces associated with each potential are calculated as a negative gradient of the above functions and the overall force applied on each follower is represented as,

$$F = F_0 + F_{ij} + D_a \tag{5.9}$$

where,

$$F_0 = -\nabla U_{att} \tag{5.10}$$

and

$$F_{ij} = -\nabla U_{rep} \tag{5.11}$$

The Control scheme described above can be illustrated as shown in Figure 5.2.

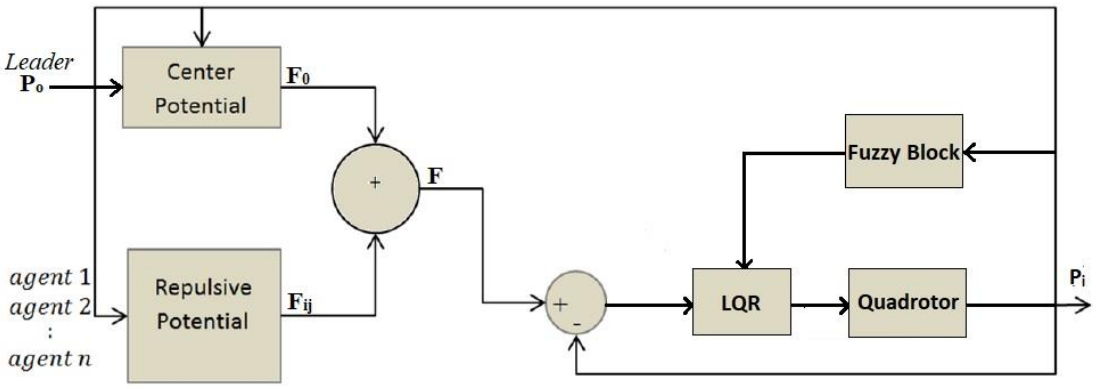

Figure 5.2 Control Scheme of a follower quadrotor using potential fields

As seen in Figure 5.2, each follower is applied with a cascaded controller in which the inner loop controller is the Fuzzy State-feedback LQR controller that has been discussed in previous chapter and the outer loop controller is the potential fields controller. The potential field controller consists of the center potential that attracts the followers towards the leader and the repulsive potential that repels adjacent followers. The center and the repulsive potentials are obtained by applying the gradient as discussed above. This formulation can be seen as follows.

a) Center Potential

Considering equations (5.7) and (5.10), we have

$$U_{att_i} = \frac{1}{2} k_{att}(r_{oi} - R)^2$$
$$F_0 = -\nabla_{P_i} U_{att_i}(P_i) \tag{5.12}$$

where

$$P_i = [x_i \; y_i \; z_i \; \psi_i]^T$$
$$P_0 = [x_0 \; y_0 \; z_0 \; \psi_0]^T \tag{5.13}$$

Hence, r_{oi} can be obtained as,

$$r_{oi} = \sqrt{(x_i - x_0)^2 + (y_i - y_0)^2 + (z_i - z_0)^2 + (\psi_i - \psi_0)^2} \tag{5.14}$$

Now, the equation (5.12) can be solved by differentiating U_{att_i} with respect to P_i as follows,

$$F_0 = -\left(\frac{\partial U_{att_i}}{\partial r_{oi}}\right)\left(\frac{\partial r_{oi}}{\partial P_i}\right) \tag{5.15}$$

From (5.12),

$$\frac{\partial U_{att_i}}{\partial r_{oi}} = k_{att}(r_{oi} - R) \tag{5.16}$$

let

$$M = (x_i - x_0)^2 + (y_i - y_0)^2 + (z_i - z_0)^2 + (\psi_i - \psi_0)^2 \tag{5.17}$$

$$r_{oi} = M^{\frac{1}{2}} \tag{5.18}$$

By using chain rule of partial derivatives, we can differentiate r_{oi} with respect to P_i as follows,

$$\frac{\partial r_{oi}}{\partial P_i} = \left(\frac{\partial r_{oi}}{\partial M}\right)\left(\frac{\partial M}{\partial P_i}\right) \tag{5.19}$$

Using (5.18),

$$\frac{\partial r_{oi}}{\partial M} = \frac{1}{2} M^{-\frac{1}{2}} \tag{5.20}$$

Also,

$$\begin{aligned} \frac{\partial M}{\partial P_i} &= \left[\frac{\partial M}{\partial x_i}\frac{\partial M}{\partial y_i}\frac{\partial M}{\partial z_i}\frac{\partial M}{\partial \psi_i}\right]^T \\ &= [2(x_i - x_0)\ 2(y_i - y_0)\ 2(z_i - z)\ 2(\psi_i - \psi_0)]^T \\ &= 2(P_i - P_0) \end{aligned} \tag{5.21}$$

Therefore, by substituting (5.20) and (5.21) in (5.19), we get

$$\begin{aligned} \frac{\partial r_{oi}}{\partial P_i} &= \frac{2}{2} M^{-\frac{1}{2}}(P_i - P_0) \\ &= \frac{1}{r_{oi}}(P_i - P_0) \end{aligned} \tag{5.22}$$

Now, by substituting (5.16) and (5.22) in (5.15), the final center potential is obtained as,

$$F_0 = -k_{att}\frac{1}{r_{oi}}(r_{oi} - R)\big(P_i(t) - P_0(t)\big) \tag{5.23}$$

b) Repulsive Potential

Considering equations (5.8) and (5.11), we have

$$U_{rep} = \begin{cases} \frac{1}{2} k_{rep} \left(r_{ij} - d\right)^2 & r_{ij} < d \\ 0 & otherwise \end{cases} \tag{5.24}$$

$$F_{ij} = -\nabla_{P_i} U_{rep}\left(P_i, P_j\right) \tag{5.25}$$

where

$$\begin{aligned} P_i &= [x_i \; y_i \; z_i \; \psi_i]^T \\ P_j &= [x_j \; y_j \; z_j \; \psi_j]^T \end{aligned} \tag{5.26}$$

Hence, r_{ij} can be obtained as,

$$r_{ij} = \sqrt{\left(x_i - x_j\right)^2 + \left(y_i - y_j\right)^2 + \left(z_i - z_j\right)^2 + \left(\psi_i - \psi_j\right)^2} \tag{5.27}$$

Proceeding with similar steps from (5.15) to (5.22), the final repulsive potential can be obtained as,

$$F_{ij} = -k_{rep} \frac{1}{r_{ij}} \left(r_{ij} - d\right) \left(\left(P_i(t) - P_j(t)\right) - \left(P_j(t) - P_i(t)\right)\right) \tag{5.28}$$

5.4 Simulation Results

The entire control scheme explained in the previous sections is implemented in MATLAB to perform the simulations. As, mentioned previously, each quadrotor has two stages of control. The outer loop controller is responsible for the formation control that allows the followers to track the trajectory of the leader by maintaining a desired shape formation. The inner control loop is the LQR controller that is responsible for the stability of the quadrotors and desired tracking.

Consider one leader quadrotor and three follower quadrotor agents, n=3. The followers are required to form a circle of radius R with center being the leader. This implies each follower is at distance of R from the leader. Also, each adjacent follower quadrotor should be at a distance of d from each other. Let R=1.5m and n=3, this implies d=2Rsin(pi/n) = 2.598m. The leader is required to follow a desired reference trajectory and the agents follow the trajectory of the leader along with the formation constraints to produce their paths that satisfy the desired shape formations.

The simulations are carried out for both types of operating points as discussed in chapter 3, i.e., for the operating points taken from [5] as well as for the new operating points. For each type of operating point, four cases are taken. The first case is when the leader moves linearly only in *x* direction, the second case is when the leader moves in *x*-*y* directions and the third case is when the leader moves in *x*-*y*-*z* direction to showcase the responses for each plane. In the fourth case, the leader is set to move in a sinusoidal path. Also, to validate the proposed T-S models and control system, the control method is applied on the nonlinear model of the quadrotor.

5.4.1 Simulation Results for Original Operating Points

a) Motion in *x* Direction

The leader and follower quadrotors are first set to their initial hovering positions. The leader then moves in x direction and the followers follow the leader while keeping the desired formation. The initial position of the leader is taken as (1,0,2) and that of the followers as (0.5,-1.4,2) , (0.1,1.2,2) and (2.5,0.2,2) respectively for each follower. The leader then moves to different positions as shown in figures (5.3) – (5.10).

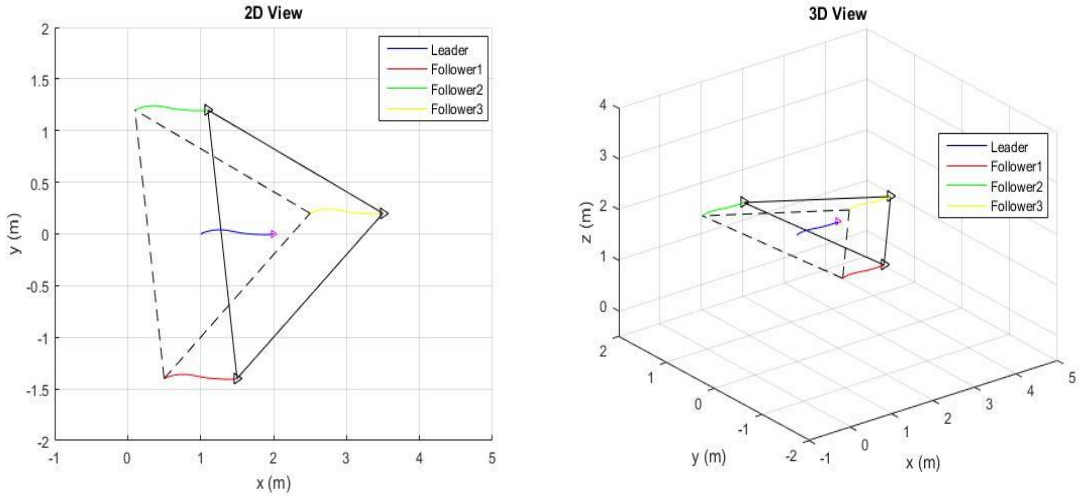

Figure 5.3 The group movement when leader moves to position (2,0,2) (different views)

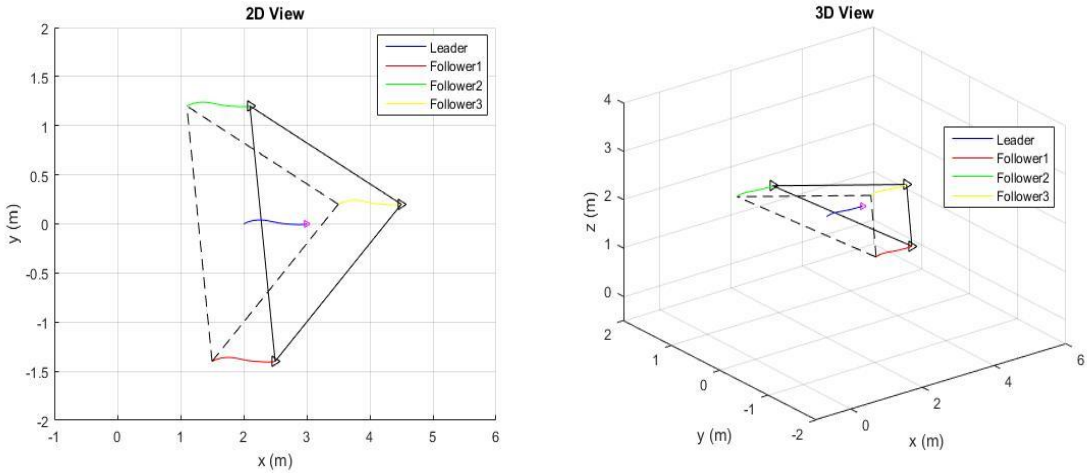

Figure 5.4 The group movement when leader moves to position (3,0,2) (different views)

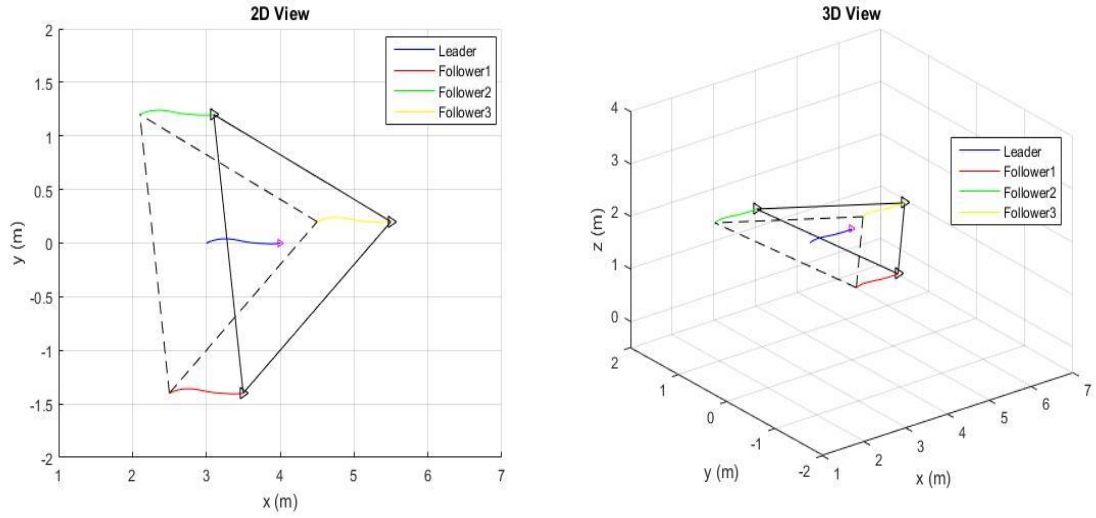

Figure 5.5 The group movement when leader moves to position (4,0,2) (different views)

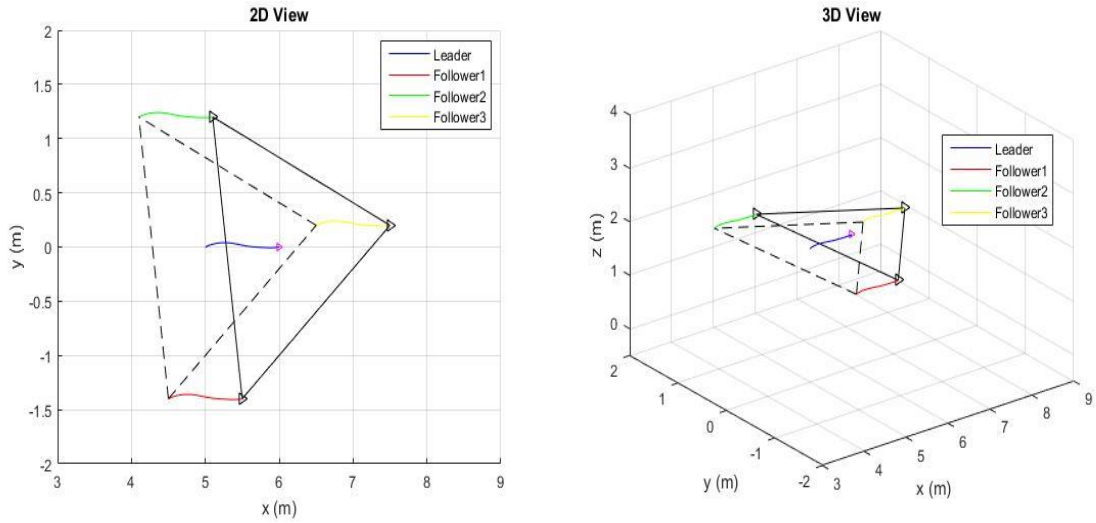

Figure 5.6 The group movement when leader moves to position (6,0,2) (different views)

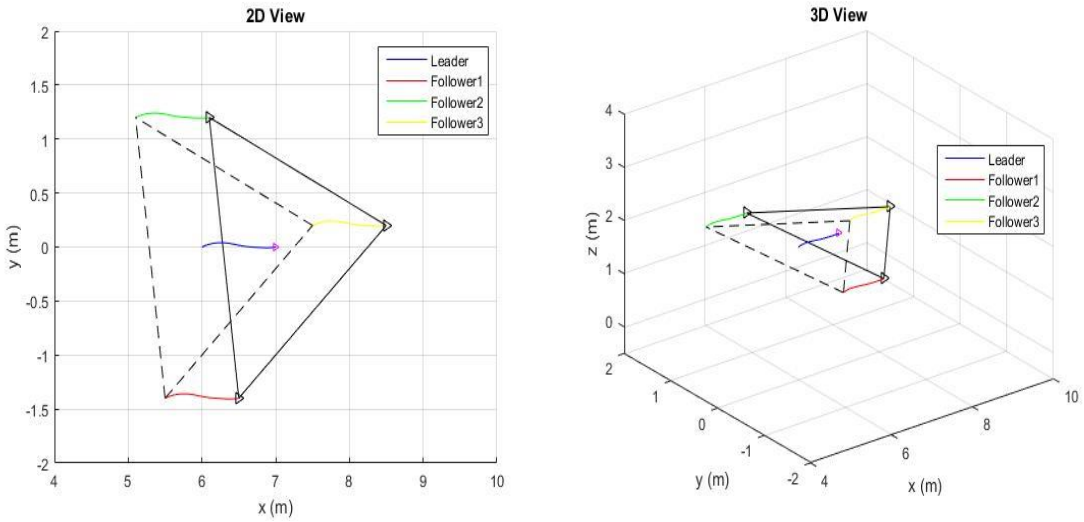

Figure 5.7 The group movement when leader moves to position (7,0,2) (different views)

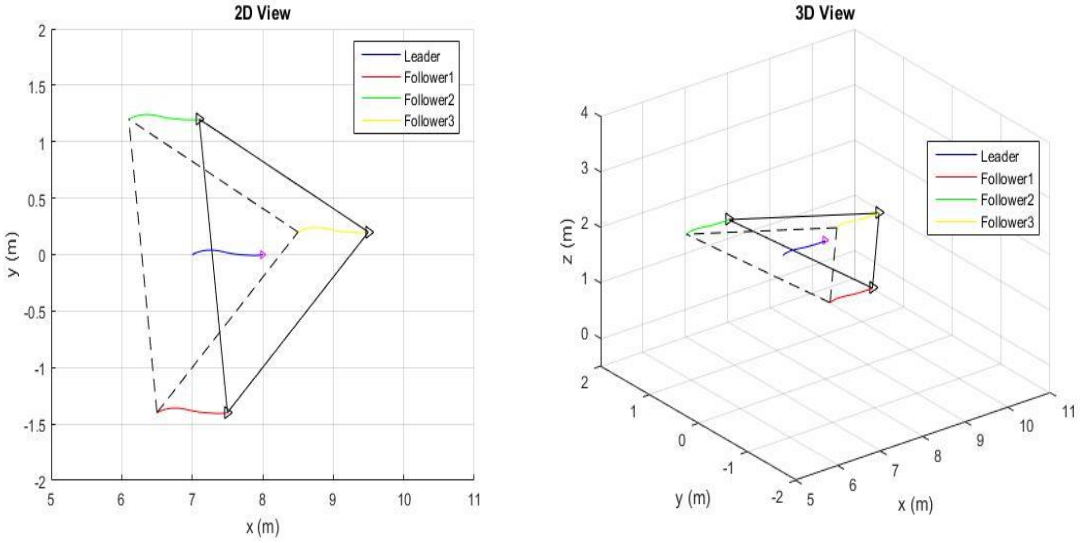

Figure 5.8 The group movement when leader moves to position (8,0,2) (different views)

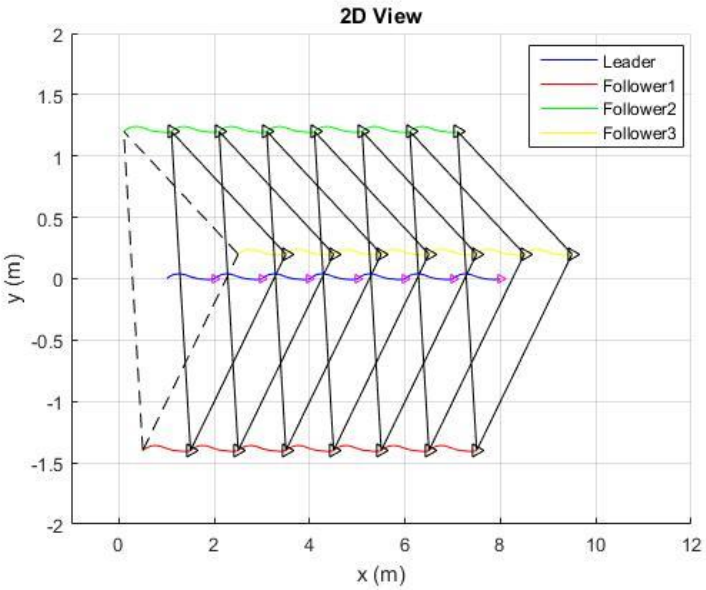

Figure 5.9 The group movement along the full path (2D view)

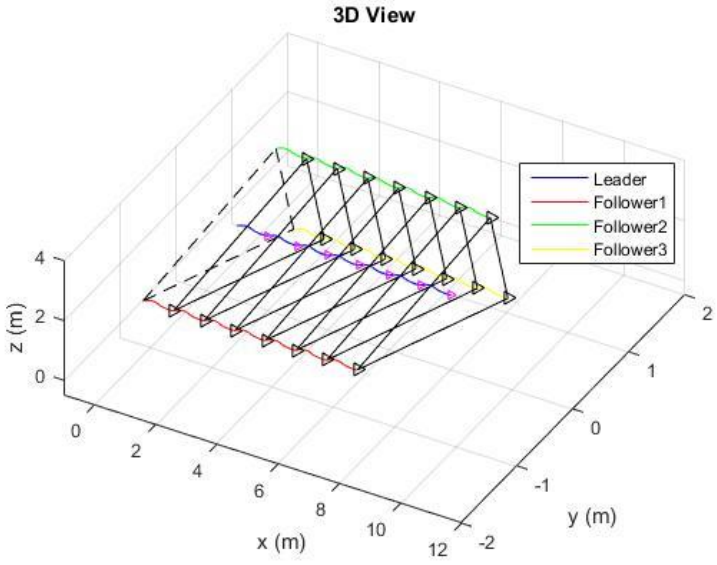

Figure 5.10 The group movement along the full path (3D view)

Figures (5.9) and (5.10) shows the 2D and the 3D views of the complete trajectory of the group of quadrotors for all the positions. From the results, we can see that we are able to obtain desired tracking and formation responses.

b) Motion in *x-y* Direction

The leader and follower quadrotors are first set to their initial hovering positions. The leader then moves in x-y direction and the followers follow the leader while keeping the desired formation. The initial position of the leader is taken as (1,0,2) and that of the followers as (0.5,-1.4,2) , (0.1,1.2,2) and (2.5,0.2,2) respectively for each follower. The leader then moves to different positions as shown in figures (5.11) – (5.18).

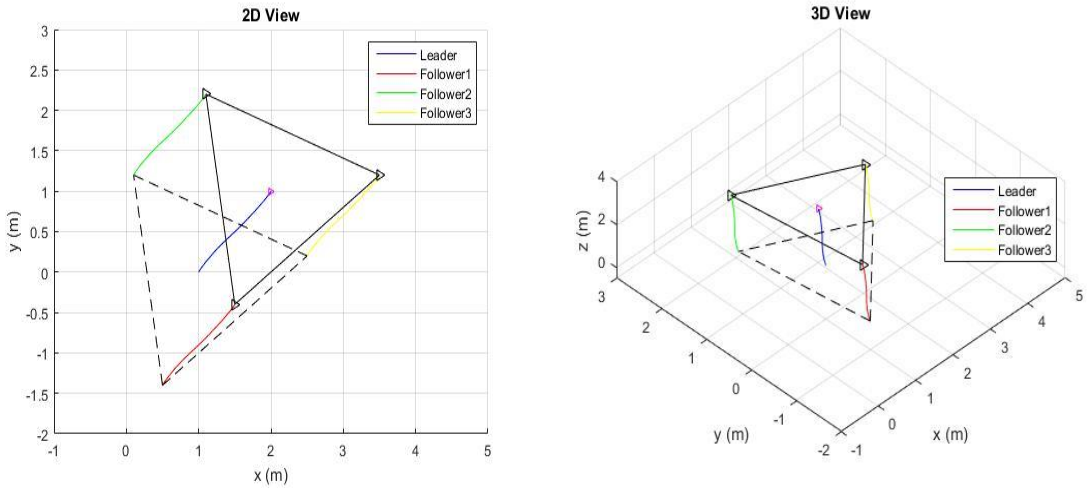

Figure 5.11 The group movement when leader moves to position (2,1,2) (different views)

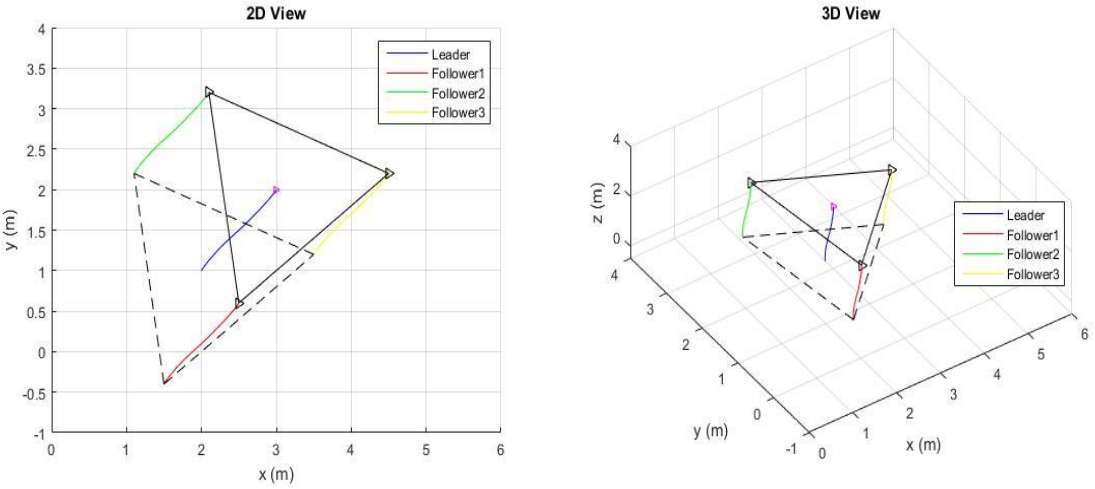

Figure 5.12 The group movement when leader moves to position (3,2,2) (different views)

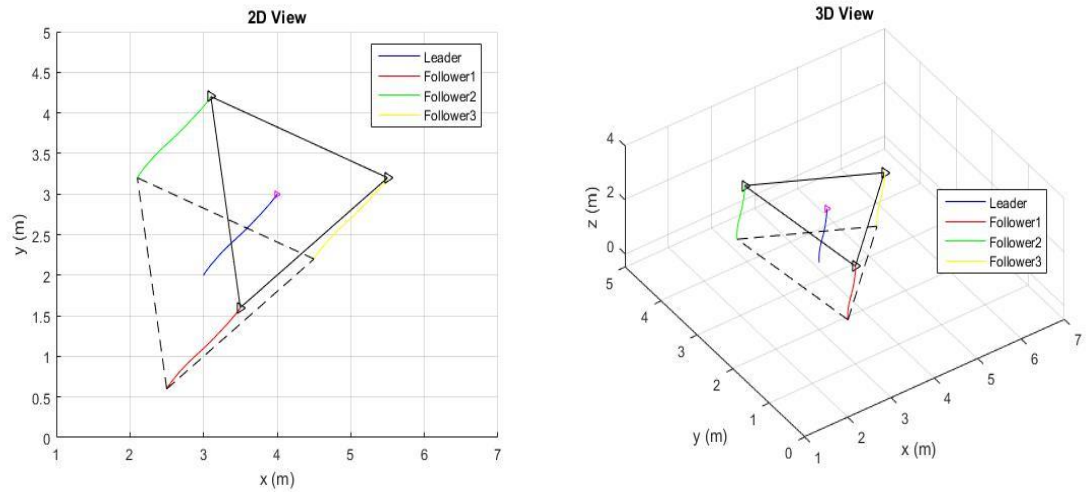

Figure 5.13 The group movement when leader moves to position (4,3,2) (different views)

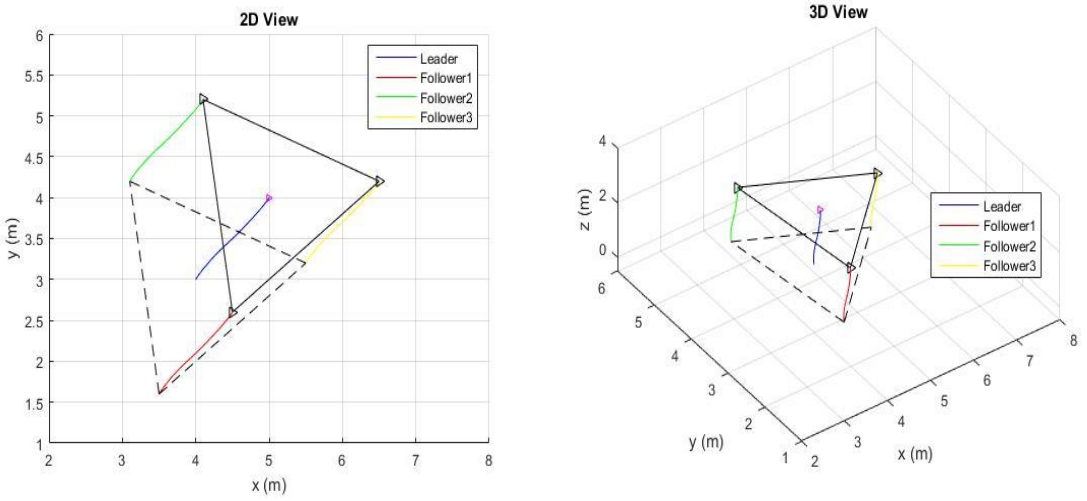

Figure 5.14 The group movement when leader moves to position (5,4,2) (different views)

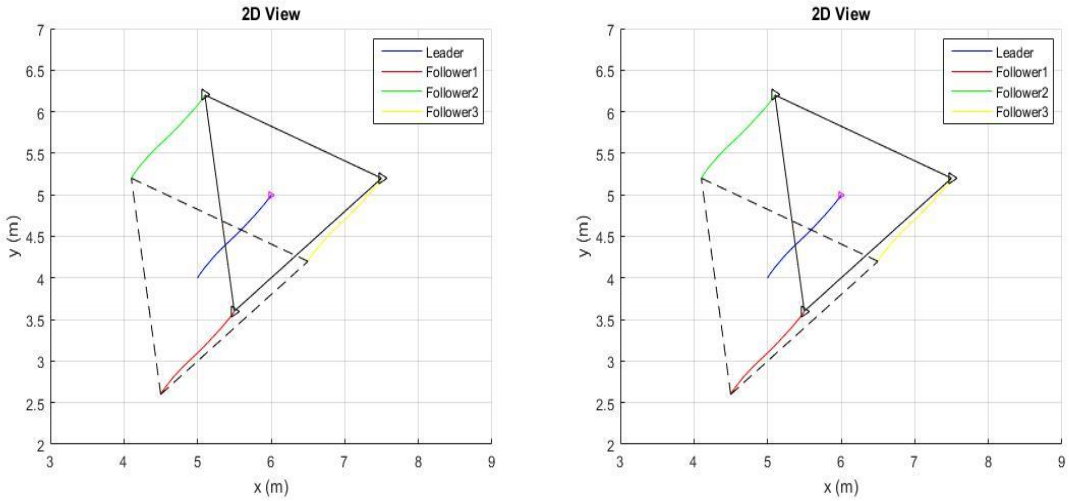

Figure 5.15 The group movement when leader moves to position (6,5,2) (different views)

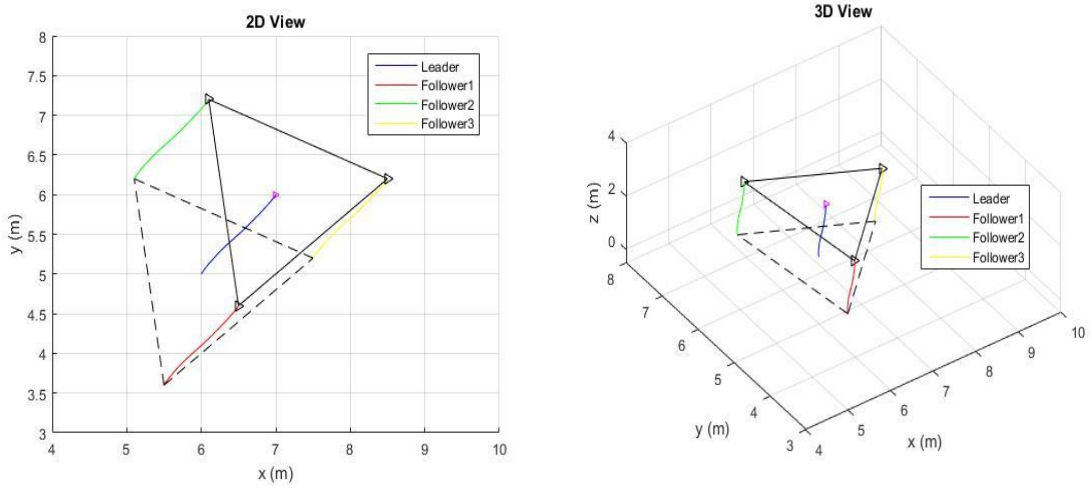

Figure 5.16 The group movement when leader moves to position (7,6,2) (different views)

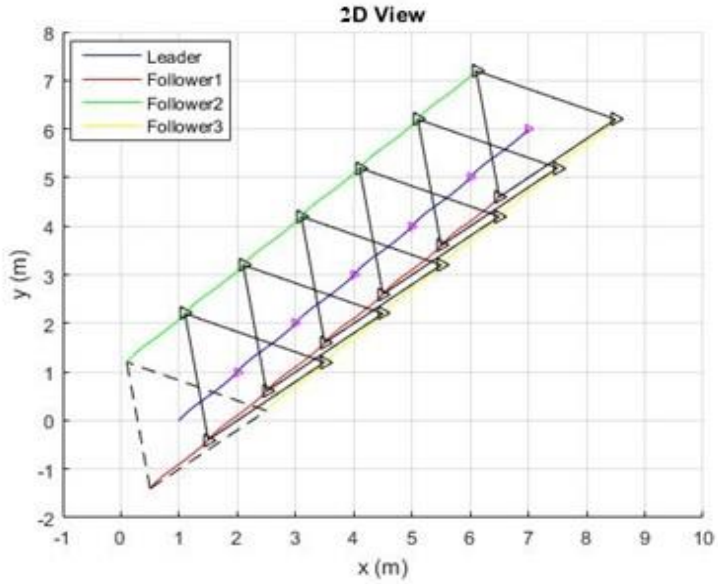

Figure 5.17 The group movement along the full x-y path (2D view)

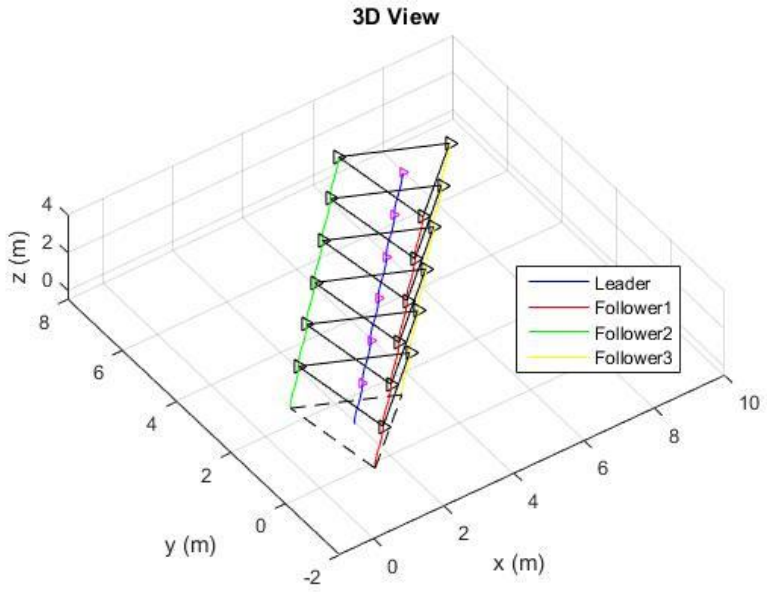

Figure 5.18 The group movement along the full x-y path (3D view)

Figures (5.17) and (5.18) shows the 2D and the 3D views of the complete trajectory of the group of quadrotors for all the positions. From the results, we can see that we are able to obtain desired tracking and formation responses.

c) Motion in x-y-z Direction

The leader and follower quadrotors are first set to their initial hovering positions. The leader then moves in x-y-z direction and the followers follow the leader while keeping the desired formation. The initial position of the leader is taken as (1,0,2) and that of the followers as (2.2,0.8,1.8) , (-0.3,0.7,2.1) and (1,-1.5,1.7) respectively for each follower to form a 3D polygon. The leader then moves to different positions as shown in figures (5.19) – (5.25).

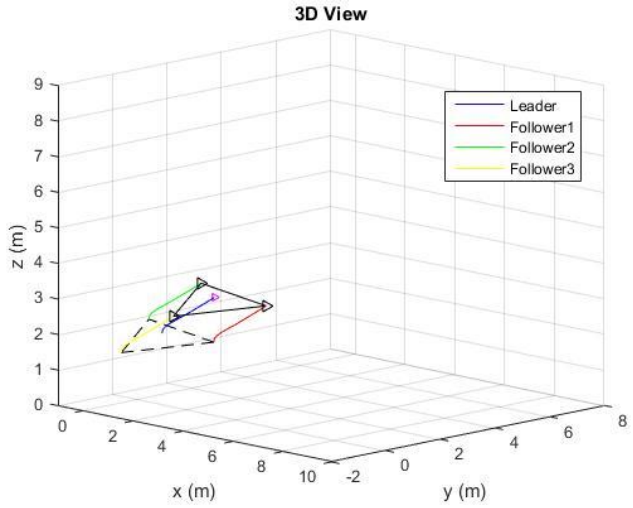

Figure 5.19 The group movement when leader moves to position (2,1,3)

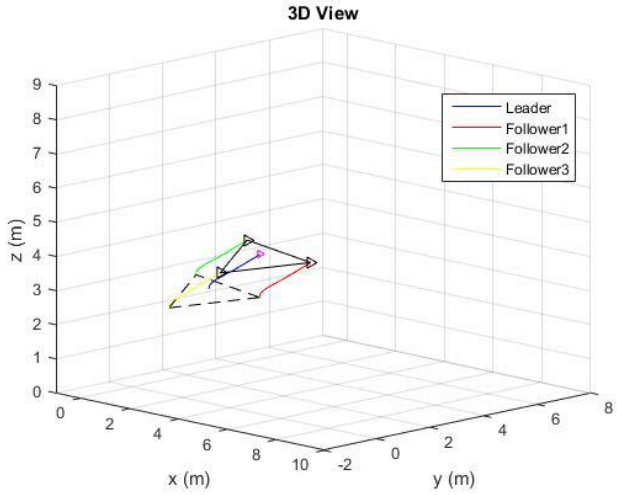

Figure 5.20 The group movement when leader moves to position (3,2,4)

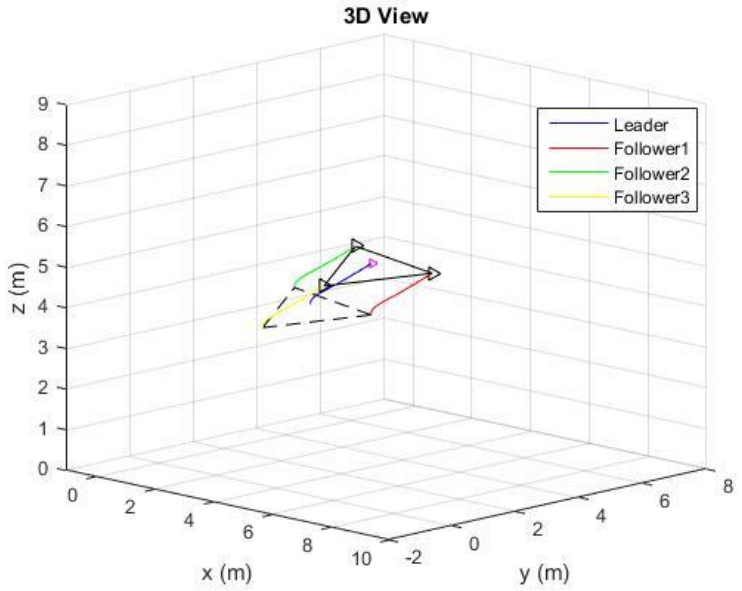

Figure 5.21 The group movement when leader moves to position (4,3,5)

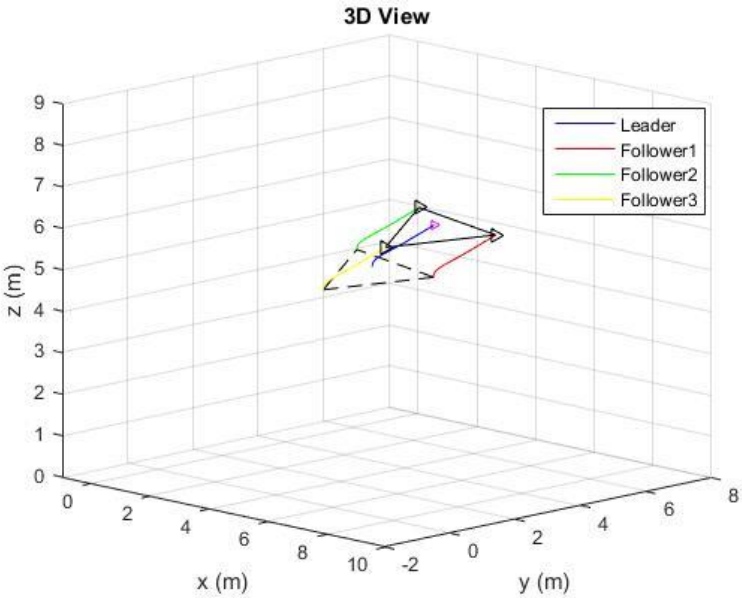

Figure 5.22 The group movement when leader moves to position (5,4,6)

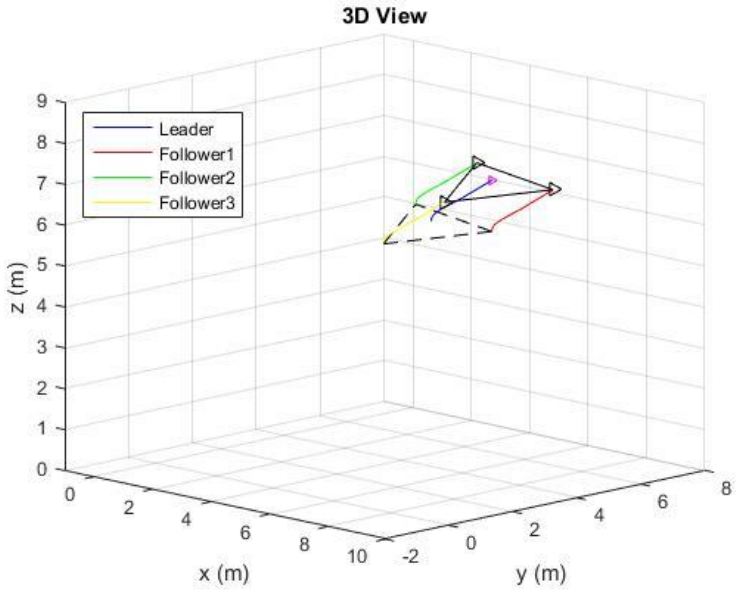

Figure 5.23 The group movement when leader moves to position (6,5,7)

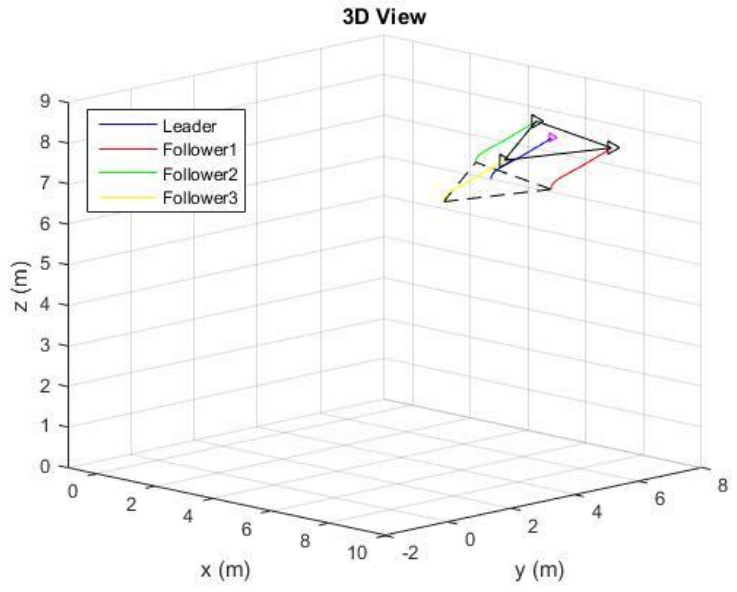

Figure 5.24 The group movement when leader moves to position (7,6,8)

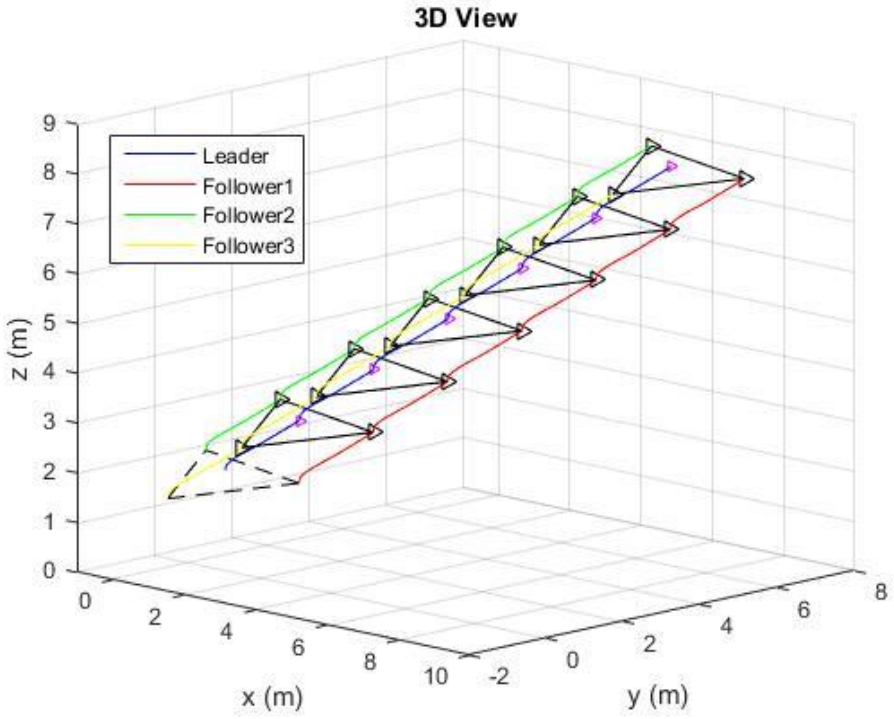

Figure 5.25 The group movement along the full x-y-z path

Figures (5.25) shows the 3D view of the complete x-y-z trajectory of the group of quadrotors for all the positions. From the results, we can see that we are able to obtain desired tracking and formation responses.

d) Sinusoidal Motion

The leader and follower quadrotors are first set to their initial hovering positions. The leader is then set to move in a sinusoidal path and the followers follow the leader while keeping the desired formation. The initial position of the leader is taken as (1,0,2) and that of the followers as (2.2,0.8,1.8) , (-0.3,0.7,2.1) and (1,-1.5,1.7) respectively for each follower to form a 3D polygon. The leader then moves in the form a sinusoidal trajectory which is of the form of $r(t) = Asin(wt + \phi)$ for each coordinate x,y and z. The different views of the simulation results can be seen from figures (5.26) - (5.29).

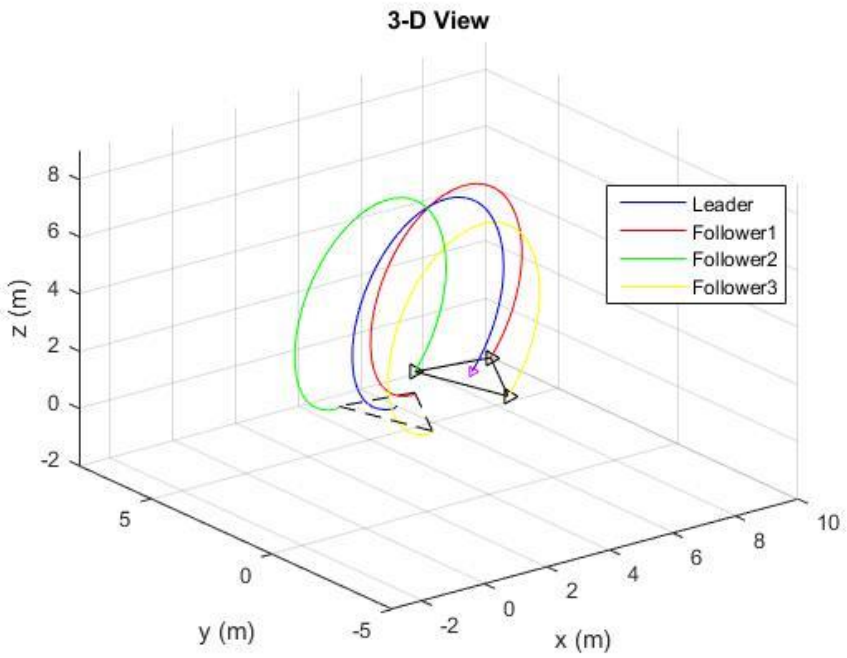

Figure 5.26 3-D view of the group movement for a sinusoidal reference trajectory

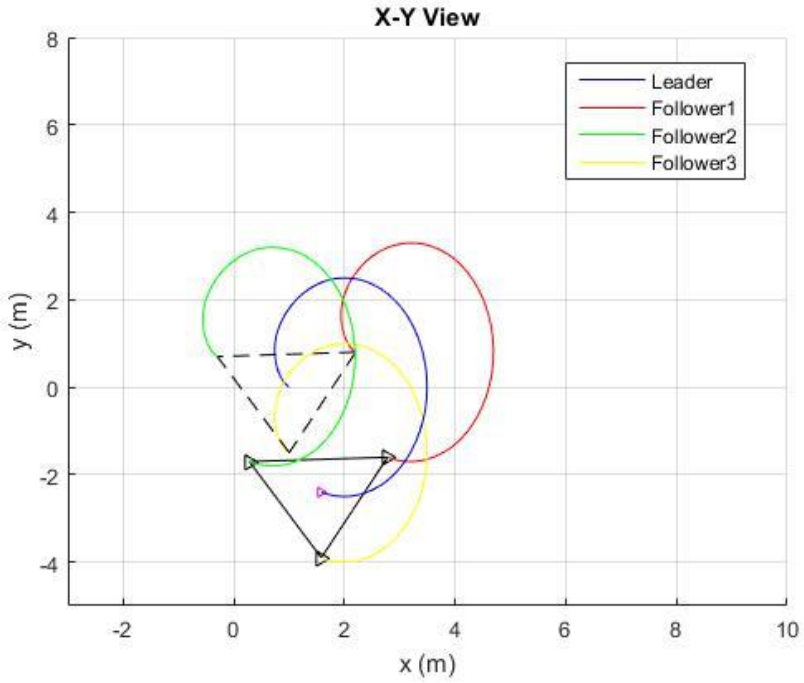

Figure 5.27 X-Y view of the group movement for a sinusoidal reference trajectory

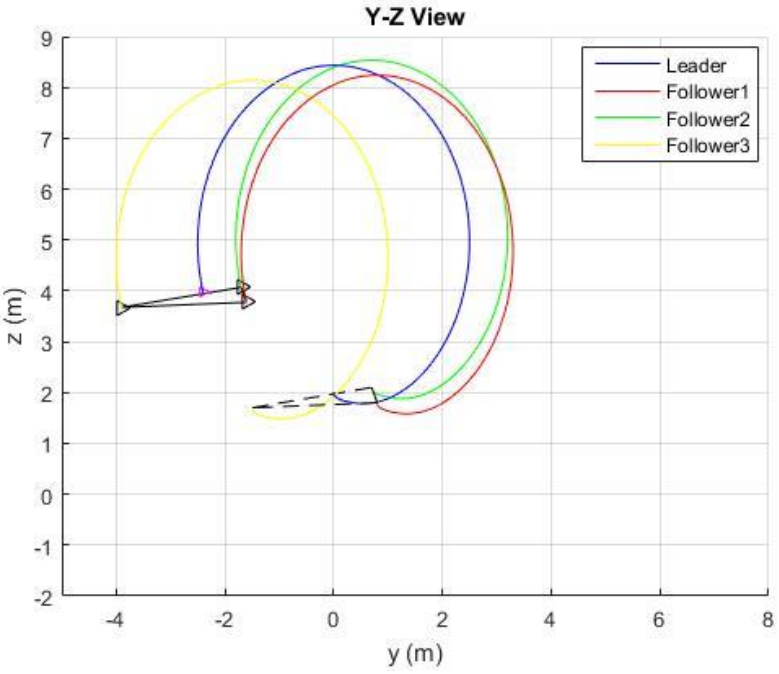

Figure 5.28 Y-Z view of the group movement for a sinusoidal reference trajectory

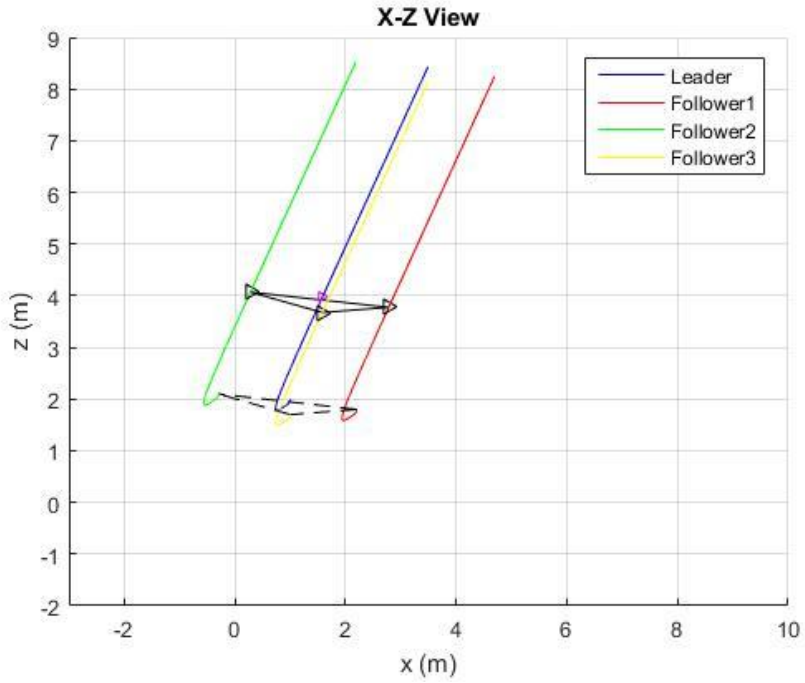

Figure 5.29 X-Z view of the group movement for a sinusoidal reference trajectory

Figures (5.26) - (5.29) shows the different views of the complete trajectory of the group of quadrotors for the sinusoidal motion. From the results, we can see that we are able to obtain desired tracking and formation responses.

5.4.2 Simulation Results for the New Operating Points

Now, the same steps done in previous section is repeated for all the four cases but the new operating points are used to design the T-S model which results in a different LQR controller for the quadrotors. The initial conditions of the leader and followers and each step motion for all the cases is taken the same as in previous section. The simulation results obtained are shown below.

a) Motion in *x* Direction

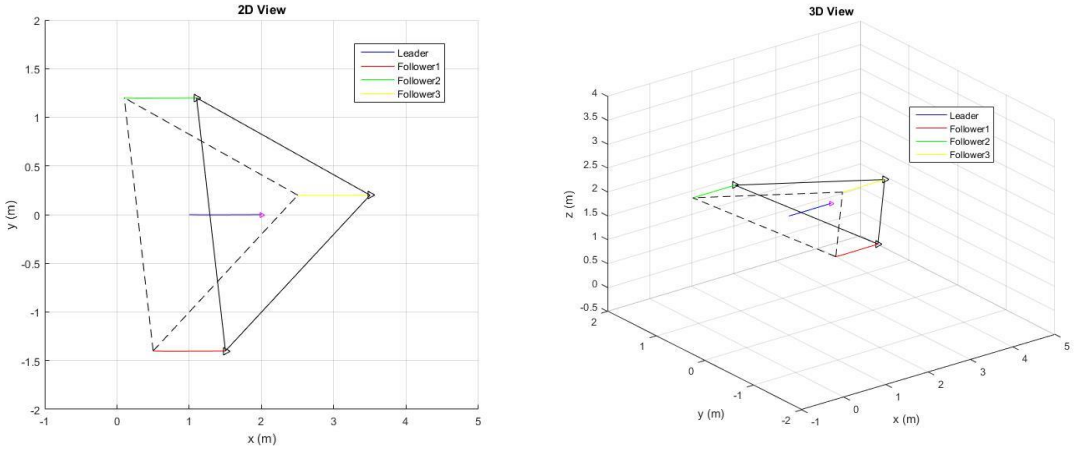

Figure 5.30 The group movement when leader moves to position (2,0,2) (different views)

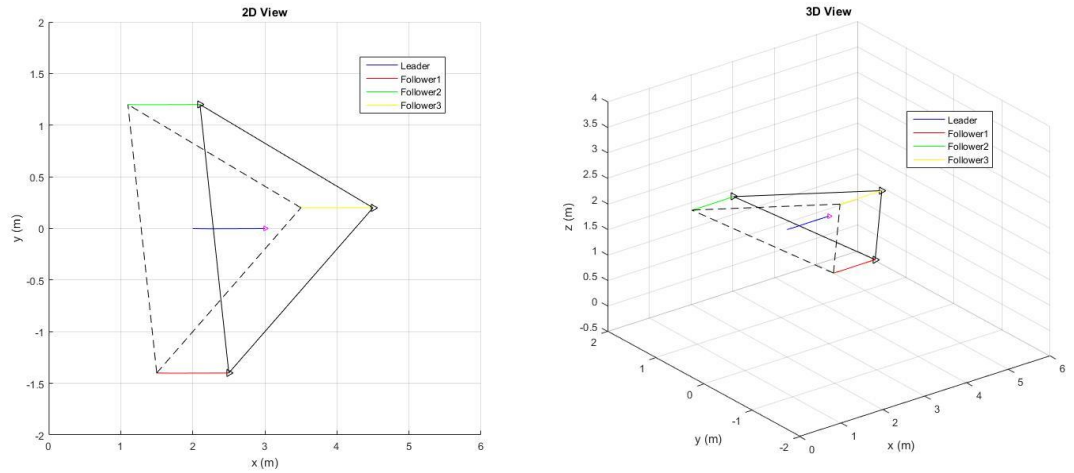

Figure 5.31 The group movement when leader moves to position (3,0,2) (different views)

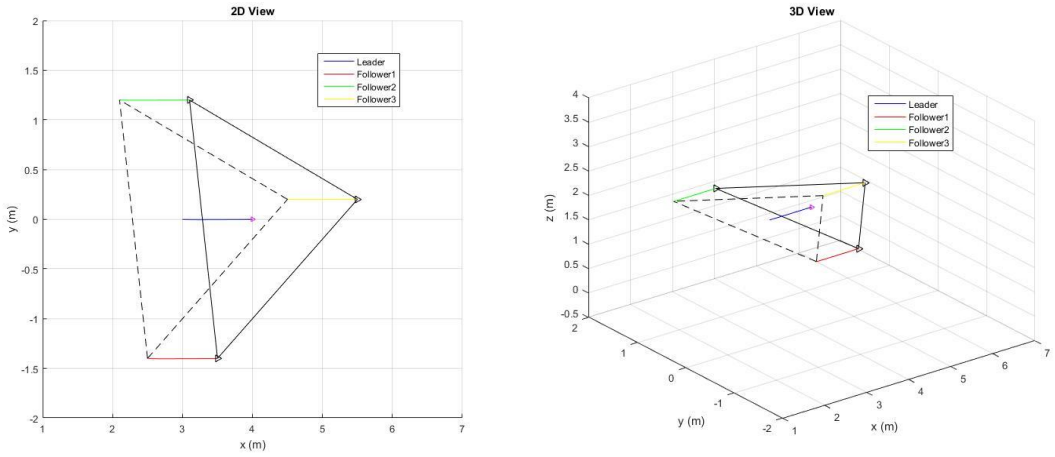

Figure 5.32 The group movement when leader moves to position (4,0,2) (different views)

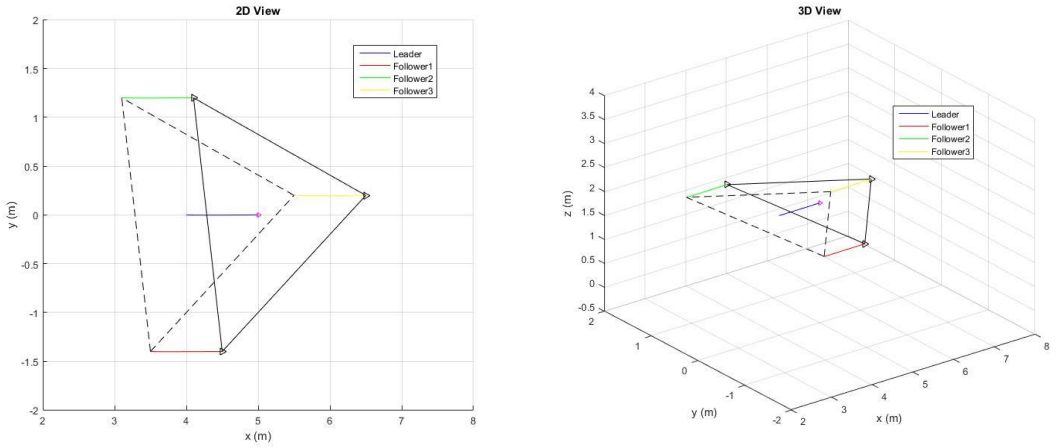

Figure 5.33 The group movement when leader moves to position (5,0,2) (different views)

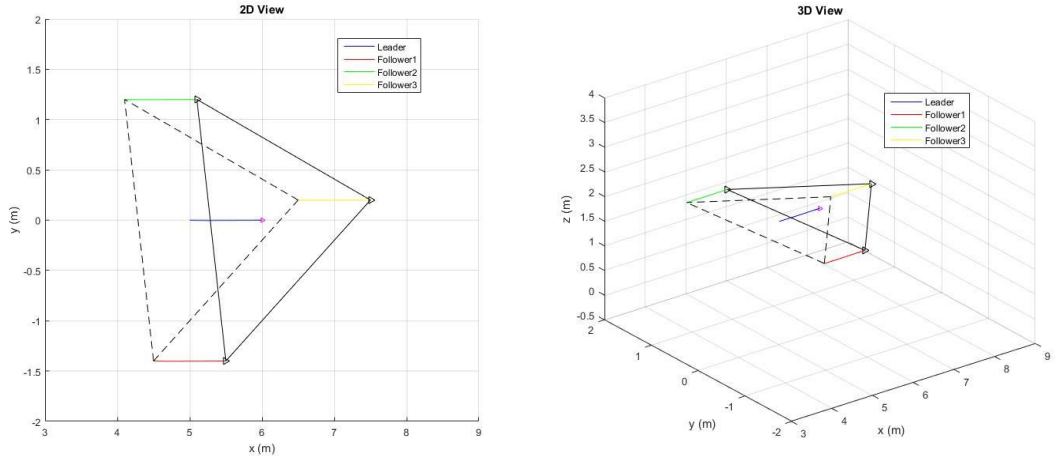

Figure 5.34 The group movement when leader moves to position (6,0,2) (different views)

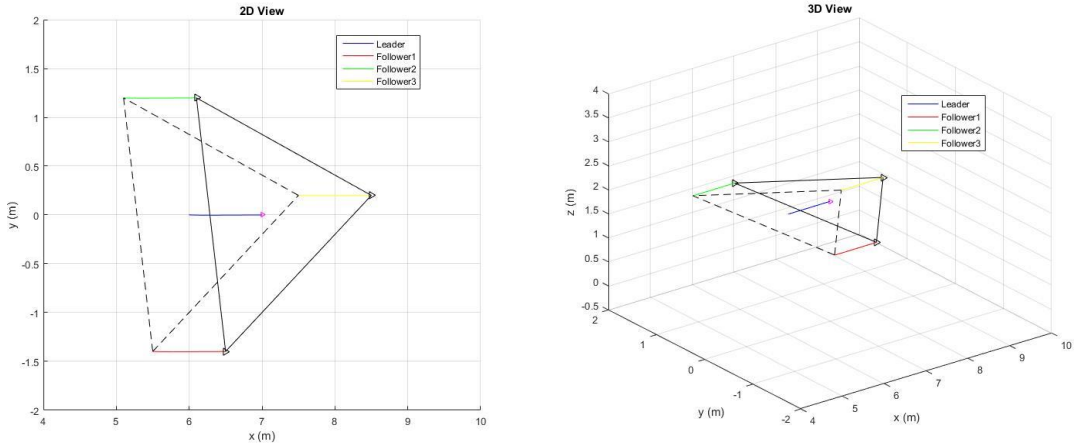

Figure 5.35 The group movement when leader moves to position (7,0,2) (different views)

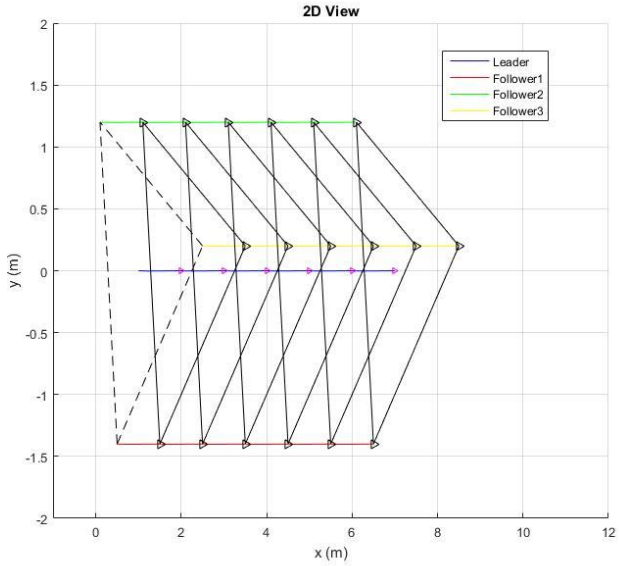

Figure 5.36 The group movement along the full path (2D view)

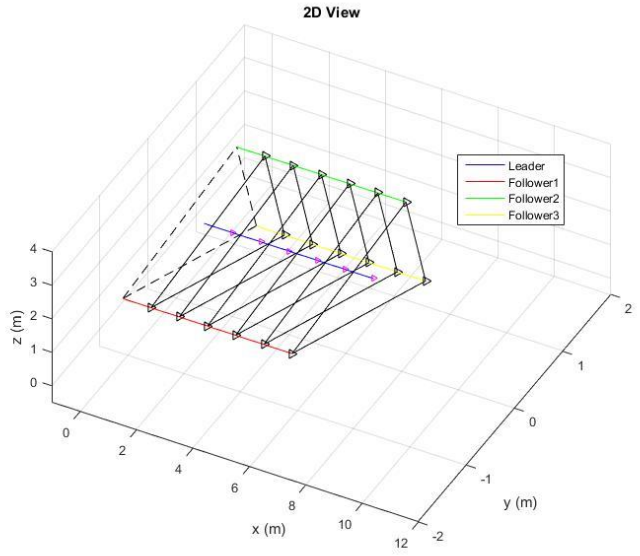

Figure 5.37 The group movement along the full path (3D view)

Figures (5.36) and (5.37) shows the 2D and the 3D views of the complete trajectory of the group of quadrotors for all the positions. From the results, we can see that we are able to obtain desired tracking and formation responses. Also, it can be observed that there are fewer ripples when compared to the results for the original operating points.

b) Motion in *x-y* Direction

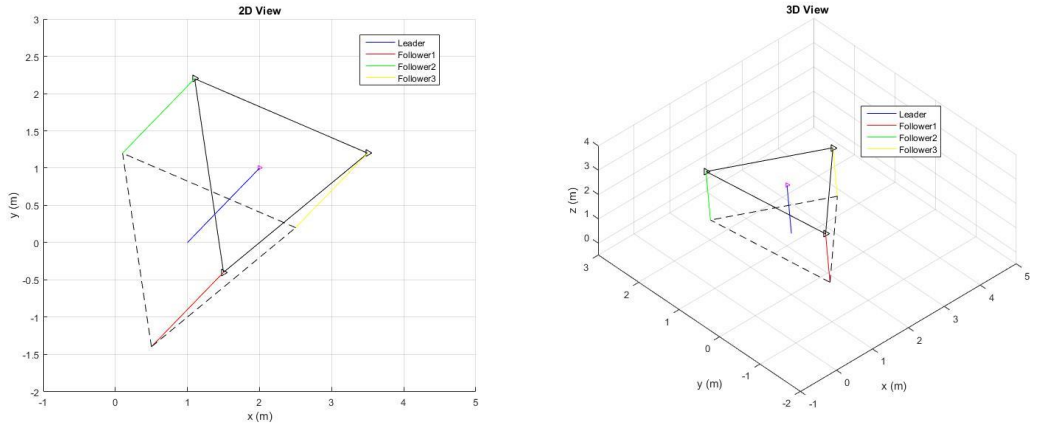

Figure 5.38 The group movement when leader moves to position (2,1,2) (different views)

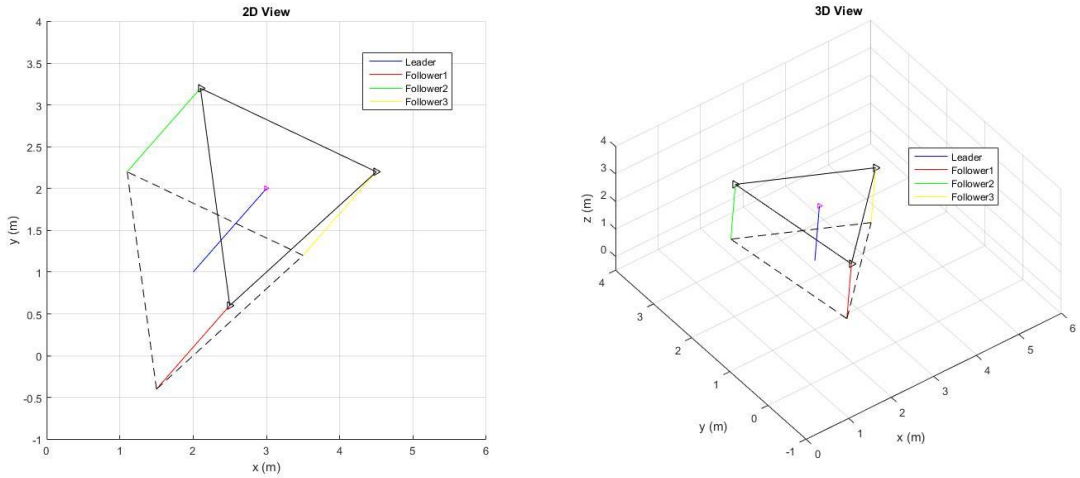

Figure 5.39 The group movement when leader moves to position (3,2,2) (different views)

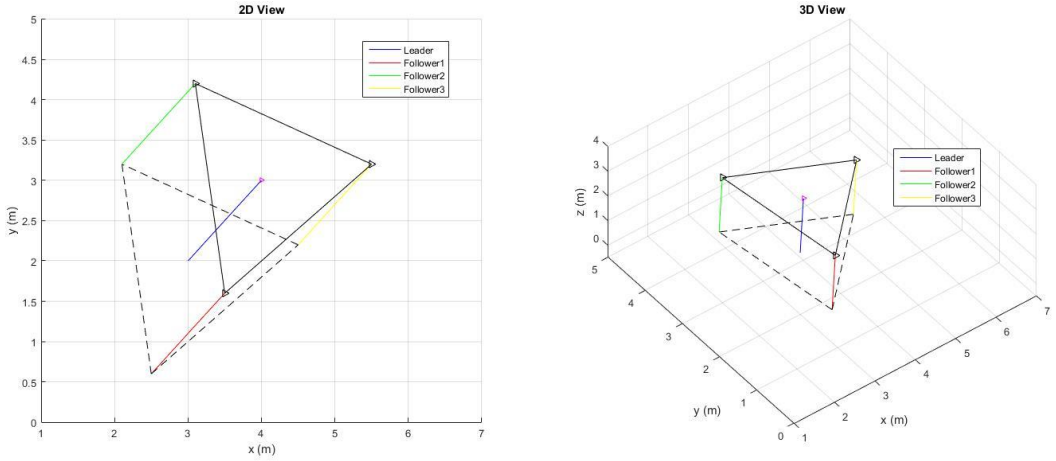

Figure 5.40 The group movement when leader moves to position (4,3,2) (different views)

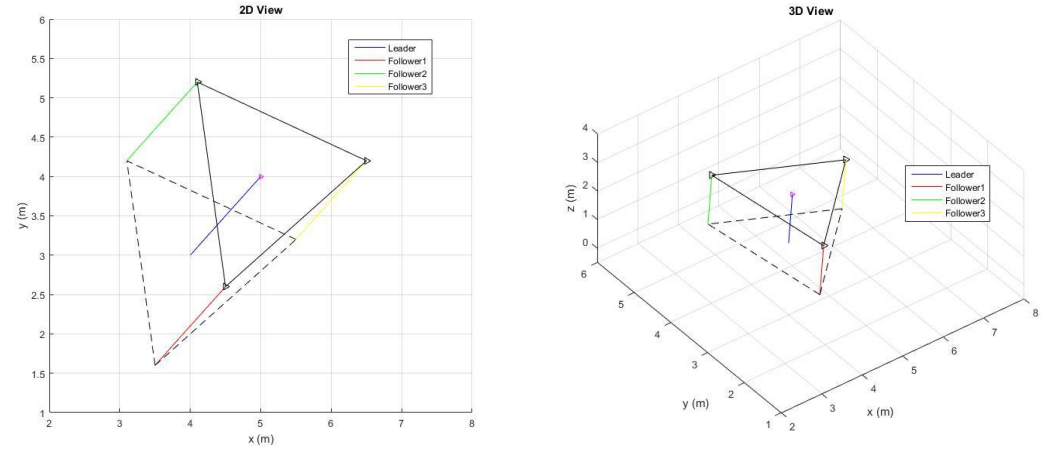

Figure 5.41 The group movement when leader moves to position (5,4,2) (different views)

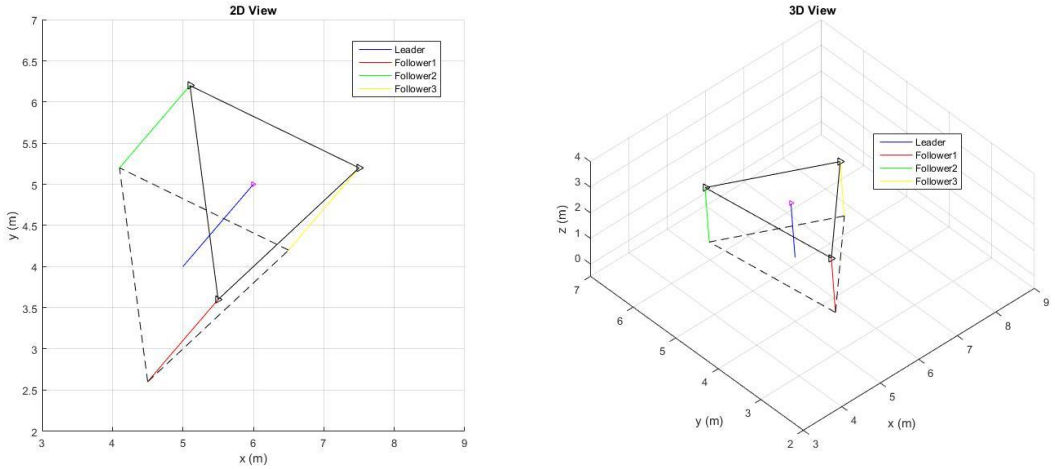

Figure 5.42 The group movement when leader moves to position (6,5,2) (different views)

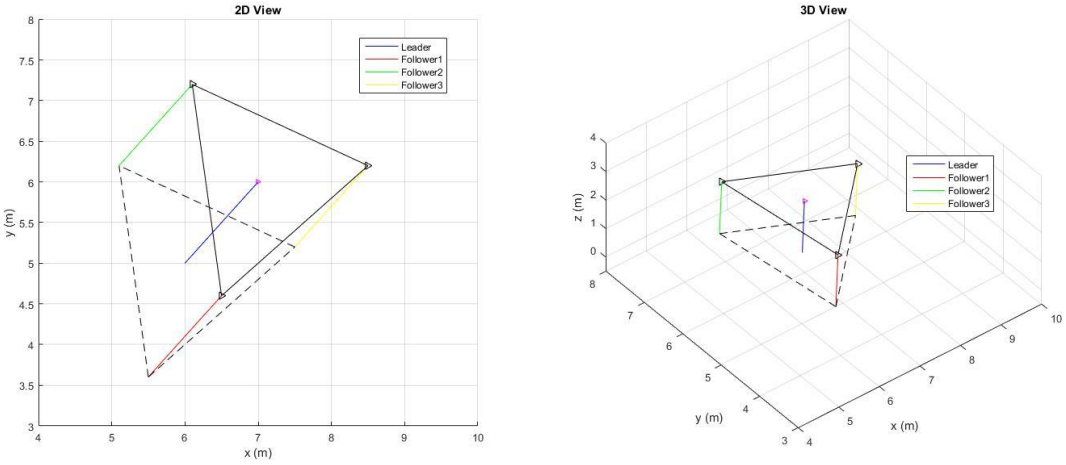

Figure 5.43 The group movement when leader moves to position (7,6,2) (different views)

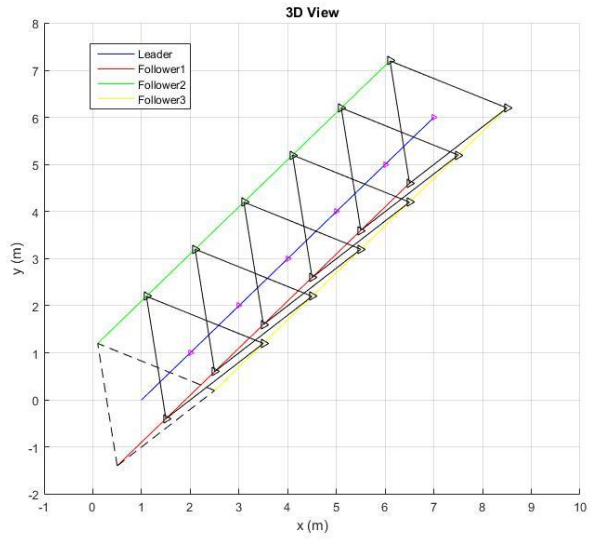

Figure 5.44 The group movement along the full path (2D view)

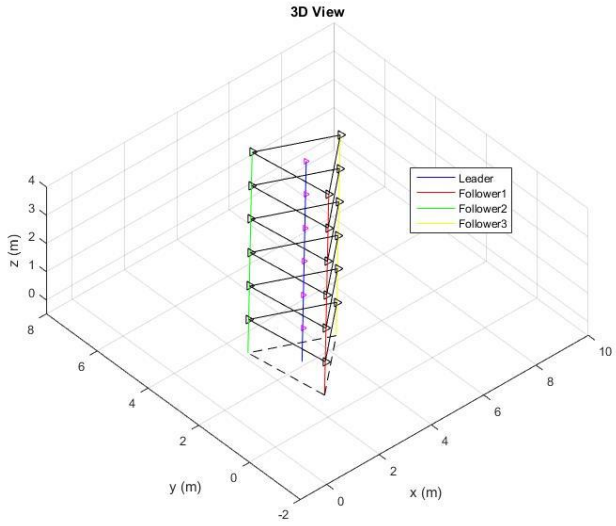

Figure 5.45 The group movement along the full path (3D view)

Figures (5.44) and (5.45) shows the 2D and the 3D views of the complete trajectory of the group of quadrotors for all the positions. From the results, we can see that we are able to obtain desired tracking and formation responses. Also, it can be observed that there are fewer ripples when compared to the results for the original operating points.

c) Motion in *x-y-z* Direction

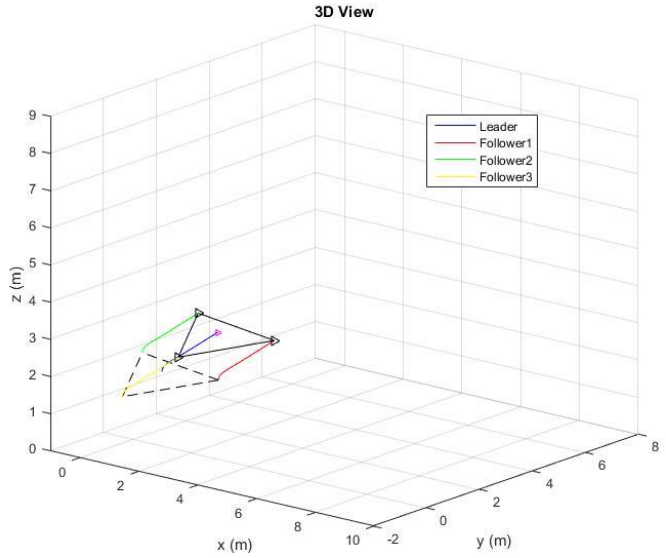

Figure 5.46 The group movement when leader moves to position (2,1,3)

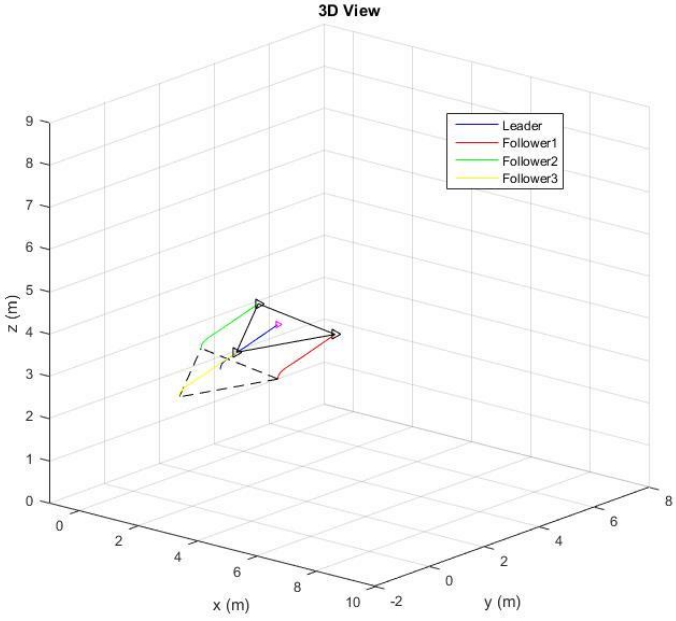

Figure 5.47 The group movement when leader moves to position (3,2,4)

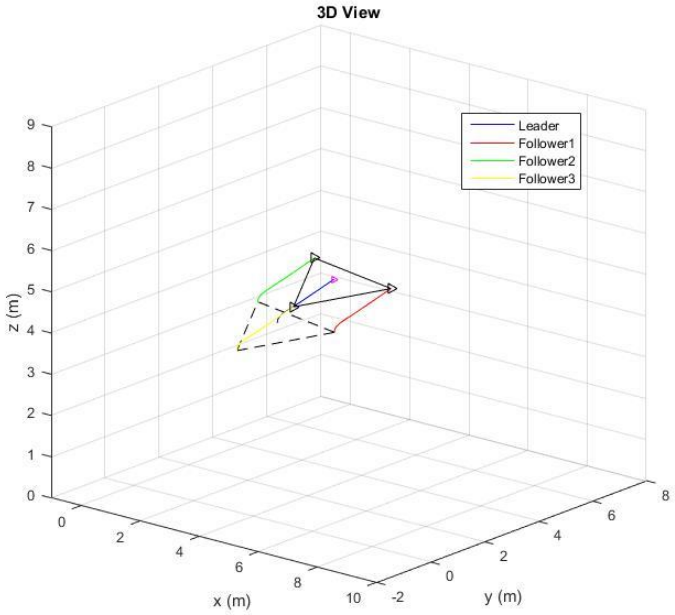

Figure 5.48 The group movement when leader moves to position (4,3,5)

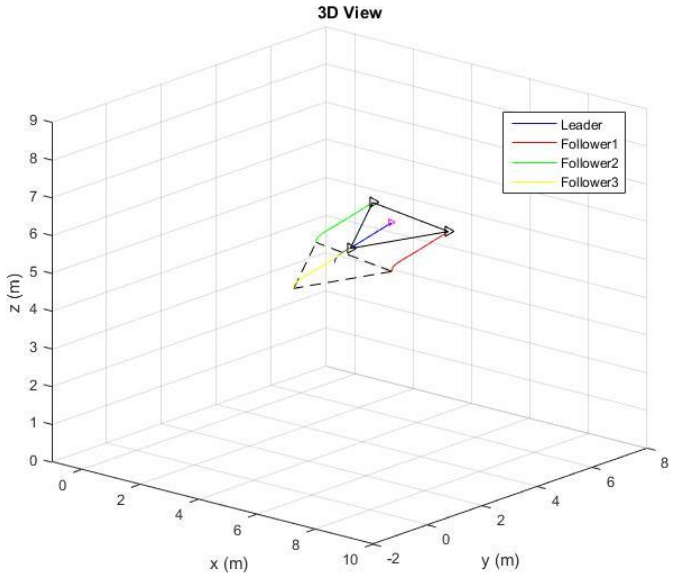

Figure 5.49 The group movement when leader moves to position (5,4,6)

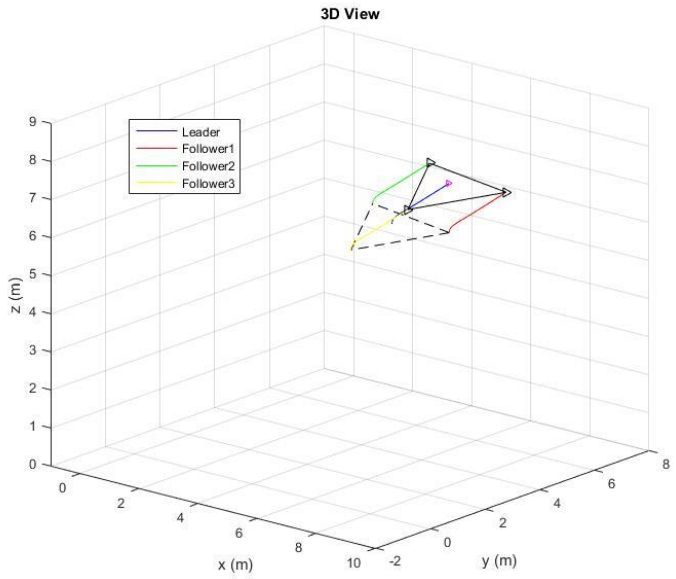

Figure 5.50 The group movement when leader moves to position (6,5,7)

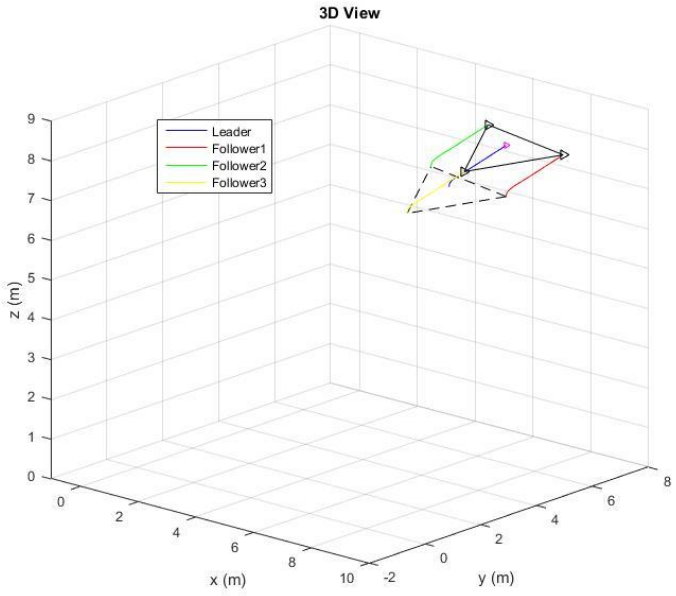

Figure 5.51 The group movement when leader moves to position (7,6,8)

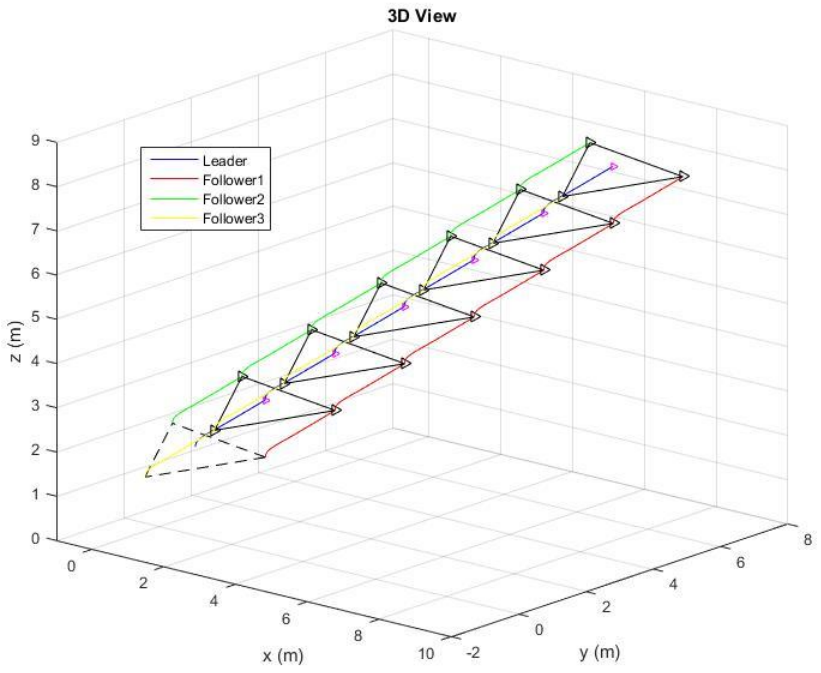

Figure 5.52 The group movement along the full x-y-z path

Figures (5.52) shows the 3D view of the complete x-y-z trajectory of the group of quadrotors for all the positions. From the results, we can see that we are able to obtain desired tracking and formation responses. Also, it can be observed that there are fewer ripples when compared to the results for the original operating points.

d) Sinusoidal Motion

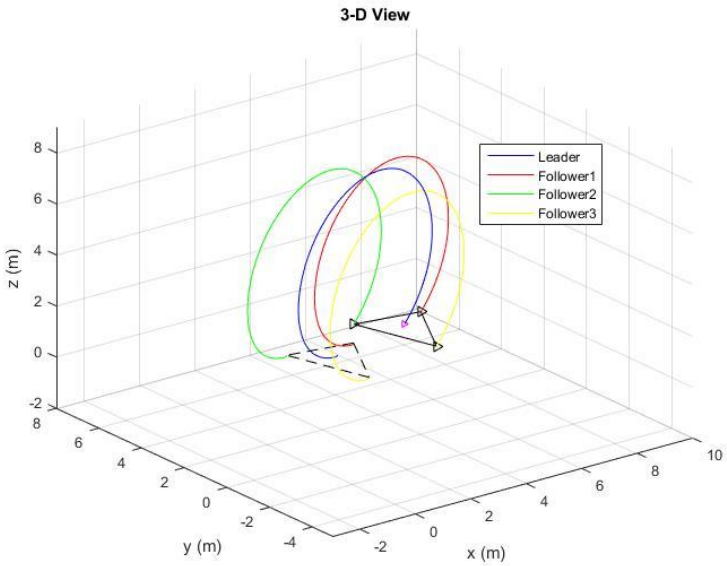

Figure 5.53 3-D view of the group movement for a sinusoidal reference trajectory

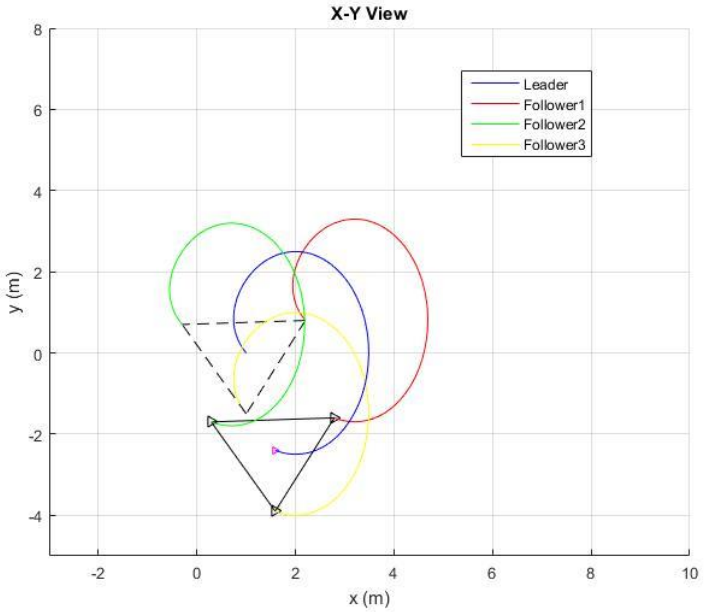

Figure 5.54 X-Y view of the group movement for a sinusoidal reference trajectory

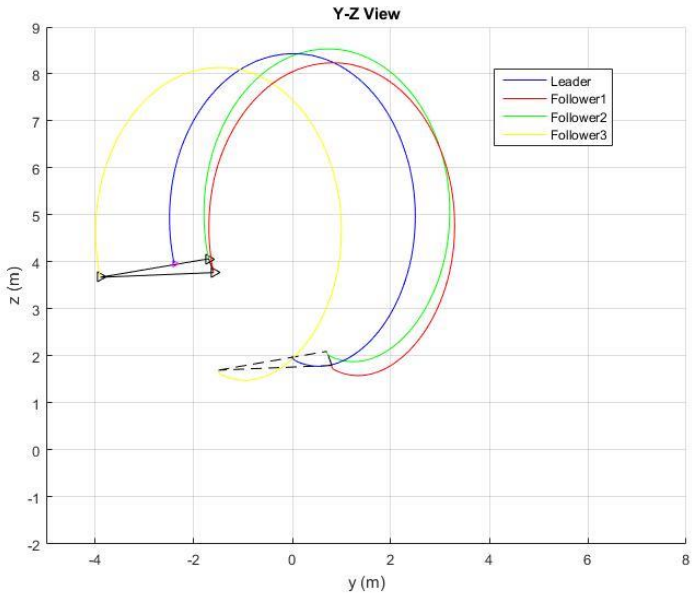

Figure 5.55 Y- Z view of the group movement for a sinusoidal reference trajectory

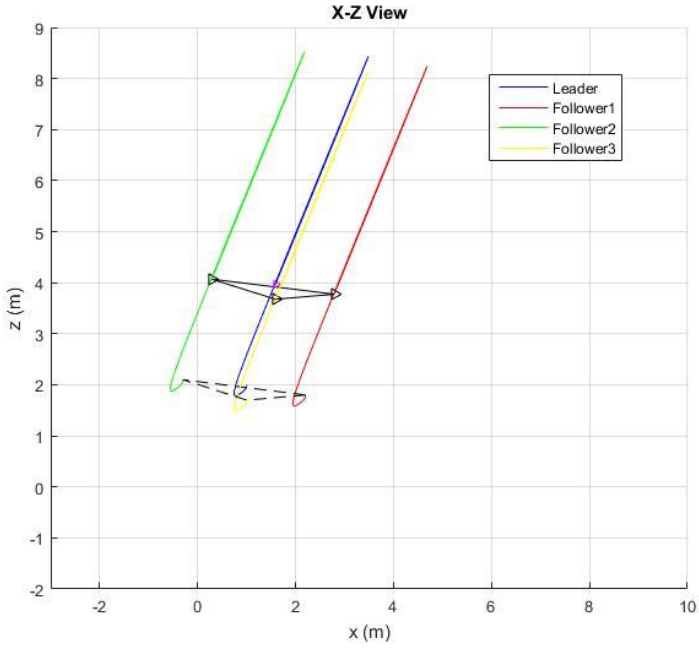

Figure 5.56 X-Z view of the group movement for a sinusoidal reference trajectory

Figures (5.53) - (5.56) shows the different views of the complete trajectory of the group of quadrotors for the sinusoidal motion. From the results, we can see that we are able to obtain desired tracking and formation responses.

Therefore, from all the simulation results, it can be concluded that the proposed formation control scheme works efficiently with the nonlinear model of the quadrotor. It provides a smooth tracking of the group of quadrotors for a desired formation flight. Also, it can be observed that the T-S model with new operating points provide a better response with fewer ripples when compared to the results when the original operating points were taken from [5].

CHAPTER 6

CONCLUSION

6.1 Conclusion

In this thesis, a cooperative flight control framework is designed for a fleet of an arbitrary number of UAVs. The Takagi-Sugeno Multiple Model approach is used to linearize the nonlinear model of the UAV and local linearized models are obtained. These local models are then interpolated using the Gaussian membership functions from Fuzzy theory to obtain the approximation of the entire nonlinear model. Then a nonlinear state-feedback controller is synthesized using the Parallel Distributed Compensation (PDC). The gains of the controller are obtained by Linear Quadratic Regulator (LQR) optimization to stabilize the system and obtain desired response. This is followed by the formation control of a set of quadrotors using the leader-follower method. In this, the potential field technique is used to obtain the desired shape formations. An attractive potential is generated that attracts the followers towards the leader and a repulsive potential is generated that repels adjacent quadrotors to avoid collisions. Simulations are performed to obtain the desired shape formation for different cases. It is observed that the formation control proposed gives a good tracking response and we are able to achieve the required formation.

6.2 Future Scope

1. The system can be addressed with the presence of communication time delays.

2. Robust controllers can be used to further enhance the system in the presence of disturbances and uncertainty.

3. The system can be implemented in an experimental platform to validate the simulations.

REFERENCES

[1] Samir Bouabdallah, “Design and control of quad rotors with application to autonomous flying”, Thesis 2007.

[2] S. Bouabdallah and R. Siegwart, “Full control of a quadrotor,” in *Proc. IEEE/RSJ Int. Conf. Intell. Robots Syst.*, San Diego, CA, USA,Oct. 29–Nov. 2 2007, pp. 153–158.

[3] Fantoni I., Lozano R. and Castillo P. A simple stabilization algorithm for the PVTOL aircraft, Proceedings of the 15th IFAC World Congress, 2002, Barcelona, Spain, pages 1225-1225, DOI: 10.3182/20020721-6-ES-1901.01227.

[4] Sanchez A., Fantoni I., Lozano R. and Morales J. D. L. Observer-based control of a PVTOL aircraft, Proceedings of the 16th IFAC World Congress, 2005, Prague, Czech Republic. p. 1980-1980 DOI: 10.3182/20050703-6-CZ-1902.01981.

[5] Yacef F., Réseau de modèles locaux pour la commande d ’ un UAV de type Quadrotor. University of Jijel, Algeria, Thesis (2011)

[6] T. Takagi & M. Sugeno, (1985) "Fuzzy identification of systems and its applications to model and control", *IEEE Transactions on Systems, Man, and Cybernetics*, vol. 15, pp. 116–132.

[7] Quadrotor Modelling and Control, Jithu G, Jayasree PR, International Conference on Electrical, Electronics, and Optimization Techniques (ICEEOT).

[8] Fuzzy State Feedback for Attitude Stabilization of Quadrotor, Fernando Torres, Abdelhamid Rabhi, David Lara, Gerardo Romero and Claude Pégard.

[9] Bouadi H., Bouchoucha M. and Tadjine M. Sliding Mode Control based on Backstepping Approach for an UAV Type-Quadrotor, International Journal of Mechanical, Aerospace, Industrial, Mechatronic and Manufacturing Engineering, 2007, Vol. 1, No. 2, pp. 39–44. URL: www.waset.org/publications/11524.

[10] Xu R. and Özgüner Ü. Sliding mode control of a class of under actuated systems, Automatica, 2008, Vol. 44, No. 1, pp. 233–241. DOI:10.1016/j.automatica. 2007.05.014.

[11] V. Mistler, A. Benallegue, and NK M'sirdi. Exact linearization and noninteracting control of a 4 rotors helicopter via dynamic feedback. In Robot and Human Interactive Communication, 2001. Proceedings. 10th IEEE InternationalWorkshop on, pages 586–593. IEEE, 2001.

[12] H. Voos. Nonlinear control of a quadrotor micro-uav using feedback-linearization. In Mechatronics, 2009. ICM 2009. IEEE International Conference on, pages 1–6. IEEE,2009.

[13] E. Altug, J.P. Ostrowski, and R. Mahony. Control of a quadrotor helicopter using visual feedback. In Robotics and Automation, 2002. Proceedings. ICRA'02. IEEE International Conference on, volume 1, pages 72–77. Ieee, 2002.

[14] Z. Zuo. Trajectory tracking control design with command-filtered compensation for a quadrotor. Control Theory & Applications, IET, 4(11):2343–2355, 2010.

[15] R. Xu and U. Ozguner. Sliding mode control of a quadrotor helicopter. In Decision and Control, 2006 45th IEEE Conference on, pages 4957–4962. IEEE, 2006.

[16] H. Bouadi, M. Bouchoucha, and M. Tadjine. Slidingmode control based on backstepping approach for an uav type-quadrotor. International Journal of AppliedMathematics and Computer Sciences, 4(1):12–17, 2007.

[17] A. Tayebi and S. McGilvray. Attitude stabilization of a four-rotor aerial robot. In Decision and Control, 2004. CDC. 43rd IEEE Conference on, volume 2, pages 1216–1221. Ieee, 2004.

[18] Remus C Avram, Xiaodong Zhang, Jonathan Muse and Matthew Clark. “Nonlinear Adaptive Control Design and Controller Integrity Monitoring for Quadrotor UAVs”. 2016 International Conference on Unmanned Aircraft Systems (ICUAS).

[19] B. J. Bialy, J. Klotz, K. Brink and W. E. Dixon. “Lyapunov-Based Robust Adaptive Control of a Quadrotor UAV in the Presence of Modeling Uncertainties”. 2013 American Control Conference (ACC), 2013.

[20] Guerrero, J. A., and Rogelio Lozano. "Flight formation of multiple mini rotorcraft based on nested saturations." Intelligent Robots and Systems (IROS), 2010 IEEE/RSJ International Conference on. IEEE, 2010.

[21] Choi, Young-Cheol, and Hyo-Sung Ahn. "Formation control of quad-rotors in three dimension based on euclidean distance dynamics matrix." Control, Automation and Systems (ICCAS), 2011 11th International Conference on. IEEE, 2011.

[22] Turpin, Matthew, Nathan Michael, and Vijay Kumar. "Decentralized formation control with variable shapes for aerial robots." Robotics and Automation (ICRA), 2012 IEEE International Conference on. IEEE, 2012.

[23] Chang-jian Ru, Rui-xuan Wei, Ying-ying Wang and Jun Che. “Multimodel Predictive Control Approach for UAV Formation Flight”. Hindawi Publishing Corporation, Mathematical Problems in Engineering, Volume 2014.

[24] Li, Xin, Daqi Zhu, and Yuang Qian. "A Survey on Formation Control Algorithms for Multi- AUV System." Unmanned Systems 2.04 (2014): 351-359.

[25] Chen, Yang Quan, and Zhongmin Wang. "Formation control: a review and a new consideration." Intelligent Robots and Systems, 2005. (IROS 2005). 2005 IEEE/RSJ International Conference on. IEEE, 2005.

[26] Latyshev, Simon. Flexible formation configuration for terrain following flight: Formation keeping constraints. 2013.

[27] Di, Long. Cognitive formation flight in multi-unmanned aerial vehicle-based personal remote sensing systems. Utah State University, 2011.

[28] Zhang, Youmin, and Hasan Mehrjerdi. "A survey on multiple unmanned vehicles formation control and coordination: normal and fault situations." Unmanned Aircraft Systems (ICUAS), 2013 International Conference on. IEEE, 2013.

[29] Lewis, F.L., Syrmos V.L.: Optimal Control, 2nd edn. Wiley (1995)

[30] J. D. Wolfe, D. F. Chichka and J. L. Speyer, “Decentralized Controllers for Unmanned Aerial Vehicle Formation Flight”, San Diego, CA, July 1996.

[31] K. Misovec, “Applied Adaptive Techniques for F/A-18 Formation Flight”, AIAA Guidance, Navigation and Control Conference, Monterrey, CA, August 2002.

[32] Oh, Kwang-Kyo, Myoung-Chul Park, and Hyo-Sung Ahn. "A survey of multi-agent formation control." Automatica (2014).

[33] R. W. Beard, J. Lawton, and F. Y. Hadaegh, "A coordination architecture for spacecraft formation control," IEEE Transactions on Control Systems Technology, vol. 9, no. 6, pp.777.790, 2001.

[34] Yacef F., Bouhali O., Khebbache H. and Boudjema F. Takagi-Sugeno model for quadrotormodelling and control using nonlinear state feedback controller, International Journal of Control Theory and Computer Modelling, 2012, Vol. 2, No. 3, pp. 9–24. DOI:10.5121/ijctcm.2012.2302.

Vitae

Name :Mohammed Ataur Rahman

Nationality :Indian

Date of Birth :12/8/1992

Email :ata.rahman36@gmail.com or g201410880@kfupm.edu.sa

Address :12-15-671, M.K. Nagar, Osmania University Campus, Hyderabad, India, 500007

Academic Background :Received Bachelor's degree in Electronics and Communications Engineering from Osmania University, Hyderabad, India in 2014. Completed Master's degree as a Research Assistant in Systems and Control Engineering at King Fahd University of Petroleum and Minerals. Dhahran, Saudi Arabia in December 2017.